

Induced pseudoscalar coupling of the proton weak interaction

Tim Gorringer*

*Department of Physics and Astronomy, University of Kentucky, Lexington,
Kentucky 40506, USA*

Harold W. Fearing†

TRIUMF, Vancouver, British Columbia, V6T 2A3, Canada

(Published 16 December 2003)

The induced pseudoscalar coupling g_p is the least well known of the weak couplings of the proton's charged-current interaction. Its size is dictated by chiral symmetry arguments, and its measurement represents an important test of quantum chromodynamics at low energies. Experiments over the past decade have produced a large body of new data relevant to the coupling g_p . These data include measurements of radiative and nonradiative muon capture on targets ranging from hydrogen and few-nucleon systems to complex nuclei. The authors review the theoretical underpinnings of g_p , the experimental studies, and the procedures and uncertainties in extracting the coupling from data. They also discuss current puzzles and future opportunities.

CONTENTS

I. Introduction	32	F. Summary and outlook for hydrogen	49
II. Theoretical Predictions for g_p	32	VI. Muon Capture in Deuterium	51
A. Proton's weak couplings	32	A. Theory of muon capture in deuterium	51
B. Chiral symmetry and g_p	33	B. Experiments on muon capture in deuterium	51
C. PCAC derivation of g_p	34	VII. Muon Capture in ^3He	53
D. ChPT derivations of g_p	34	A. Theory of ordinary muon capture in ^3He	53
III. Sources of Information on g_p	35	B. Experiments on ordinary muon capture in ^3He	54
IV. Muon Chemistry and the Initial Spin State	36	1. ^3He capture rate experiments	54
A. Muons in pure hydrogen	36	2. ^3He recoil asymmetry experiments	54
B. Muons in pure deuterium	38	C. Radiative muon capture in ^3He	55
C. Muons in hydrogen-deuterium mixtures	38	1. Theoretical calculations	55
V. Muon Capture in Hydrogen	39	2. Experimental results	56
A. Theory of ordinary muon capture	39	VIII. Other Few Body Processes	56
1. Standard diagram calculations	39	IX. Exclusive Ordinary Muon Capture on Complex Nuclei	57
2. ChPT calculations	39	A. Free couplings versus effective couplings	58
3. Spin effects	40	B. Physical observables	58
B. Theory of radiative muon capture	40	1. Capture rates	58
1. Standard diagram calculations	40	2. Recoil asymmetries	58
2. ChPT calculations	41	3. Recoil orientations	59
3. Model calculations	42	4. Gamma-ray correlations	59
4. Spin effects	42	C. Helicity representation	60
C. Experimental methods for hydrogen and deuterium	43	1. Capture on zero-spin targets	60
1. Bubble chamber studies	43	2. Capture on nonzero-spin targets	60
2. Lifetime method	43	D. Induced currents	61
3. Neutron method	43	1. Asymmetries, orientations, and correlations	61
4. Radiative capture	44	2. Hyperfine dependences	61
D. Comparison of experiment and theory	45	3. Capture rates	62
E. Attempts to resolve the discrepancy	47	E. Experimental studies of partial transitions	62
1. General comments	47	1. $^{12}\text{C}(0^+,0) \rightarrow ^{12}\text{B}(1^+,0)$	62
2. Value of the ortho-para transition rate Λ_{op}	47	2. $^{11}\text{B} \rightarrow ^{11}\text{Be}$ and $^{23}\text{Na} \rightarrow ^{23}\text{Ne}$	64
3. Admixtures of a $J=3/2$ ortho-molecular state	48	3. $^{16}\text{O}(0^+,0) \rightarrow ^{16}\text{N}(0^-,120)$	65
4. Direct singlet-para transitions	48	4. $^{28}\text{Si}(0^+,0) \rightarrow ^{28}\text{Al}(1^+,2201)$	66
5. Large Δ resonance effects	49	F. Theoretical framework for exclusive ordinary muon capture	67
6. Other possibilities	49	1. Multipole operators	67
		2. Impulse approximation	68
		3. Exchange currents	68
		G. Nuclear models for partial transitions	69
		1. $^{11}\text{B}(3/2^-,0) \rightarrow ^{11}\text{Be}(1/2^-,320)$	69
		2. $^{12}\text{C}(0^+,0) \rightarrow ^{12}\text{B}(1^+,0)$	70
		3. $^{23}\text{Na}(3/2^+,0) \rightarrow ^{23}\text{Ne}(1/2^+,3458)$	70
		4. $^{28}\text{Si}(0^+,0) \rightarrow ^{28}\text{Al}(1^+,2201)$	70

*Electronic address: gorringer@pa.uky.edu

†Electronic address: fearing@triumf.ca

5. $^{16}\text{O}(0^+,0) \rightarrow ^{16}\text{N}(0^-,120)$	70
H. The coupling g_p from partial transitions	71
1. Recommended values of g_p/g_a	71
2. Model sensitivities of g_p/g_a	72
3. Conclusions and outlook for g_p/g_a	73
X. Inclusive Radiative Muon Capture on Complex Nuclei	74
A. Theory of nuclear radiative muon capture	74
B. Measurement of nuclear radiative muon capture	76
C. Interpretation of nuclear radiative muon capture	76
XI. Other Observables in Muon Capture	79
A. Neutron asymmetries in nuclear ordinary muon capture	79
B. Photon asymmetries in nuclear radiative muon capture	80
XII. Summary	80
Acknowledgments	82
References	82

I. INTRODUCTION

Our topic is g_p , the induced pseudoscalar coupling of the proton's axial current. This coupling is the least well known of the four weak couplings appearing in the proton's charged-current weak interaction.

Interest in determining the coupling is twofold. First, g_p is obviously important as a basic parameter of the proton's interaction. Second, there is a theoretical prediction for g_p which is related to our modern understanding of spontaneously broken chiral symmetry and the origins of hadronic mass, and to explicit chiral symmetry breaking and the effects of nonzero quark masses. Thus the determination of g_p permits an important test of the internal symmetries of the standard model, in particular the approximate chiral symmetry of quantum chromodynamics (QCD), and its realization in the low-energy regime.

The investigation of g_p covers a wide range of experimental phenomena and theoretical methods. In one corner of the experimental program are the challenging studies of the rare processes of ordinary muon capture and radiative muon capture on hydrogen. In another corner are studies of muon capture on complex nuclei, where one tries to tune the observables and transitions to isolate the contribution of g_p . Theoretically the tools range from effective field theories in elementary processes to large-scale shell model computations in complex nuclei. Understanding the rich chemistry of muonic molecules is also a necessity in the studies on muonic hydrogen and muonic deuterium.

The main purpose of this review is to discuss in detail the information currently available, both theoretical and experimental, regarding the value of g_p . In Sec. II we discuss the theoretical prediction for g_p which came originally from the hypothesis of the partially conserved axial current (PCAC) and current algebra, but which nowadays is derived using chiral perturbation theory. Section III concerns some general remarks on different sources of experimental information on g_p and Sec. IV contains a general discussion of the muon chemistry that is necessary to understand the muon processes in hydro-

gen isotopes. The remainder of the review is divided into three main parts which discuss the three main areas which have provided information on the coupling g_p . In the first major part, Secs. V–VIII, we deal with ordinary muon capture (OMC) and radiative muon capture (RMC) on the proton, deuteron, and ^3He . Here experiments are difficult, but the results presumably are not obscured by uncertain details of nuclear structure. In the next major part, Sec. IX, exclusive ordinary muon capture on complex nuclei is examined, with particular emphasis on spin observables in partial transitions. Here the sensitivity to g_p is high, but the experiments are often difficult and their interpretation is model dependent. In the third major part, Sec. X, inclusive radiative muon capture on complex nuclei is examined. Radiative muon capture on complex nuclei is quite sensitive to g_p and nowadays measurements of inclusive radiative muon capture on $Z > 2$ targets are relatively straightforward. However, the model dependence of the theoretical calculations makes the extraction of the coupling a very difficult problem. Two lesser topics, the gamma-ray asymmetry in inclusive radiative muon capture on complex nuclei and the neutron asymmetry in inclusive ordinary muon capture on complex nuclei, are tackled in Sec. XI. Finally in Sec. XII we summarize the current situation with regard to g_p , and make suggestions for further work.

Related review articles include those of Mukhopadhyay (1977), Grenacs (1985), Gmitro and Truöl (1987), Measday (2001), and Bernard *et al.* (2002).

II. THEORETICAL PREDICTIONS FOR g_p

A. Proton's weak couplings

It is well known that the weak interactions of leptons are governed by a current-current interaction, where the currents are given by a simple $V-A$ form, $\gamma_\mu(1-\gamma_5)$. When hadrons are involved, the interaction is still current-current and still $V-A$ but the individual vector and axial vector currents become more complicated, picking up both form factors and new structures involving the momentum transfer q . The couplings associated with these new structures are the so-called "induced" couplings which have been a topic of investigation, both theoretical and experimental, for a long time. In this review we are concerned with one of these, the induced pseudoscalar coupling g_p .

The most general weak current, actually the matrix element of that current, for, say, a neutron and proton can be written as

$$\bar{u}_n \left(+g_v \gamma^\mu + \frac{ig_m}{2m_N} \sigma^{\mu\nu} q_\nu + \frac{g_s}{m_\mu} q^\mu - g_a \gamma^\mu \gamma_5 - \frac{g_p}{m_\mu} q^\mu \gamma_5 - \frac{ig_t}{2m_N} \sigma^{\mu\nu} q_\nu \gamma_5 \right) u_p, \quad (1)$$

where the notation for gamma matrices, spinors, etc., is that of Bjorken and Drell (1964) and m_μ and m_N are, respectively, the muon and nucleon masses. The momen-

tum transfer $q = p_n - p_p$, with p_p, p_n , respectively, the proton and neutron momenta. This most general form for the current contains six coupling “constants,” which are actually functions of q^2 , namely, g_v and g_a , the vector and axial vector couplings, g_m , the weak magnetism coupling, g_p , the induced pseudoscalar coupling, and g_s and g_t , the second class induced scalar and induced tensor couplings.¹ For the most part we will refer to these as “couplings” rather than “constants” to emphasize the fact that they do depend on q^2 , but we will exhibit the q^2 dependence explicitly only when the context requires it.

Of these six, the second class terms g_s and g_t transform differently than the others under G parity, which is a combination of charge conjugation and a rotation in isospin space. In the standard model they are generated only via quark mass differences or electromagnetic effects and are thus predicted to be small (Grenacs, 1985; Shiomi, 1996). Thus although the experimental evidence is not unequivocal (Wilkinson, 2000a, 2000b; Minamisono *et al.*, 2001), they are normally assumed to be zero and will be ignored in this review. Within the standard model the vector piece of the weak charged-current interaction and the isovector piece of the electromagnetic current are just different isospin components of a common isovector current. Thus the static values of g_v and g_m are related to the charge and anomalous magnetic moments of the nucleons and their q^2 dependence is given by measurements of the isovector electromagnetic form factors of the proton and neutron. The axial vector coupling g_a can be determined precisely from neutron beta decay and its q^2 dependence from neutrino scattering (Ahrens *et al.*, 1988) or from pion electroproduction (Del Guerra *et al.*, 1976; Esaulov *et al.*, 1978; Bernard, Kaiser, and Meissner, 1992; Choi *et al.*, 1993; Liesenfeld *et al.*, 1999).

This leaves the induced pseudoscalar coupling g_p , which is by far the least well known. The coupling is predicted by arguments founded on the approximate chiral symmetry of quantum chromodynamics. These arguments were originally formulated in the terms of the PCAC hypothesis and dictate a specific relationship between the induced coupling g_p and the axial coupling g_a known as the Goldberger-Treiman expression (Goldberger and Treiman, 1958). Nowadays they are derived

¹There is an unfortunate confusion about the signs of the axial couplings which has arisen as conventions have changed over the years. In very early calculations in a different metric, the signs were such that g_a was positive. With the widespread use of the metric of Bjorken and Drell (1964) it became conventional to write the weak current like Eq. (1) only with all signs positive. This was the convention used in Beder and Fearing (1987, 1989), Fearing (1980), and most other modern papers, and implies that g_a and g_p are negative. With the advent of chiral perturbation theory, for which g_a is normally taken to be positive, the convention changed again. We have adopted this latter convention. This means that the axial current of Eq. (1) has an explicit overall minus sign and that g_a and g_p are positive numbers.

from heavy baryon chiral perturbation theory. The details of these derivations will be discussed in the next sections. Physically the dominant diagram is one in which the nucleon emits a pion which propagates and then couples to the μ - ν or e - ν vertex. The coupling g_p thus contains a pion pole. In practice, however, it has been difficult to verify this relation and there are some situations, notably radiative muon capture in liquid hydrogen, where experiment and theory do not agree.

B. Chiral symmetry and g_p

According to our present understanding, the strong interactions are described by the Lagrangian of QCD which satisfies an approximate chiral symmetry. The prediction for g_p is based on this approximate chiral symmetry. For that reason a test of that prediction becomes an important test of QCD and its underlying symmetry.

To understand this, consider first the limiting case of massless u and d quarks, and neglect the s quark. In that limit the u and d quarks have definite handedness, and left-handed quarks and right-handed quarks can themselves be regarded as distinct. Likewise in such a limit the strong interaction possesses an exact $SU(2)_L \times SU(2)_R$ chiral symmetry, that is, separate copies of isospin symmetry for left-handed quarks and right-handed quarks. This symmetry generates two conserved currents, a polar vector isovector current V_μ that is associated with a conserved sum of left-handed and right-handed quark currents, and a conserved axial vector isovector current A_μ that is associated with a conserved difference of left-handed and right-handed quark currents.

The chiral symmetry of QCD, unlike isospin symmetry of QCD, is not reflected in the multiplet structure of the hadronic masses. Instead chiral symmetry is realized as a spontaneously broken symmetry. The signature of spontaneously broken chiral symmetry is the appearance of massless pseudoscalar Goldstone bosons, one of which it is natural to identify with the pion. Through spontaneous symmetry breaking the vacuum acquires a particular chirality and the hadrons acquire their non-zero masses, thus hiding or masking the underlying chiral symmetry.

The strict conservation of the axial current, which applies in the massless limit, implies a relation between g_a and g_p . To see this apply current conservation to the axial part of Eq. (1). A sensible result is obtained only if g_p has a pole at $q^2=0$ and if g_p is proportional to g_a .

We know, however, that the quarks are not exactly massless and that the chiral symmetry of the QCD Lagrangian is explicitly broken by quark mass terms, so that the divergence of the axial current is not zero, i.e., the axial current is not exactly conserved. In this situation, by considering coupling of the quarks to external fields,² one can show that the divergence of axial current

²See Fuchs and Scherer (2003) for a good pedagogical discussion of this.

is in fact proportional to the pion mass and to the pion field. Thus one derives from the underlying symmetries of QCD what was earlier known as the PCAC hypothesis and one-pion dominance. This allows us to derive, as we will outline below, a modified relation between g_a and g_p which is known as the Goldberger-Treiman expression.

Given our modern understanding of the symmetries of QCD, however, one can go even further. The crucial observation is that a Lagrangian which satisfies these symmetries will also generate the correct divergence of the axial current. One such Lagrangian is provided by chiral perturbation theory. What is new and important is that with such a Lagrangian one can calculate not only the leading term but higher-order corrections. Thus we can now generate a prediction for g_p in terms of g_a , based purely on the underlying chiral symmetry of the QCD Lagrangian, which reproduces the old PCAC result and in addition generates higher-order corrections.

Thus the relation between g_a and g_p is intimately tied to modern ideas of approximate chiral symmetry and approximate axial current conservation, and tests our understanding of both spontaneous and explicit symmetry breaking in the QCD Lagrangian.

C. PCAC derivation of g_p

Historically the original prediction for g_p was derived more than 40 years ago by Goldberger and Treiman (1958) using a dispersion relation approach. Shortly thereafter the prediction was shown to be based on the notion of the partially conserved axial current (PCAC) and the principle of pion dominance. This work was striking because it predates the discovery of quarks and quantum chromodynamics and our modern understanding of the role of approximate chiral symmetry in the nonconservation of the axial current.

Detailed derivations of these historic approaches are given in textbooks, e.g., Bjorken and Drell (1964) or Weinberg (1996), so we simply outline the basic ideas here. The underlying assumption is that the divergence of the axial current is proportional to the pion field. Applying this idea to the divergence of the axial current of Eq. (1), taking matrix elements, and evaluating at four-momentum transfer $q^2=0$, gives the relation known as the Goldberger-Treiman relation:

$$g_{\pi NN}(0)F_\pi = m_N g_a(0), \quad (2)$$

where $g_{\pi NN}$ is the pion-nucleon coupling, $F_\pi = 92.4 \pm 0.3$ MeV is the pion decay constant, and m_N is the nucleon mass. This equation is rather well satisfied when one uses a modern value of $g_{\pi NN}$ and neglects the possibility that it varies significantly with momentum. A measure of the difference, which is known as the Goldberger-Treiman discrepancy, and which reflects to some extent the momentum dependence of $g_{\pi NN}$, is given by the equation

$$\Delta_{GT} = 1 - \frac{m_N g_a(0)}{g_{\pi NN}(m_\pi^2)F_\pi}, \quad (3)$$

where m_π is the charged pion mass. The value of Δ_{GT} was about 6% using the older (larger) value of $g_{\pi NN} = 13.4$, and there were a number of papers discussing possible sources of this discrepancy. See, e.g., Coon and Scadron (1981, 1990), Jones and Scadron (1975), and references cited therein. With the newer and somewhat smaller value of $g_{\pi NN}(m_\pi^2) = 13.05 \pm 0.08$ (Stoks *et al.*, 1993; Arndt *et al.*, 1995; de Swart *et al.*, 1997), and updated values of g_a and F_π the discrepancy is now 2% or less; see, e.g., Goity *et al.* (1999), Nasrallah (2000), and references cited therein. Thus at $q^2=0$ the Goldberger-Treiman relation is quite well satisfied.

Now consider the matrix element of the divergence of the axial current for nonzero q^2 . This leads, using Eq. (2) and again neglecting the momentum dependence of $g_{\pi NN}$, to an expression for g_p given by

$$g_p(q^2) = \frac{2m_\mu m_N}{m_\pi^2 - q^2} g_a(0). \quad (4)$$

This is known as the Goldberger-Treiman expression for g_p . Observe the explicit presence of a pion pole. At $q^2 = -0.88m_\mu^2$, which is the relevant momentum transfer for muon capture on the proton, this formula gives $g_p(-0.88m_\mu^2) = 6.77g_a = 8.58$, where we have used the value of $g_a(0) = 1.2670 \pm 0.0035$ from the Particle Data Group (2000) and taken for m_N the average of neutron and proton masses. At $q^2 = -m_\mu^2$ the result is $g_p(-m_\mu^2) = 6.47g_a = 8.20$.

Somewhat later the first-order correction to this, proportional to the derivative of g_a , was derived using current algebra techniques (Adler and Dothan, 1966). Numerically, however, the correction is rather small, as described in the next section.

D. ChPT derivations of g_p

As was noted above, in the years since the original derivations of the Goldberger-Treiman relation there have been major advances in our understanding of the way to include chiral symmetry in such analyses and of the role of the underlying QCD Lagrangian. Particularly useful in this regard has been the framework of what is known as chiral perturbation theory (ChPT), or, when nucleons are involved, heavy baryon chiral perturbation theory (heavy-baryon ChPT). This approach provides a way of incorporating the symmetries of QCD into a systematic low-energy expansion, where the expansion parameter is something of the order m_π/m_N . Thus one can reproduce all the old current algebra results, but more importantly calculate in a systematic way the corrections to these results.

This approach was applied (Bernard, Kaiser, and Meissner, 1994) to obtain for g_p the result

$$g_p(q^2) = \frac{2m_\mu g_{\pi NN}(q^2)F_\pi}{m_\pi^2 - q^2} - \frac{1}{3}g_a(0)m_\mu m_N r_A^2, \quad (5)$$

where r_A^2 is the axial radius of the nucleon, defined in the usual way via $g_a(q^2) = g_a(0)[1 + q^2 r_A^2/6 + \mathcal{O}(q^4)]$.

This is essentially the result obtained much earlier by Adler and Dothan (1966) and by Wolfenstein (1970), but the systematic approach allows us to be confident that the corrections are of higher order.

The most recent antineutrino-nucleon experiment (Ahrens *et al.*, 1988) gives the value of the axial radius $r_A^2 = 0.42 \pm 0.04 \text{ fm}^2$ while the most recent pion electroproduction experiment on the nucleon (Liesenfeld *et al.*, 1999) gives $r_A^2 = 0.40 \pm 0.03 \text{ fm}^2$, with the difference being understood in terms of corrections which can be calculated in ChPT (Bernard, Kaiser, and Meissner, 1992; Bernard *et al.*, 2002). We take the world average of the neutrino experiments, including those on nuclei, $r_A^2 = 0.44 \pm 0.02 \text{ fm}^2$, as quoted by Liesenfeld *et al.* (1999). Using this value and taking $g_{\pi NN}(q^2) \rightarrow g_{\pi NN}(m_\pi^2) = 13.05 \pm 0.08$, Eq. (5) leads to $g_p(-0.88m_\mu^2) = 8.70 - 0.47 = 8.23$, so the correction term is indeed rather small.

Very recently Kaiser (2003) has estimated the two loop correction to this relation, and found it to be tiny. There may be a slight caveat to this result in that it was necessary to assume that some undetermined low-energy constants (LEC's) of the theory were of natural size. There are examples where this is not the case, e.g., some of the LEC's needed for pion radiative capture (Fearing *et al.*, 2000), but it appears in this case that such LEC's would have to be huge to make a significant difference.

An alternative approach, still within heavy-baryon ChPT and differing really only in algebraic details, is simply to calculate the amplitude for muon capture, as was done by Fearing *et al.* (1997), and identify g_p by comparing with Eq. (1). This gives, up to corrections of $\mathcal{O}(p^4)$,

$$g_p(q^2) = \frac{2m_\mu m_N}{(m_\pi^2 - q^2)} \left[g_a(q^2) - \frac{m_\pi^2}{(4\pi F_\pi)^2} (2b_{19} - b_{23}) \right], \quad (6)$$

where b_{19} and b_{23} are low-energy constants (LEC's) of the basic Lagrangian. At first glance this appears to be different than the result above, but can be put in the form of Eq. (5) by noting that in the same approach $g_{\pi NN}$ and the axial radius squared r_A^2 are given by

$$g_{\pi NN}(q^2) = \frac{m_N}{F_\pi} \left(g_a(0) - \frac{m_\pi^2 b_{19}}{8\pi^2 F_\pi^2} \right) \quad (7)$$

and

$$r_A^2 = -6 \frac{b_{23}}{g_a(0)(4\pi F_\pi)^2}, \quad (8)$$

which are valid through $\mathcal{O}(p^3)$.

If one wants to express g_p in terms of g_a as has been conventional, rather than $f_\pi g_{\pi NN}$, some simple manipulation of Eq. (5) using Eq. (3) gives

$$g_p(q^2) = \frac{2m_\mu m_N}{(m_\pi^2 - q^2)} g_a(0)(1 + \bar{\epsilon}) - \frac{m_\mu m_N g_a(0) r_A^2}{3}, \quad (9)$$

where $(1 + \bar{\epsilon}) = [g_{\pi NN}(q^2)/g_{\pi NN}(0)][1 - \Delta_{GT}]^{-1}$. Note that $(1 + \bar{\epsilon}) = 1$ if one neglects the q^2 dependence of $g_{\pi NN}$, which we will normally do in this review, and also neglects the small correction due to Δ_{GT} , which historically has usually been done. This gives $g_p(-0.88m_\mu^2) = 8.58 - 0.47 = 8.11$ where the slight difference from the result of Eq. (5) originates in the difference between the left- and right-hand sides of Eq. (2) when experimental values are used, i.e., in Δ_{GT} .

For the purposes of this review we will take as the leading order, or PCAC, prediction for g_p at $q^2 = -0.88m_\mu^2$ that obtained from the first term of Eq. (5), i.e., $g_p^{PCAC} = 8.70$, though in almost all previous fits to data the corresponding term of Eq. (9) has been used instead. When the constant correction term of Eq. (5) or Eq. (9) is included, as it should be nowadays, this becomes 8.23. When we want to distinguish the two values, we will refer to this latter value as “ g_p^{PCAC} with constant term included,” or “ g_p^{PCAC} with the next to leading order (NLO) correction from ChPT included,” or “ g_p^{PCAC} including one-loop corrections.”

It is important to note that the specific formulas in terms of the LEC's of ChPT depend on the specific choice of starting Lagrangian and the details of the calculation. The expressions of Eqs. (6), (7), and (8) come from Fearing *et al.* (1997), but similar results were subsequently obtained by Bernard *et al.* (1998) and Ando *et al.* (2000). However, the expressions in terms of the physically measurable quantities, as given in Eqs. (5) or (9) are independent of the detailed conventions of the approach.

Finally we can summarize this section by observing that theoretical prediction for g_p as given in Eqs. (5) or (9) and based on chiral symmetry seems to be quite robust. The original Goldberger-Treiman relation is understood as the first term in an expansion and correction terms have been evaluated and are understood via a ChPT calculation carried out through the first three orders. Thus a test of this prediction should be an important test of our understanding of chiral symmetry and of low-energy QCD.

III. SOURCES OF INFORMATION ON g_p

At the simplest level g_p appears as a phenomenological parameter in the fundamental definition of the weak nucleon current, Eq. (1), so it should be obtainable from any process which directly involves this current. This would include beta decay and muon capture and, to a good approximation, radiative muon capture, as well as in principle any of the crossed versions of these reactions, as, for example, processes initiated by neutrinos. The g_p term is proportional to the momentum transfer, however, so in practice beta decay is not a useful source of information since the momentum transfer is so small. Neutrino processes are of course extremely difficult to measure. This leaves ordinary muon capture and radiative muon capture as the two main sources of information on g_p .

For ordinary, i.e., nonradiative, muon capture, g_p can be considered as a purely phenomenological parameter

which appears in the most general weak current whose matrix element gives directly the amplitude for the process. Theoretical input, such as PCAC, is not needed and it is quite reasonable to simply fit to data, treating g_p as a free parameter. This is what has typically been done, with the result looked upon as a clean test of the PCAC prediction and of the higher-order corrections from ChPT.

At a somewhat deeper level the g_p coupling is understood to arise from the pole diagram in which a pion, emitted from a nucleon, couples to the weak leptonic current. Since this pion-nucleon coupling is a component of the axial current, other processes involving this current such as pion electroproduction, for example, also in principle allow one to obtain information on g_p . The interpretation of information from such processes must be somewhat different, however, than that obtained from processes like muon capture which contain the phenomenological weak current explicitly. For processes like electroproduction the direct information available is really information about the pion pole diagram. Thus the connection to g_p is only via the theoretical infrastructure of chiral symmetry, PCAC, ChPT, and the interpretation that g_p originates in a pion exchange diagram. If this theoretical approach were in fact wrong, the whole connection would break down and there would be no convincing physical reason why fitting data using for g_p the PCAC expression containing the pion pole should work.

It is interesting to note that radiative muon capture is somewhere in between the situations corresponding to ordinary muon capture and pion electroproduction. The dominant diagrams contain the phenomenological weak current directly, albeit with one leg off shell, but there is also a diagram which explicitly contains pion exchange and which requires additional theoretical input to connect to g_p .

Finally there is a third level where the weak current and one pion exchange do not appear directly but where, in the context of heavy-baryon ChPT, some of the LEC's needed for g_p do appear. For such processes it is, at least in principle, possible to determine those LEC's, and thus determine g_p , at least indirectly, via an equation analogous to Eq. (6). Again such information must be interpreted in a context which accepts the validity of heavy-baryon ChPT.

For all of these processes it may be that measurable quantities such as correlations relative to some of the particle spins, or capture from hyperfine states, or capture to or from a specific nuclear state, or some such more detailed observable may provide more information than just the overall rate, so these should be considered.

We will begin by looking at these various processes, starting with the simplest, muon capture on the proton, and working up through reactions on nuclei to see what has been learned and what potentially could be learned with regard to g_p .

IV. MUON CHEMISTRY AND THE INITIAL SPIN STATE

When a negative muon is stopped in matter a muonic atom is formed. Unfortunately in hydrogen and deuterium such atoms undergo a complicated sequence of chemical processes, changing the spin-state populations with time, as the muons eventually reach the level from which they are captured. As discussed elsewhere, the capture rates for muonic hydrogen and muonic deuterium are strongly dependent on the spin state of the μ -nucleus system. Thus a detailed knowledge of this muon chemistry is required in order to determine g_p from H_2/D_2 experiments and it is appropriate to discuss this chemistry before considering the capture process. Below we denote the two hyperfine states of the muonic atom by $F_{\pm} = I \pm 1/2$ where $I = 1/2$ for the proton and $I = 1$ for the deuteron, so that F is the total spin of the atom.

Before we discuss the details we make a few general comments. One important aspect of muon chemistry is μ -atom scattering from surrounding molecules which results in the hyperfine depopulation of the upper F state into the lower F state. Another important aspect is collisional formation of muonic molecules which results in additional arrangements of μ -nucleus spin states. Also muon recycling from molecular states to atomic states via μ -catalyzed fusion occurs for $d\mu d$ molecules and $p\mu d$ molecules. How these effects unfold for muons in hydrogen and deuterium, as a function of the density, is the focus of our discussion in this section.

In Secs. IV.A and IV.B, respectively, we discuss the chemistry of μp atoms in pure H_2 and μd atoms in pure D_2 . In Sec. IV.C we describe the chemistry of muons in H_2/D_2 mixtures. Related review articles are those of Ponomarev (1973), Bracci and Fiorentini (1982), Breunlich *et al.* (1989), and Froelich (1992).

A. Muons in pure hydrogen

To assist the reader a simplified diagram of muon chemistry in pure H_2 is given in Fig. 1. The figure shows the F_+ and F_- states of the μp atom, the ortho ($I=1$) and para ($I=0$) states of the $p\mu p$ molecule, and relevant atomic and molecular transitions.

The μp atom is initially formed in a highly excited state with a principal quantum number $n \sim 14$ and a kinetic energy ~ 1 eV. The excited atom then rapidly de-excites via combinations of Auger emission,

$$(\mu p)_n + e \rightarrow (\mu p)_{n'} + e, \quad (10)$$

radiative decay,

$$(\mu p)_n \rightarrow (\mu p)_{n'} + \gamma, \quad (11)$$

and Coulomb deexcitation,

$$(\mu p)_n + p \rightarrow (\mu p)_{n'} + p. \quad (12)$$

Note that in Auger emission and radiative decay the μp recoil has a relatively small kinetic energy, since the e or γ carry the released energy, while in Coulomb deexcitation the μp recoil has a relatively large kinetic en-

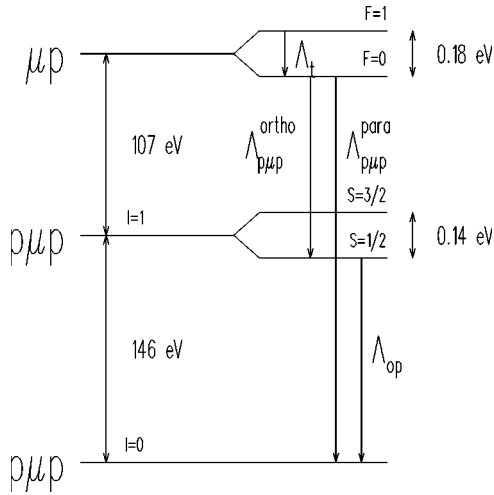


FIG. 1. A simplified diagram of the various atomic and molecular states and transitions relevant to muon capture in pure H_2 . A more detailed diagram of the level structure is given in Bakalov *et al.* (1982) and a more complete diagram of the muon chemistry is given in Wright *et al.* (1998).

ergy, since the μp and p share the released energy. Consequently when formed the ground-state atom has kinetic energies of typically about 1 eV but occasionally up to 100 eV. For recent experiments on energy distributions of ground state $\mu p/\pi p$ atoms see Sigg *et al.* (1996) and Schottmüller *et al.* (1999). Note that at formation of the ground-state atom the hyperfine states are statistically populated, i.e., 3:1 for $F_+ : F_-$.

This “hot” ground state atom is rapidly thermalized by elastic scattering,



and spin-flip collisions,



from the atomic nuclei of the neighboring molecules. Here $\uparrow\uparrow$ denotes the triplet state and $\uparrow\downarrow$ denotes the singlet state. Once the μp kinetic energy falls below the 0.18-eV μp hyperfine splitting the singlet-to-triplet transitions are energetically forbidden and triplet-to-singlet transitions depopulate the upper F_+ state. The resulting F_+ state lifetime is about 0.1 ns in liquid H_2 and about 10 ns in 10 bar H_2 gas. The short lifetime arises from the large μp scattering cross sections due to a near-threshold $\mu p + p$ virtual state. For further details of experimental studies of μp scattering in H_2 environments see Abbott *et al.* (1997) and references therein.

At sufficient densities, i.e., at pressures exceeding 10 bars, the formation of $p\mu p$ molecules is important. The molecule (see Fig. 1) comprises a para-molecular ground state, with total orbital angular momentum $\ell=0$ and nuclear spin $I=0$, and an ortho-molecular excited state, with total orbital angular momentum $\ell=1$ and nuclear spin $I=1$. Note that spin-spin and spin-orbit interactions produce a fivefold splitting of the ortho-molecular state with two $S=1/2$ substates and four $S=3/2$ substates, where S is the total spin angular momentum of the $p\mu p$ complex. Importantly the different states have different

makeups in terms of μp components with parallel spins (i.e., F_+) and antiparallel spins (i.e., F_-). Specifically the para state is 3:1 triplet-to-singlet, the $S=1/2$ ortho states are 1:3 triplet-to-singlet, and the $S=3/2$ ortho states are pure triplet. For further details, see Bakalov *et al.* (1982).

The $p\mu p$ molecules are formed by Auger emission,



Calculations of the rates for the process have been performed by Zel’dovich and Gershtein (1959), Ponomarev and Faifman (1976), Faifman (1989), and Faifman and Men’shikov (1999). Formation of the ortho state involves an $E1$ transition with a predicted rate $\Lambda_{p\mu p}^{ortho} \approx n/n_o \times 1.8 \times 10^6 \text{ s}^{-1}$ and formation of the para state involves an $E0$ transition with a predicted rate $\Lambda_{p\mu p}^{para} \approx n/n_o \times 0.75 \times 10^4 \text{ s}^{-1}$, where n/n_o is the H_2 target number density normalized to the liquid- H_2 number density. Recent measurements of the summed, i.e., ortho and para, rate are typically 30% greater than the calculated rate.³ See Mulhauser *et al.* (1996) for further details.

Note that the $E1$ transition feeding the ortho-molecular state populates only the $S=1/2$ substates (i.e., yielding a 1:3 ratio of $F_+ : F_-$ spin states). Weinberg (1960) and Ando *et al.* (2000) have discussed the possible mixing of the $S=1/2, 3/2$ levels which would lead to changes in the 1:3 triplet-to-singlet ratio for the ortho molecule. However, the available calculations of Halpern (1964a, 1964b), Wessel and Phillipson (1964), and Bakalov *et al.* (1982) have suggested that such effects are negligible.⁴

At first glance the $\Delta I=0$ selection rule for $E1$ transitions forbids decay of the ortho excited state to the para ground state. However, as discussed by Bakalov *et al.* (1982), via the small components of the relativistic wave functions, the ortho state contains $I=0$ admixtures and the para state contains $I=1$ admixtures. Therefore ortho-to-para $E1$ transitions occur via cross combinations of the small components and the large components of the molecular wave functions. Note that the rate Λ_{op} for this Auger process is a function of the electron environment of the $p\mu p$ molecule. Bakalov *et al.* (1982) obtained $\Lambda_{op} = 7.1 \pm 1.2 \times 10^4 \text{ s}^{-1}$ assuming an environment consisting of 75% $[(p\mu p)^+ 2p2e]^+$ and 25% $[(p\mu p)^+ e]$. These proportions are a consequence of the Hirshfelder reaction (Hirshfelder *et al.*, 1936) involving $p\mu p$ complexes and H_2 molecules as discussed by Faifman (1989) and Faifman and Men’shikov (1999). Note

³We note that the most recent measurement of the ortho-para transition rate of Mulhauser *et al.* (1996), yielding $\Lambda_{op} = (3.21 \pm 0.10 \pm 0.14) \times 10^6 \text{ s}^{-1}$, was performed in solid hydrogen not liquid hydrogen. Thus solid-state effects may explain their observation of a higher rate than the earlier experiments.

⁴In addition the relative rates for μ capture in H_2 gas (mostly singlet-atom capture) and H_2 liquid (mostly ortho-molecule capture) are consistent with a 1:3 triplet:singlet makeup of the ortho molecule. For details, see Sec. V.D.

that the only published experimental value of $\Lambda_{op} = (4.1 \pm 1.4) \times 10^4 \text{ s}^{-1}$ from Bardin *et al.* (1981b) and Bardin (1982) is in marginal disagreement with the calculation at the 2σ level.

In summary, in H_2 gas at pressures $0.1 < P < 10$ bars, where the $F=1$ atoms disappear very quickly and the $p\mu p$ molecules form very slowly, the capture process is essentially dominated by singlet atoms. However, in liquid H_2 the molecular formation rate $\Lambda_{p\mu p}$ and ortho-to-para transition rate Λ_{op} are important. Here the rate is a superposition of singlet atomic capture, ortho-molecule capture, and para-molecule capture and depends on $\Lambda_{p\mu p}$, Λ_{op} , and the measurement time window.

B. Muons in pure deuterium

The atomic capture and cascade processes for muons in pure D_2 and pure H_2 are very similar. Most importantly for muons in D_2 the ground state μd atoms are rapidly formed in a statistical mixture of the hyperfine states, i.e., 2:1 for $F_+ : F_-$.

The μd atoms are then thermalized by elastic scattering,



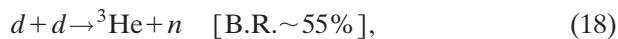
and spin-flip collisions,



on surrounding nuclei. When the μd kinetic energy falls below the 0.043-eV hyperfine splitting the spin-flip collisions then depopulate the higher lying F_+ state. However, the cross sections are considerably smaller for $\mu d + d$ than $\mu p + p$ and consequently the F_+ lifetime is considerably longer in deuterium than hydrogen. For example, in liquid D_2 at 23.8 K, the hyperfine depopulation rate is $\Lambda = (3.05 \pm 0.07) \times 10^7 \text{ s}^{-1}$. For further details see Kammel *et al.* (1982, 1983) and Nägele *et al.* (1989).

An interesting feature of μd chemistry is resonant formation of $d\mu d$ molecules. For example, in liquid D_2 , while $d\mu d$ formation from $F=1/2$ μd atoms involves a nonresonant Auger process, the $d\mu d$ formation from $F=3/2$ μd atoms involves a resonant excitation process, i.e., one where the $d\mu d$ binding energy is absorbed by D_2 vibro-rotational modes. In liquid D_2 at 23.8 K the effective rates are $\Lambda_{d\mu d}^{1/2} = (5.00 \pm 0.40) \times 10^4 \text{ s}^{-1}$ for nonresonant, i.e., doublet, formation and $\Lambda_{d\mu d}^{3/2} = (3.25 \pm 0.33) \times 10^6 \text{ s}^{-1}$ for resonant, i.e., quartet, formation. Note that the resonant formation is temperature dependent. For further details, see Breunlich *et al.* (1989) and Nägele *et al.* (1989).

When $d\mu d$ molecules are formed, the two deuterons immediately fuse via μ -catalyzed fusion,



which quickly recycles the muon from the molecular states to the atomic states. Consequently for muons in

pure D_2 the deuterium capture is from μd atoms and not $d\mu d$ molecules, independent of density and temperature. However, the μ sticking probability in μ catalyzed fusion, 13% in Eq. (18) and 1% in Eq. (19), is non-negligible. Consequently with increasing D_2 target density an increasing $\mu^3\text{He}$ capture background is unavoidable.

In summary, for muons in pure D_2 the capture is a superposition of the rates from the doublet atom and the quartet atom and μ capture from $d\mu d$ molecules is completely negligible. Actually for the particular conditions of the μd experiments by Bardin *et al.* (1986) and Cargnelli *et al.* (1989) the deuterium capture is almost entirely from doublet atoms. See Sec. VI.B for details. However, due to muon sticking in the $d\mu d$ fusion process, a correction for backgrounds from $\mu^3\text{He}$ capture is necessary in liquid D_2 .

C. Muons in hydrogen-deuterium mixtures

Our interest in hydrogen-deuterium mixtures is two-fold. First, “pure- H_2 ” experiments and “pure- D_2 ” experiments must inevitably be concerned with contamination from other isotopes. Second, some early experiments on deuterium capture used hydrogen-deuterium mixtures, e.g., Wang *et al.* (1965) used 0.3% D_2 in H_2 liquid and Bertin *et al.* (1973) used 5% D_2 in H_2 gas.

Muon transfer from μp atoms to μd atoms,



occurs with an energy release of 135 eV and a transfer rate of $n/n_o \times c_d \times 1.7 \times 10^{10} \text{ s}^{-1}$, where c_d is the D_2 concentration in the H_2 target and n/n_o the target number density relative to liquid H_2 (Adamczak *et al.*, 1992). Consequently, in H_2 liquid a 10^{-3} D_2 concentration and in $P > 10$ bars H_2 gas a 10^{-2} D_2 concentration, is sufficient to engineer the transfer in roughly 100 ns.

Following transfer, the μd atom is thermalized via collisions with H_2 molecules. An interesting feature of $\mu d + p$ scattering is the Ramsauer-Townsend minimum at a kinetic energy 1.6 eV. The tiny $\mu d + p$ cross section means slow thermalization and large diffusion of μd atoms in H_2 gas. In addition, the slow thermalization and small deuterium concentration makes hyperfine depopulation via spin-flip collisions,



very slow by comparison to μp atoms in pure H_2 and μd atoms in pure D_2 .

At sufficient densities the formation of $p\mu d$ molecules occurs by Auger emission,



with a rate in liquid H_2 of $\Lambda_{p\mu d} = 5.6 \times 10^6 \text{ s}^{-1}$ (Petitjean *et al.*, 1990/91). The formation of molecules is important as (i) capture is consequently a superposition of μd reactions and μp reactions, and (ii) the various $p\mu d$ states

have different decompositions into μd F states. Further the parent distribution of μd atom F states effects the resulting distribution of $p\mu d$ molecule states, making the relative population of $p\mu d$ states a complicated function of target density and deuterium concentration.

Muon catalyzed fusion from $p\mu d$ molecules occurs via both radiative reactions,



and nonradiative reactions



The radiative rates (Petitjean *et al.*, 1990/91) are $\Lambda_{1/2} = 0.35 \times 10^6 \text{ s}^{-1}$ and $\Lambda_{3/2} = 0.11 \times 10^6 \text{ s}^{-1}$ and the nonradiative rates are $\Lambda_{1/2} = 0.056 \times 10^6 \text{ s}^{-1}$ and $\Lambda_{3/2} = 0$, where the subscripts 1/2, 3/2 denote the p - d spin states. The slow rates make μ capture from $p\mu d$ molecules an important contribution at high target densities. Further, the 100% sticking probability for the radiative reaction makes μ capture in muonic ${}^3\text{He}$ a troublesome background.

In summary, both $\sim 10^{-3}$ D_2 admixtures in H_2 liquid and $\sim 10^{-2}$ D_2 admixtures in H_2 gas have been used in the study of μd capture. Unfortunately the hyperfine depopulation of μd atoms in H_2/D_2 mixtures is slow and therefore the doublet-quartet makeup in H_2/D_2 experiments is dependent on target density and deuterium concentration. Further at densities where $p\mu d$ molecules are formed, the observed rate of muon capture is a complicated superposition of the μp , μd , and $\mu^3\text{He}$ rates and thus disentangling the outcome is difficult.

V. MUON CAPTURE IN HYDROGEN

A. Theory of ordinary muon capture

1. Standard diagram calculations

The simplest of the muon capture reactions is ordinary muon capture on the proton, $\mu + p \rightarrow n + \nu$, which has been studied theoretically for many years. Some of the early work included that of Fujii and Primakoff (1959) and Primakoff (1959). Opat (1964) evaluated amplitudes for both ordinary and radiative muon capture in an expansion in powers of $1/m_N$. Many other authors have performed similar evaluations of the ordinary muon capture rate.

The basic physics is completely determined by the weak nucleon current given in Eq. (1), which is the most general possible form consistent with the known current-current form of the weak interaction. Given this current, the ordinary muon capture amplitude is determined by its product with the leptonic weak current. One then uses standard techniques to square the amplitude, put in phase space, and thus obtain an expression for the rate in terms of the coupling parameters g_v , g_m , g_a , and g_p . This expression is the same whether the couplings are obtained from purely phenomenological sources or from some detailed fundamental model.

Fortunately a lot is known about the couplings. The weak vector current is completely determined by the well-established conserved vector current (CVC) theory which tells us that the weak vector current is simply an isospin rotation of the isovector electromagnetic current. In practice this means that $g_v(q^2) = F_1^p(q^2) - F_1^n(q^2)$ and $g_m(q^2) = \kappa_p F_2^p(q^2) - \kappa_n F_2^n(q^2)$ where $\kappa_p = 1.79285$, $\kappa_n = -1.91304$ are the proton and neutron anomalous magnetic moments and where $F_1^p(q^2)$, $F_1^n(q^2)$, $F_2^p(q^2)$, and $F_2^n(q^2)$ are the usual proton and neutron isovector electromagnetic form factors. The coupling g_a is well determined from neutron beta decay, $g_a(0) = 1.2670 \pm 0.0035$ (Particle Data Group, 2000). The momentum dependence is known, at least at low-momentum transfers, from neutrino scattering on the proton (Ahrens *et al.*, 1988) or from pion electroproduction (Del Guerra *et al.*, 1976; Esaulov *et al.*, 1978; Choi *et al.*, 1993; Liesenfeld *et al.*, 1999). For a long time there was some disagreement between these two sources, but that has now been resolved by a more careful analysis of the corrections necessary in pion electroproduction (Bernard, Kaiser, and Meissner, 1992; Bernard *et al.*, 2002). Thus all of the ingredients for a theoretical calculation of the ordinary muon capture rate on the proton are well determined by general principles which have been verified in many other situations, except for the value of g_p , which is given primarily by the theoretical predictions discussed in Sec. II above.

2. ChPT calculations

The amplitude for ordinary muon capture on the proton has also been evaluated in the context of heavy-baryon ChPT by Fearing *et al.* (1997). Such calculations start with the general ChPT Lagrangian, in this case through $O(p^3)$, and evaluate the amplitude consisting of tree and one-loop diagrams. The outcome of such calculations are expressions for couplings appearing in the most general amplitude of Eq. (1) in terms of the LEC's appearing in the Lagrangian. This approach thus provides a systematic way of calculating couplings and their corrections, as was described for g_p in Sec. II.D above. However, the vector part of the amplitude must still satisfy CVC, g_a must still reproduce neutron beta decay, etc., so in actual fact the couplings to be used are exactly the same as those which have always been used in the phenomenological approach and there is no new information arising from a ChPT calculation, except perhaps for the (small) correction term appearing in g_p , Eq. (5). What is accomplished by such a calculation, however, is to evaluate some of the LEC's which are needed for other calculations, such as radiative muon capture.

Similar ChPT evaluations of ordinary muon capture were subsequently carried out by Bernard *et al.* (1998) and Ando *et al.* (2000). In the latter case the so-called small scale expansion was used, which is a way of including the Δ as an explicit degree of freedom in the ChPT formalism, rather than absorbing its effects in the LEC's.

TABLE I. Numerical values of the parameters and derived quantities used in the text and in our evaluations of rates for comparison with experiment.

Symbol	Description	Value	Reference
F_π	pion decay constant	92.4 ± 0.3 MeV	Particle Data Group (2000)
$g_{\pi NN}(m_\pi^2)$	pion nucleon coupling	13.05 ± 0.08	de Swart <i>et al.</i> (1997)
$G_F V_{ud}$	Fermi constant for β decay	$1.135 48 \times 10^{-5}$ GeV $^{-2}$	Particle Data Group (2000)
$g_a(0)$	axial coupling from β decay	1.2670 ± 0.0035	Particle Data Group (2000)
r_A^2	rms radius squared for g_a	0.44 ± 0.02 fm 2	Liesefeld <i>et al.</i> (1999)
g_p^{PCAC}	PCAC value, $g_p(-0.88m_\mu^2)$	$6.87 g_a(0) = 8.70$	Eq. (5), leading term only
	PCAC value, NLO constant term included	$6.50 g_a(0) = 8.23$	Eq. (5), including NLO correction
$\Lambda_{p\mu p}$	$p\mu p$ molecular formation rate	2.5×10^6 s $^{-1}$	average, Wright <i>et al.</i> (1998)
$\Lambda_{p\mu p}^{ortho} / \Lambda_{p\mu p}^{para}$	ratio of ortho to para molecular formation	240:1	Faifman and Men'shikov (1999)
Λ_{op}	ortho to para transition rate	$4.1 \pm 1.4 \times 10^4$ s $^{-1}$	Bardin <i>et al.</i> (1981a)
$2\gamma^{ortho}$	ortho-molecular overlap factor	1.009 ± 0.001	Bakalov <i>et al.</i> (1982)
$2\gamma^{para}$	para-molecular overlap factor	1.143 ± 0.001	Bakalov <i>et al.</i> (1982)
$g_m(0)$	weak magnetism coupling, $\kappa_p - \kappa_n$	3.705 89	Particle Data Group (2000)
r_m^2	rms radius squared for g_m	0.80 fm 2	Mergell <i>et al.</i> (1996)
r_v^2	rms radius squared for g_v	0.59 fm 2	Mergell <i>et al.</i> (1996)

3. Spin effects

When a muon is stopped in hydrogen it proceeds via a rather complicated series of atomic and molecular processes, as was described above, to a low-level state in either a μp atom or a $p\mu p$ molecule from which the muon is captured. The details of this cascade process and relative probabilities for population of the various states depend on the density of the target and the time at which one starts detecting the captures. For now it suffices to note that the capture from any initial state will be a linear combination of captures from the singlet and triplet μp states. Thus it is important to calculate separately the rates from these two spin states.

Figure 2 shows the individual singlet and triplet captures rates for ordinary muon capture, using a standard diagram calculation (Fearing, 1980), plotted versus the value of g_p . The calculation has been updated to include form factors and modern values of the couplings, particularly g_a . The general table of numerical values, Table I, gives the values of parameters and constants used. Clearly the capture rate from singlet state is much larger than that from the triplet state. However, it is also much less sensitive to the value of g_p . Unfortunately, although one can increase the sensitivity to g_p to some extent by choosing conditions that enhance the triplet contribution, the singlet rate is so much larger that it dominates in essentially all circumstances.

B. Theory of radiative muon capture

We now want to consider the radiative muon capture process $\mu + p \rightarrow n + \nu + \gamma$. The basic ingredients are the same as for ordinary muon capture and the additional coupling of the photon is known. However, the presence of the photon changes the range of momentum transfers available and leads to contributions coming from regions much closer to the pion pole than for ordinary muon

capture. More specifically, for ordinary muon capture on the proton the momentum transfer is fixed at $q^2 = -0.88m_\mu^2$. For radiative muon capture, however, the momentum transfer for some of the diagrams can approach $+m_\mu^2$. These diagrams, all of which involve radiation from hadronic legs, are not the dominant ones. The muon radiating diagram dominates, at least in the usual transverse gauge, and it involves similar momentum transfer as for ordinary muon capture. However, the other diagrams contribute enough in the measurable photon energy region $k > 60$ MeV that the overall sensitivity of radiative muon capture to g_p is significantly increased as compared to ordinary muon capture.

1. Standard diagram calculations

The standard approach to radiative muon capture on the proton has been a Feynman diagram approach, Figs. 3(a)–(e), which includes the diagrams involving radiation from the muon, the proton, the neutron via its magnetic moment, and from the exchanged pion which generates the induced pseudoscalar term. The fifth diagram makes the result gauge invariant using a minimal substitution. Opat (1964) performed one of the earliest such calculations, using, however, a $1/m_N$ expansion of the amplitude. The completely relativistic calculation of Fearing (1980) is an example of a more modern calculation using this approach.⁵

There are some possible enhancements to this basic approach. For example, the intermediate nucleon, between weak and electromagnetic vertices, can in prin-

⁵Hwang and Primakoff (1978) also evaluated radiative muon capture in hydrogen using what they called a linearity hypothesis. This was shown to be incorrect, however, by Wullschlegler and Scheck (1979), Fearing (1980), and Gmitro and Ovchinnikova (1981).

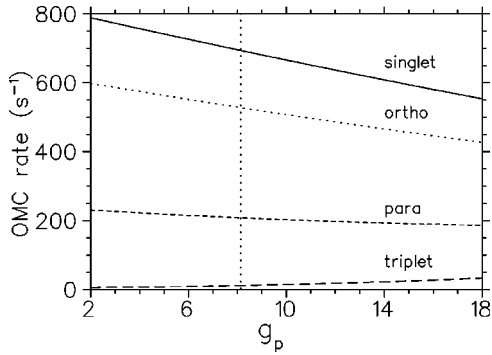


FIG. 2. Capture rates for ordinary muon capture on a proton plotted versus g_p ($-0.88m_\mu^2$) for the muon initially in the singlet or triplet state of the μp atom or in the ortho or para state of the $p\mu p$ molecule. The vertical line corresponds to the PCAC value of $g_p = 8.23$, as defined in Eq. (5), which includes the constant term coming from next-to-leading-order corrections. Details of the model used are described in Sec. V.D.

ciple be a Δ . Such effects, Figs. 3(f) and (g), were considered by Beder and Fearing (1987, 1989). They increase the photon spectrum by amounts ranging from 2–3% at 60 MeV to 7–8% at the upper endpoint. Truhlik and Khanna (2002) found a similar sized effect.

Some additional terms, higher order in an expansion of the radiative muon capture amplitude in powers of the photon momentum k or the momentum transfer q , were obtained originally by Adler and Dothan (1966). These arise via the requirements of gauge invariance and PCAC for the full amplitude. Similar terms were obtained by Christillin and Servadio (1977) and by Klieb (1985). They, however, seem to be fairly small.

This basic diagrammatic approach clearly contains most of the important physics. However, there are some things it does not contain. In particular in the simplest approach gauge invariance is imposed only via a minimal substitution $p \rightarrow p - eA$ on the explicit momentum dependence of the operators in the weak vertex, Eq. (1). Thus one picks up only two terms, one from the explicit q in the g_m term and one from the q in the g_p term. In principle there may be many other terms, gauge invariant by themselves, for example, coming from situations where the photon couples to some internal loop structure of the πNN vertex.

Also for radiative muon capture it is difficult to put form factors in at the various vertices in a general way, though lowest-order form factor effects can be included via a low-energy expansion as done by Adler and Dothan (1966). This is because the momentum transfer at the various vertices in different diagrams is different and so putting in form factors evaluated at these different momenta would destroy the delicate cancellation needed for gauge invariance. This is not a problem unique to radiative muon capture. It appears in any electromagnetic process described by more than one diagram if the momentum transfers are different. Various prescriptions have been proposed to address this problem, but all are pretty much *ad hoc*. In ordinary muon capture introducing form factors reduces the rate, but

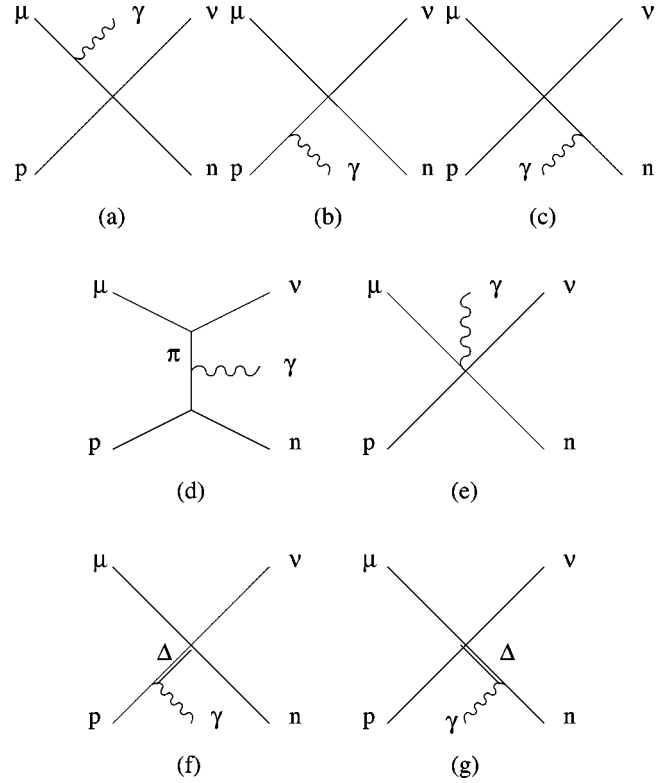


FIG. 3. Diagrams contributing to the standard diagrammatic approach to radiative muon capture: (a)–(e) are the standard diagrams, (f) and (g) are those involving Δ contributions.

only by a few percent. This is because the relevant momentum transfer is small compared to the scale relevant for the form factor. In radiative muon capture all momentum transfers are comparable or smaller than that for ordinary muon capture, so hopefully the form factors introduce only a small correction in radiative muon capture as well. This turns out to be the case in the simple approach described below.

2. ChPT calculations

Just as for ordinary muon capture, it is possible to calculate the amplitude for radiative muon capture using heavy-baryon ChPT. Unlike ordinary muon capture, however, such a calculation introduces some new physics. The ChPT Lagrangian is constructed to satisfy gauge invariance and also CVC and PCAC. Thus the calculated amplitude will satisfy all of these general principles. This means, for example, that such a calculation may contain explicitly gauge terms beyond the simple minimal substitution used in the standard diagrammatic approach. Figure 4 shows some examples of such terms present in a ChPT calculation which are not present in the diagrammatic calculation. A second advantage of such a calculation is that it automatically incorporates form factors, at least to the order of the calculation. One can calculate weak and electromagnetic form factors explicitly as was done by Fearing *et al.* (1997) or Bernard and co-workers (Bernard, Kaiser, Kambor, and Meissner, 1992; Bernard *et al.*, 1998) within ChPT. The same-

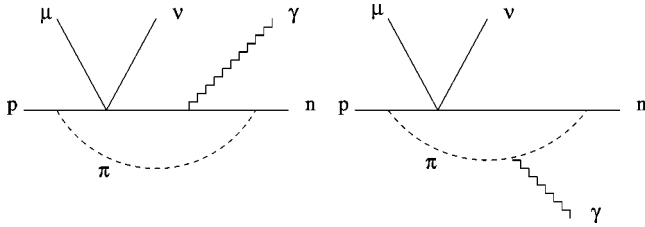


FIG. 4. Several examples of diagrams which appear in a heavy-baryon ChPT calculation but which are not included in the usual minimal substitution gauge contribution of the diagrammatic approach.

subdiagrams responsible for these form factors will appear in the radiative muon capture calculation, so the form factors will be present in such a calculation, and in a gauge invariant way.

The ChPT approach has one disadvantage, however, not shared by the diagrammatic approach. It is an expansion in a small parameter. Thus the calculations are usually done at best to $\mathcal{O}(p^3)$ which is sufficient to include contributions from tree level through this order and the lowest contribution to one-loop diagrams. In contrast in a diagrammatic calculation, at least when done relativistically, no expansion in $1/m_N$ is made and one thus keeps all orders of whatever diagrams are initially included. In practice, however, diagrammatic calculations are limited to tree level graphs, so they do not include the loop contributions of ChPT. Furthermore, they probably at most have only a few higher-order terms coming from relativistic corrections to the tree graphs which would not be included in the ChPT approach.

A heavy-baryon ChPT calculation of radiative muon capture involving just tree level diagrams and working only to $\mathcal{O}(p^2)$ was performed by Meissner *et al.* (1998). They initially found a photon spectrum harder by 10% or so than that of the diagrammatic approach in the region of photon energies greater than 60 MeV, but this was later attributed (Myhrer, 1999) to unwarranted approximations made in the phase-space evaluation.

The most complete of the heavy-baryon ChPT calculations of radiative muon capture has been done by Ando and Min (1998), who worked to third order, i.e., $\mathcal{O}(p^3)$, or in their terminology NNLO (next-to-next-to-leading order). They found that the loop contributions constituted a less than 5% correction to the tree level amplitude and that the result was in reasonable agreement with the standard diagrammatic approach.

An $\mathcal{O}(p^2)$ calculation was also done by Bernard, Hemmert, and Meissner (2001) who, however, used the so-called small scale expansion which allows one to put the Δ in explicitly. Such an approach is not fundamentally different from the usual heavy-baryon ChPT approach. It just allows one to extract explicitly the contribution of the Δ to the various LEC's. In the usual approach the Δ degrees of freedom are integrated out and their effects absorbed in the LEC's. These authors found results similar to those of earlier diagrammatic calculations and specifically that the Δ contribution was

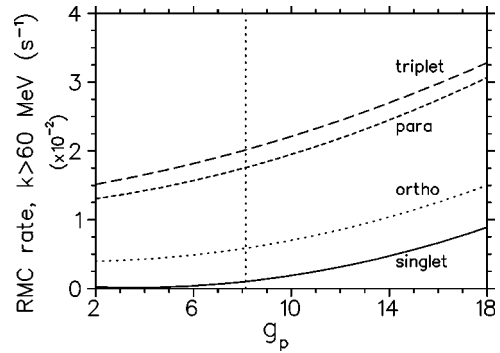


FIG. 5. The photon spectrum for radiative muon capture on a proton, integrated from 60 MeV to the upper end point, shown as a function of $g_p (-0.88m_\mu^2)$. Shown separately are the rates for the muon initially in the singlet or triplet state of the μp atom or in the ortho or para state of the $p\mu p$ molecule. The vertical line corresponds to the PCAC value of $g_p = 8.23$, as defined in Eq. (5), which includes the constant term coming from next-to-leading-order corrections. Details of the model used are described in Sec. V.D.

only of order of a few percent, consistent with the findings of Beder and Fearing (1987, 1989).

3. Model calculations

Recently there has been a somewhat different model calculation of radiative muon capture (Truhlik and Khanna, 2002) based on a $\pi\rho\omega a_1$ Lagrangian which also includes Δ 's (Smejkal *et al.*, 1999). This is basically a diagrammatic approach, but based on a Lagrangian which has a number of additional pieces, and which thus results in an explicitly gauge invariant expression, which also satisfies CVC and PCAC and which generates some of the higher-order terms analogous to those derived by Adler and Dothan (1966). For the best values of the parameters the Δ contributions range from about 3–7% which can be increased to roughly 7–11% at the extreme edge of the allowed parameter space. Thus their results are very similar to those obtained by Beder and Fearing (1987, 1989), and so this model would seem to give a result only a few percent different from the ChPT result or from the standard diagrammatic approach including the Δ .

4. Spin effects

For radiative muon capture, just as for ordinary muon capture, there are fairly dramatic differences in the capture rate from singlet and triplet initial states, and likewise in sensitivities to g_p . Figure 5 shows the integrated photon spectrum above 60 MeV plotted versus g_p for radiative muon capture on the proton. Now it is the triplet state which dominates and the singlet which is most sensitive to g_p , just the opposite situation from ordinary muon capture. Furthermore, if one looks at the RMC photon spectrum before integration (Beder and Fearing, 1989) one sees that variations in g_p about the PCAC value tend to affect the singlet rate more at the upper

end of the spectrum than at the lower end, whereas for the triplet state the change is more uniform across the spectrum. This further enhances the sensitivity to g_p , since it is the upper end of the spectrum which is experimentally accessible.

Finally one should note that the effects which change the relative proportion of singlet and triplet states work in different directions for ordinary muon capture and radiative muon capture. This is because triplet capture is most important for radiative muon capture whereas singlet capture is most important for ordinary muon capture. Thus, for example, some effect which increases the proportion of the triplet state relative to the singlet will decrease the ordinary muon capture rate and increase the radiative muon capture rate, for a given value of g_p .

C. Experimental methods for hydrogen and deuterium

Herein we discuss the experimental methods for muon capture on hydrogen and deuterium. They include measurements of ordinary capture via neutron detection, Sec. V.C.3, Michel electron detection, Sec. V.C.2, and radiative capture via γ -ray detection, Sec. V.C.4.

1. Bubble chamber studies

The first observations of ordinary muon capture on hydrogen were reported by Bertolini *et al.* (1962), Hildebrand (1962), and Hildebrand and Doede (1962). In these early bubble chamber experiments the muons were identified by range and curvature and neutrons were identified via their knock-on protons. An attractive feature of bubble chamber studies is the determination of the neutron energy from the measurement of the proton kinematics. This is helpful in distinguishing the neutrons from ordinary muon capture in H_2 from combinatorial backgrounds of uncorrelated muons and knock-on protons. Recall the neutrons from ordinary muon capture in H_2 are monoenergetic $E_n = 5.2$ MeV. However, the bubble chamber studies were limited by statistics.

2. Lifetime method

The “lifetime method” involves comparing the negative muon lifetime and positive muon lifetime when stopped in hydrogen or deuterium. For positive muons the lifetime is the inverse of the μ decay rate, whereas for negative muons the lifetime is the inverse of the sum of the μ decay rate and the μ capture rate. The lifetime difference thus determines the capture rate. This approach was used at Saclay to determine the μ capture rate in liquid H_2 (Bardin *et al.*, 1981a) and liquid D_2 (Bardin *et al.*, 1986).

The Saclay experiments used a pulsed beam with typically a 3000-Hz repetition rate and typically a 3.0- μ s pulse width. The beam entered via a lead collimator and a copper degrader, stopping in a 24-cm-diameter copper-walled target. The target was filled with liquid H_2 or liquid D_2 with high elemental and isotopic purity. The target was viewed by six Michel electron telescopes each

comprising a three-ply plastic scintillator sandwich. A quartz oscillator was used to determine the time between the beam pulse start signal and the decay electron stop signal. Note that the stop signals were recorded in time windows of about $1 < t < 16$ μ s following the end of the beam pulse.

The major challenge in the lifetime experiment is the required accuracy. Since the μ decay rate is about 1000 times the μ capture rate, the $\mu^+ - \mu^-$ lifetime difference is only about 0.1%. Consequently a determination of the capture rate Λ to about 5% requires a measurement of the lifetime τ to about 5×10^{-5} . Therefore both high statistics and low systematics are important.

One concern is muon stops in nonhydrogen materials. Detection of decay electrons from extraneous materials will alter the time spectrum and distort the measured lifetime. Note that the degrader, collimator, and target cell were all constructed from high- Z materials, so muon stops were rapidly absorbed. Also special care was taken to avoid the occurrence of muon stops in plastic scintillator. Last, H_2 or D_2 of ultrahigh elemental and isotopic purity was used. For μp experiments a small quantity of D_2 in H_2 will result in μ transfer (see Sec. IV.C). For μd experiments, where muons are quickly recycled from $d\mu d$ molecules to μd atoms (see Sec. IV.B), the effects of muon transfer to high- Z contaminants are especially troublesome.

Another concern is a time distortion due to rate effects, i.e., distortion arising from finite resolving time and electron pulse pileup. Bardin *et al.* (1981a) found the main effect of pulse pileup is an additional time component with an effective lifetime $\tau/2$. They corrected for this effect by measuring lifetimes at different rates and extrapolating to zero. The correction to τ was roughly ~ 0.1 ns. Additionally time-dependent and time-independent physical backgrounds were accounted for.

In μd experiments a correction is also necessary for μ capture on ^3He nuclei. The $\mu^3\text{He}$ atoms are produced via $d\mu d$ formation and dd fusion (see Sec. IV.B). The ^3He background, which was monitored by the detection of the 2.5-MeV neutrons from the dd fusion, was a 10% correction in the Saclay μd experiment.

Finally we note that although the Saclay group measured both the μ^+ and μ^- lifetimes they employed the then available world average values for τ_+ in order to extract the capture rates in liquid H_2 and liquid D_2 . The earlier hydrogen experiment used $\tau_+ = 2197.148 \pm 0.066$ ns (Bardin *et al.*, 1981a), though this was later updated by Martino (1982, 1984). The later deuterium measurement (Bardin *et al.*, 1986) used $\tau_+ = 2197.03 \pm 0.04$ ns. This point is discussed in detail in Sec. V.D.

3. Neutron method

The “neutron method” involves directly detecting the recoil neutrons from muon capture in H_2 or D_2 . For hydrogen capture the neutrons are monoenergetic with $E_n = 5.2$ MeV while for deuterium capture the neutrons are peaked at $E_n \sim 1.5$ MeV. Hydrogen data are available on liquid targets from Bleser *et al.* (1962) and Roth-

berg *et al.* (1963) and on gas targets from Alberigi-Quaranta *et al.* (1969) and Bystritskii *et al.* (1974). Deuterium data are available in pure D₂ from Cargnelli *et al.* (1989) and H₂/D₂ mixtures from Wang *et al.* (1965) and Bertin *et al.* (1973).

The neutron method involves (i) counting the incoming muons and outgoing neutrons and (ii) determining their corresponding detection efficiencies. In a typical setup the μ beam is directed into the target vessel via a scintillator telescope and the neutrons are detected in a liquid scintillator counter array. Pulse-shape analysis enables the separation of neutrons from γ rays and veto counters enable the separation of neutrons from electrons. Both electrons and gammas from μ decay are intense backgrounds. Typically the detection of neutrons is initiated about 1 μ s after μ arrival.

The low yield of capture neutrons from ordinary muon capture in H₂ or D₂ means neutron backgrounds from μ capture in surrounding materials, μ transfer to target impurities, and other sources, are troublesome. In gas targets the diffusion of μp atoms or μd atoms to the walls of the target is also a concern. By using high- Z materials for the collimator, vessel, etc., the neutron backgrounds from μ stops in extraneous materials are short lived.⁶ By using high-purity gas/liquid with small $Z > 1$ contamination the problem of transfer is minimized. Additionally a neutron background generated by the combination of Michel bremsstrahlung and (γ, n) reactions is observed. These photoneutrons have the 2.2- μ s lifetime of the μ stops. Therefore studies with μ^+ stops, yielding photo neutrons without capture neutrons, are necessary to subtract this background.

Also the accurate determination of the neutron detection efficiency is a difficult problem. Calibration via the 8.9-MeV neutrons from the $\pi^- p \rightarrow \gamma n$ reaction is helpful, but careful simulations of neutron interactions in counters, target, etc., are necessary.

Note that the deuterium experiment using the neutron method is especially challenging. First, the deuterium neutrons form a continuous distribution peaking at 1.5 MeV. Second, a large background is produced by dd fusion following $d\mu d$ formation.

4. Radiative capture

Radiative muon capture on H₂ has a yield per muon stop of $\sim 10^{-8}$ and a continuum gamma-ray spectrum with $E_\gamma \leq 99.2$ MeV. The first measurement of radiative muon capture on H₂ was recently accomplished at TRIUMF (Jonkmans *et al.*, 1996; Wright *et al.*, 1998).

⁶Further, the experiments of Alberigi-Quaranta *et al.* (1969), Bertin *et al.* (1973), and Bystritskii *et al.* (1974) used a counter arrangement in the target vessel to define the μ stops in hydrogen.

The experiment detected photons from μ stops in liquid H₂. An ultrapure muon beam ($\pi/\mu = 10^{-3}$) was directed into a liquid-H₂ target via a scintillator telescope. The target flask and vacuum jacket were constructed from Au and Ag in order to ensure wall stops in high- Z materials. The flask contained pure hydrogen with a D₂ contamination of about 1 ppm and a $Z > 1$ contamination of less than 1 ppb. The γ -ray detector was a high acceptance, medium resolution, pair spectrometer and comprised a lead cylinder for γ -ray conversion, cylindrical multiwire and drift chambers for e^+e^- tracking, and axial B field for momentum analysis. The photon detection efficiency was $\epsilon\Omega \sim 10^{-2}$ and photon energy resolution was $\Delta E/E \sim 10\%$.

The major difficulty in radiative muon capture on H₂ is the tiny yield. Consequently, photon backgrounds from pion stops in liquid hydrogen, muon capture in nearby materials, and μ decay are dangerous.

Pion stops in liquid H₂ undergo both charge exchange, $\pi^- p \rightarrow \pi^0 n$, and radiative capture, $\pi^- p \rightarrow \gamma n$. The resulting photons comprise a Doppler spectrum of 55–83 MeV and monoenergetic peak at 129 MeV, thus endangering the region of interest for radiative muon capture on H₂. Wright *et al.* (1998) suppressed this background via an ultrahigh-purity muon beam, prompt photon timing cut, and the difference in the π/μ ranges. Additionally the authors determined the residual background from the 55–83-MeV photons via the residual signal from the 129-MeV γ -ray peak.

The bremsstrahlung of electrons from μ decay yields a continuum background with $E_\gamma < m_\mu/2$. It prevents the measurement of the radiative muon capture spectrum below 53 MeV and threatens the measurement of the radiative muon capture spectrum above 53 MeV, because of the finite resolution of the pair spectrometer. Wright *et al.* (1998) designed their spectrometer to minimize the contribution of the high-energy tail in the response function. Additionally the remaining background from Michel bremsstrahlung was measured by stopping a μ^+ beam in liquid H₂, yielding the photon background from μ decay without the photon signal from μ capture.

In addition the backgrounds from μ stops in extraneous materials and μ transfer to target impurities were minimized by (i) using high- Z materials in the target vicinity and (ii) using high isotopic purity H₂ as the target material. Also ancillary measurements were employed to determine the photon backgrounds from accelerator sources and cosmic-ray interactions.

The experiment recorded 397 ± 20 photons with energies $E_\gamma > 60$ MeV and times $t > 365$ ns. After subtracting the backgrounds from μ -decay bremsstrahlung (48 ± 7), Au/Ag radiative μ capture (29 ± 11), and other sources, a total of 279 ± 26 photons from radiative muon capture in liquid H₂ was obtained. The resulting partial branching ratio for radiative muon capture on liquid H₂, i.e., the integrated photon spectrum for $k > 60$ MeV divided by the sum of the muon decay and capture rates, was $R_\gamma(k > 60 \text{ MeV}) = (2.10 \pm 0.21) \times 10^{-8}$. Note that this value corresponds to the particular occupancy of the

TABLE II. Summary of world data for ordinary and radiative muon capture on hydrogen. The columns correspond to the target density in units of liquid-hydrogen density n_o , the time delay between μ stop and start of counting, the effective, time averaged, singlet/ortho/para ratio corresponding to the particular experimental conditions, the capture rate corresponding to these ratios, and the value of g_p implied using the calculation described in the text. For radiative muon capture the value given in the rate column corresponds to $R_\gamma(k>60 \text{ MeV})$, the partial branching ratio obtained by integrating the photon spectrum above $k = 60 \text{ MeV}$ and dividing by the sum of the μ decay and capture rates. Note that the ratios of molecular states in the S:O:P column depend on the parameters, e.g., Λ_{op} , used, and are given only for those experiments that measure the neutron or gamma yield. For the Saclay experiment (Bardin *et al.*, 1981a) the relationship between the measured rate and the ortho capture rate depends on details of the experiment and is given in the original paper. With respect to radiative muon capture, the “original theory” is that of Beder and Fearing (1987, 1989), Fearing (1980) as used in the analysis of the experiment. The “new theory” has updated couplings and form factors were included as described in the text.

Ref.	n/n_o	Δt (μs)	S:O:P	Rate (s^{-1})	$g_p(-0.88m_\mu^2)$
Ordinary muon capture					
Hildebrand (1962)	1.0	0.0	0.15:0.77:0.07	420 ± 120	19.5 ± 11.6
Hildebrand and Doede (1962)	1.0	0.0	0.15:0.77:0.07	428 ± 85	18.7 ± 8.2
Bertolini <i>et al.</i> (1962)	1.0	0.0	0.15:0.77:0.07	450 ± 50	16.4 ± 4.9
Bleser <i>et al.</i> (1962)	1.0	1.0	0.01:0.88:0.11	515 ± 85	6.3 ± 8.7
Rothberg <i>et al.</i> (1963)	1.0	1.2	0.01:0.88:0.12	464 ± 42	11.4 ± 4.2
Alberigi-Quaranta <i>et al.</i> (1969)	0.014	0.9	1.00:0.00:0.00	651 ± 57	11.0 ± 3.8
Bystritskii <i>et al.</i> (1974)	0.072	1.4	1.00:0.00:0.00	686 ± 88	8.7 ± 5.7
Bardin <i>et al.</i> (1981a) (original τ_+)	1.0	2.5		460 ± 20	7.9 ± 3.0
(new τ_+)				435 ± 17	10.6 ± 2.7
Radiative muon capture					
Wright <i>et al.</i> (1998) (original theory)	1.0	0.365	0.06:0.85:0.09	$(2.10 \pm 0.21) \times 10^{-8}$	$12.4 \pm 0.9 \pm 0.4$
(new theory)					$12.2 \pm 0.9 \pm 0.4$

μp spin states in the TRIUMF experiment, i.e., with $t > 365 \text{ ns}$ at liquid- H_2 densities.

D. Comparison of experiment and theory

In Table II we summarize the results of the various measurements of muon capture on hydrogen. For each experiment we have shown the density of the target n/n_o , relative to liquid hydrogen, the approximate time delay from muon stop until counting starts Δt , the time averaged proportion of singlet, ortho, and para states relevant for the experiment, and the rate obtained under these conditions. Note that the singlet/ortho/para ratios depend on the muon chemistry, and the underlying parameters determining that chemistry, and on the delay time Δt . In Table II we used a $p\mu p$ molecular formation rate $\Lambda_{p\mu p} = 2.5 \times 10^6 \text{ s}^{-1}$, a ratio of ortho-state formation to para-state formation of 240:1 (Zel'dovich and Gershtein, 1959; Ponomarev and Faifman, 1976; Faifman and Men'shikov, 1999), an ortho-to-para transition rate $\Lambda_{op} = 4.1 \times 10^4 \text{ s}^{-1}$ (Bardin *et al.*, 1981a). The gamma factors, which account for the difference between the μ density at the proton in the $p\mu p$ and μp systems, were taken as $2\gamma^{ortho} = 1.009$ and $2\gamma^{para} = 1.143$ (Bakalov *et al.*, 1982). It should be emphasized that the rates tabulated correspond to different experimental conditions and so are not directly comparable.

First we stress that the various experiments are sensitive to different combinations of the μ atomic and molecular states, i.e., the triplet, singlet, ortho, and para states. The situation is simplest in the H_2 gas experiments of Alberigi-Quaranta *et al.* (1969) and Bystritskii

et al. (1974) where muon capture is almost exclusively from the $F=0$ atomic state and $p\mu p$ molecule formation is a few percent correction. However, for experiments in liquid H_2 , while capture from the ortho state is the largest, capture from other states is significant. The precise blend of states is determined by the delay Δt between the muon arrival time and the counting start time. The greater the delay the smaller the contribution from the $F=0$ atomic state and the larger the contribution from the para molecular state, as the muon has additional time to form the $p\mu p$ molecular state and convert from ortho to para state, in accord with the processes described in Sec. IV. Thus, for example, the bubble chamber experiments, where $\Delta t = 0$, have therefore the largest contribution of singlet atom capture and smallest contribution of para molecule capture. In contrast, the Saclay lifetime experiment, where $\Delta t \sim 2.5 \mu\text{s}$, had the smallest contribution of singlet atom capture and, though still dominated by ortho capture, the largest contribution of capture from the para state.⁷

In the last column of this table is given the value of g_p corresponding to the experimental rate. To get these numbers the singlet and triplet capture rates were calculated and combined as appropriate for the experimental conditions of the individual experiment. The model used was the standard diagrammatic approach of Fearing (1980) updated to the extent that modern values of the

⁷ $\Delta t \sim 2.5 \mu\text{s}$ is an approximate average value for the Saclay experiment. In analyzing the data the detailed time structure had to be explicitly treated.

couplings, particularly $g_a=1.267$, were used and form factors were included. These form factors were taken to be of the form $f(q^2)=1+q^2\langle r^2\rangle/6$ with the values of the rms radii squared $\langle r^2\rangle$ taken as 0.59 and 0.80 fm² for g_v and g_m (Mergell *et al.*, 1996), respectively, and 0.44 fm² for g_a (Liesenfeld *et al.*, 1999). At the momentum transfer appropriate for ordinary muon capture these form factors are typically 0.98–0.96 so that including them reduces the theoretical ordinary muon capture rate by 2–4 %. The constant term appearing in g_p , as in Eqs. (5) or (9), was included and g_p was parametrized as

$$g_p(q^2)=R\frac{2m_\mu m_N}{(m_\pi^2-q^2)}g_a(0)-\frac{m_\mu m_N g_a(0)r_A^2}{3}. \quad (25)$$

Here R is not intended to have physical significance, but just be a conventional way of parametrizing the variation of the data from the value predicted by theory using the expected value of g_p . At the PCAC (plus next-to-leading-order corrections) point, $R=1$ and $g_p(-0.88m_\mu^2)=8.58-0.47=8.11$.

For radiative muon capture form factors were included also using the $1+q^2\langle r^2\rangle/6$ form and the necessary gauge terms were generated via a minimal substitution. This gives a gauge invariant result which includes most of the terms found by Adler and Dothan (1966). For radiative muon capture these form factors make essentially no difference, e.g., <1 % in the rate corresponding to the TRIUMF experiment, presumably because both spacelike and timelike momentum transfers contribute and, with the linear approximation for the form factors, tend to cancel. The Δ was included as in Beder and Fearing (1987, 1989).

The ordinary muon capture results obtained from this calculation are in very good agreement with other modern ordinary muon capture calculations such as those of Ando *et al.* (2000) and Bernard, Hemmert, and Meissner (2001). It is interesting to observe, however, that the values of g_p quoted in Table II are 0.3–0.8 higher than those in a similar table given in Bardin *et al.* (1981b). This can be traced to two main effects, namely, the increase in g_a to its modern value, 1.254→1.267, and the use of more modern form factors which fall somewhat less rapidly with q^2 than those used in Bardin *et al.* (1981b). Both of these effects lead to a larger theoretical rate for a given value of g_p and thus, as can be seen from Fig. 2, to a larger g_p to fit a given experimental rate.

A further comment is required concerning the value of g_p obtained from the Saclay experiment (Bardin *et al.*, 1981a, 1981b). In analyzing their data the authors extracted the capture rate from the difference between their measured value for τ_- and the world average value for τ_+ . They used the world average for comparison because their measured value for τ_+ , although consistent with the world average, had a larger uncertainty. Since the publication of Bardin *et al.* (1981a) the world average of τ_+ has changed from 2197.15±0.07 ns to 2197.03±0.04 ns (Particle Data Group, 2000). In determining g_p for Table II we decided it best to update the

μ^+ lifetime in extracting the μ^- capture rate,⁸ which now becomes 435±17 s⁻¹ instead of 460±20 s⁻¹. Therefore the value of $g_p(-0.88m_\mu^2)=10.6±2.7$ in Table II is one standard deviation larger than $g_p(-0.88m_\mu^2)=7.9±3.0$ which is obtained from the original published rate with our theoretical calculation, and even larger than the value $g_p(-0.88m_\mu^2)=7.1±3.0$ given in the original paper (Bardin *et al.*, 1981b).

The values of $g_p(-0.88m_\mu^2)$ obtained from the five more recent, electronic, ordinary muon capture experiments are all in general agreement within their errors and result in a world average value 10.5±1.8. The single determination with the smallest uncertainty is that of Bardin *et al.* (1981b) which gives 10.6±2.7. Both of these values are somewhat larger than the prediction $g_p(-0.88m_\mu^2)=8.23$, which includes the constant term arising from next-to-leading-order corrections, though are consistent with it at the 1–1.3 standard deviation level. Note that if one does not update the μ^+ lifetime in the Bardin *et al.* (1981b) analysis the Saclay result is $g_p(-0.88m_\mu^2)=7.9±3.0$ and world average is $g_p(-0.88m_\mu^2)=9.4±1.9$, both of which are also consistent with the prediction $g_p(-0.88m_\mu^2)=8.23$, but both still about 0.7 larger than the corresponding numbers, 7.1±3.0 and 8.7±1.9 quoted in the original paper, because of the updates to the parameters of the theory.

However, the result $g_p(-0.88m_\mu^2)=12.4±0.9±0.4$, or 12.2±1.1 using the updated theory, from the TRIUMF radiative capture experiment (Wright *et al.*, 1998) is 50% larger than, and clearly inconsistent, with the prediction derived from symmetry arguments. Note that the radiative muon capture result is quite consistent with the world average from ordinary muon capture or the Saclay result for g_p if one uses the updated μ^+ lifetime. However, with the older μ^+ lifetime that Bardin *et al.* (1981b) have used, the Saclay result and radiative muon capture result do not overlap within their uncertainties.

We can thus summarize the situation in hydrogen as follows. The radiative muon capture result is several standard deviations larger than the prediction $g_p(-0.88m_\mu^2)=8.23$ and clearly inconsistent with it. The ordinary muon capture results have always been considered to be in agreement with theory, based on the results of the Saclay experiment. We have seen though that, as a result of updates to the parameters in the theory and to subsequent measurements of the μ^+ lifetime, the value of g_p obtained from the ordinary muon capture result has increased. The increase is only about one standard deviation, so the result is still marginally consistent with $g_p(-0.88m_\mu^2)=8.23$. The central value, however, is now also high, and actually somewhat closer to the radiative muon capture result than the chiral symmetry based prediction.

⁸This was also done, in a conference proceedings, by one of the members of the original experimental group. See Martino (1984).

E. Attempts to resolve the discrepancy

1. General comments

In the previous section we saw that the results for g_p obtained from radiative muon capture were significantly higher than the prediction $g_p(-0.88m_\mu^2)=8.23$ and in definite disagreement. The new interpretation of the ordinary muon capture results suggest that they are too high also, being in good agreement with the radiative muon capture result, but perhaps only marginally consistent with predicted value. Since the older interpretation of the ordinary muon capture data seemed to be in good agreement with theory, there has been essentially no consideration of possible difficulties with ordinary muon capture. However, the discrepancy between the radiative muon capture results and theory has generated a lot of discussion and a number of attempts to find additional effects to explain it, some of which will be now discussed.

Suppose that the values of g_p extracted from ordinary and radiative muon capture were in fact different. Is that possible, and what would be the implications of such a result? Clearly in principle the value of g_p should be the same in the two processes as it originates in each case from the same fundamental axial current which contributes to both processes. However, given the present state of analysis, an apparent difference could arise simply because radiative muon capture is much more complicated than ordinary muon capture and involves a lot of additional diagrams. Thus if something is left out of the radiative muon capture analysis, a fit to the data using the standard approach may require a different value of g_p to compensate for the piece left out. In this view a difference in the values of g_p extracted from ordinary and radiative muon capture using current theory may reflect something wrong or missing in the theory rather than a failure of the chiral symmetry based relation of Eq. (5). Note, however, that while a difference between the values of g_p extracted from ordinary and radiative muon capture might be rationalized this way, this would not explain any differences between the ordinary muon capture and ChPT/PCAC results since for ordinary muon capture g_p is a parameter in the most general weak amplitude. It can thus be determined from data largely independently of the details of the weak capture part, as opposed to the molecular and atomic part, of the theory.

A second question to ask is what does it take to bring the radiative muon capture result closer to the prediction $g_p(-0.88m_\mu^2)=8.23$, and what does that do to ordinary muon capture? As discussed earlier the rates for both radiative and ordinary muon capture depend strongly on the proportion of singlet versus triplet components in the initial state. To get the radiative muon capture result to agree better with theory we need to increase the predicted rate for a given g_p , which can be done by increasing the amount of triplet capture and reducing the singlet capture. Since ordinary muon capture is dominated by the singlet rate, this reduces the ordinary muon capture rate, which also moves the ex-

tracted g_p toward the predicted value. However the sensitivity of ordinary and radiative muon capture to increasing triplet is different, and thus it becomes difficult to completely fix one without destroying the agreement of the other.⁹

In any case, in the subsequent paragraphs we will discuss several aspects of the muon chemistry which change the average singlet/ortho/para ratio for each experiment and thus in principle affect the comparison of the results with theory. We will also discuss two other suggestions, dealing specifically with the radiative muon capture calculation which have been put forward as potentially resolving the discrepancy implied by the radiative muon capture results.

2. Value of the ortho-para transition rate Λ_{op}

As has been noted, the experimental combination of singlet and triplet states is important, and this is determined by the various transition rates governing the chemical processes the muon undergoes between stopping and capture. The least certain of these rates is Λ_{op} , the ortho-para transition rate. There is a single theoretical value $\Lambda_{op}=(7.1\pm 1.2)\times 10^4\text{ s}^{-1}$ (Bakalov *et al.*, 1982) which, however, is nearly a factor of 2 larger than the experimental value $(4.1\pm 1.4)\times 10^4\text{ s}^{-1}$ (Bardin *et al.*, 1981b; Bardin, 1982),¹⁰ though another experiment is in progress (Armstrong *et al.*, 1995). A larger value of Λ_{op} increases the relative amount of para state, and thus increases the amount of the triplet component contained in the initial state. Figure 6 shows the region in the g_p - Λ_{op} plane allowed by the TRIUMF radiative muon capture experiment (Wright *et al.*, 1998) and the latest ordinary muon capture experiment (Bardin *et al.*, 1981a).

For these experiments an increase in the value of Λ_{op} , which leads to a greater triplet component in the initial state, increases the predicted radiative muon capture rate and decreases the ordinary muon capture rate for a given value of g_p . In the vicinity of the predicted value of g_p , the radiative muon capture rate increases and the ordinary muon capture rate decreases with increasing g_p . This means that for fixed value of the ex-

⁹To get simultaneous agreement of both the TRIUMF radiative muon capture result and Saclay ordinary muon capture result with theory a larger increase in triplet occupancy is needed for radiative than for ordinary muon capture. Since the TRIUMF radiative muon capture experiment detected the majority of its photons with muon capture times less than a few μs , whereas the Saclay ordinary muon capture experiment detected the majority of its electrons with muon decay times more than a few μs , in principle such circumstances are possible. For example, a long-lived, i.e., ~ 1 - μs lifetime, triplet atom component could increase triplet occupancy for the TRIUMF radiative muon capture experiment much more than for the Saclay ordinary muon capture experiment. However, such a long-lived triplet atom is completely at odds with our current knowledge of muon chemistry in liquid hydrogen.

¹⁰This group also obtained a value $7.7\pm 2.7\times 10^4\text{ s}^{-1}$ via a measurement of the electron time spectrum. See Martino (1982).

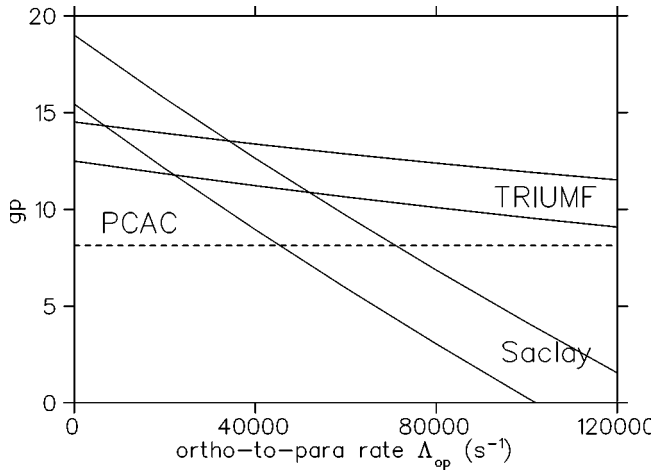


FIG. 6. The region in the g_p - Λ_{op} plane which is allowed by the TRIUMF radiative muon capture experiment (Wright *et al.*, 1998) and the Saclay ordinary muon capture experiment (Bardin *et al.*, 1981a). The dashed line indicates the value, $g_p = 8.23$, as defined in Eq. (5), which includes the constant term coming from next-to-leading-order corrections. Details of the model used are described in Sec. V.D. Note that in determining the error bands the uncertainty included in the experimental results due to the uncertainty in Λ_{op} has not been included, as the results are being plotted against Λ_{op} .

perimental rate the extracted value of g_p decreases with increasing Λ_{op} for both ordinary and radiative muon capture, as can be seen from the figure. However, the Saclay ordinary muon capture experiment is much more sensitive to Λ_{op} than the TRIUMF radiative muon capture experiment.

The updates and improvements we have made in the theory, which raise the ordinary muon capture band in this figure, make it a little easier to accommodate a larger value of Λ_{op} and still have consistency between ordinary and radiative muon capture. In fact now a modest increase in Λ_{op} from the experimental value which has normally been used improves the agreement of both ordinary and ordinary muon capture with theory while keeping them consistent. However, increasing Λ_{op} enough to get agreement of ordinary muon capture with $g_p(-0.88m_\mu^2) = 8.23$ or increasing it further to the theoretical value still leaves radiative muon capture several standard deviations above the predicted value. Increasing it sufficiently to produce the ChPT/PCAC value of g_p from the radiative muon capture data would lead to a catastrophic disagreement between the Saclay ordinary muon capture experiment and the predicted value. Thus while one can envision a value of Λ_{op} which slightly improves the agreement with the chiral symmetry based prediction for both ordinary and radiative muon capture, there still appears to be no value which will simultaneously result in good agreement of current experimental results with the prediction for both cases.

3. Admixtures of a $J=3/2$ ortho-molecular state

It was pointed out in the very early work of Weinberg (1960) that the ortho state could also include a compo-

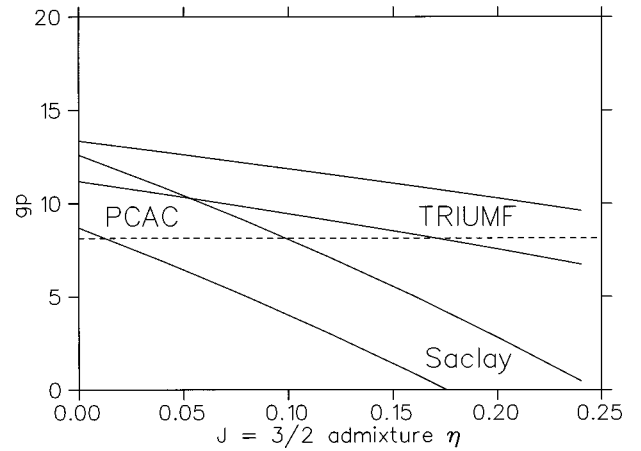


FIG. 7. The region in the g_p - η plane which is allowed by the TRIUMF radiative muon capture experiment (Wright *et al.*, 1998) and the Saclay ordinary muon capture experiment (Bardin *et al.*, 1981a). The dashed line indicates the value, $g_p = 8.23$, as defined in Eq. (5), which includes the constant term coming from next-to-leading-order corrections. Details of the model used are described in Sec. V.D. Λ_{op} has been taken as $4.1 \times 10^4 \text{ s}^{-1}$ and the uncertainty in its value has not been included in the plotted error bands.

nent of total spin angular momentum $S=3/2$. Subsequent theoretical calculations (Halpern, 1964a, 1964b; Wessel and Phillipson, 1964; Bakalov *et al.*, 1982) seemed to indicate that this component was zero or very small. Nevertheless, if there were such a component it would effectively increase the amount of triplet state in the initial state. This has been suggested as a possible explanation by Ando, Myhrer, and Kubodera (2000, 2002). Their original numbers were not quite right, due to a misinterpretation of the appropriate initial state in the ordinary muon capture experiment, but the idea is worth examining. Figure 7 shows the region in the η - g_p plane allowed by the TRIUMF radiative muon capture experiment and the most recent ordinary muon capture experiment. Here η is the fraction of the spin-3/2 state present in the ortho state. The ordinary muon capture calculation here differs slightly from that of Ando *et al.* (2000) by virtue of the fact that form factors have now been included. The theoretical prediction, $\eta=0$ corresponding to no additional spin 3/2 component, gives the most consistent result. The updates to the ordinary muon capture theory, which again raise the band from the Saclay experiment, make it possible to slightly improve both radiative and ordinary muon capture results with a small nonzero value of η . However, analogous to the previous case, a value of η which makes ordinary muon capture agree with theory leaves radiative muon capture too high and a value which makes radiative muon capture agree leads to dramatic disagreement of ordinary muon capture. Thus this effect does not appear to resolve the discrepancy.

4. Direct singlet-para transitions

As shown in Fig. 1 it is in principle possible for the μp singlet atom to make a direct transition to the para $p\mu p$

molecule. This also would increase the proportion of the triplet component in the initial state. This transition is governed by the rate $\Lambda_{p\mu p}^{para}$ which is predicted to be $\approx 0.75 \times 10^4 \text{ s}^{-1}$ for liquid hydrogen, which is two orders of magnitude smaller than the transition rate to the ortho state, $\Lambda_{p\mu p}^{ortho} \approx 1.8 \times 10^6 \text{ s}^{-1}$ (Faifman and Men'shikov, 1999) and so should be a negligible effect.

5. Large Δ resonance effects

In a recent calculation of radiative muon capture in a Lagrangian based model, described in Sec. V.B.3 above, Truhlik and Khanna (2002) argue that the discrepancy is at least partially resolved by a contribution coming primarily from the Δ . The first observation to be made, however, is that using their best parameters the Δ contribution they obtain is essentially the same size as the contribution obtained earlier (Beder and Fearing, 1987, 1989) which was already included in the analysis of the TRIUMF radiative muon capture experiment. Other values of the parameters, but still within the region allowed by other experiments, can raise this Δ contribution by 3–4% in the most important part of the spectrum, where the discrepancy is more than 40%. It would appear, as they in fact note, that their primary results really basically agree with previous ones and so do not provide an explanation of the discrepancy. They go on to observe, however, that one can change one of the parameters corresponding to off-shell properties of the Δ and thus fit the experimental spectrum. That is certainly possible, as one can usually arbitrarily change one parameter to get a fit to another. However, it requires the Δ contribution to be an order of magnitude larger than what they consider most reasonable. Furthermore one would have to reconcile such an explanation with the general result that changing off-shell properties cannot change physically measurable quantities; see, e.g., Fearing (1998b, 2000), Fearing and Scherer (2000), Scherer and Fearing (2001), and references cited therein. Although it is clear that there are uncertainties in any attempt to include a Δ in a calculation such as this, their best estimate of the Δ contribution is quite consistent with the (small) contribution found in the two previous independent calculations which included the Δ (Beder and Fearing, 1987, 1989; Bernard, Hemmert, and Meissner, 2001). An enhancement obtained by varying off-shell parameters which is large enough to explain the full discrepancy does not seem too likely.¹¹

6. Other possibilities

Another suggestion was made by Bernard, Hemmert, and Meissner (2001), namely, that the discrepancy be-

¹¹There was also a suggestion by Cheon and Cheoun (1998, 1999) and Cheoun and Cheon (2003) of an additional term in the Lagrangian which could contribute, but it was shown that such a term was already included in standard calculations, and so was not an additional effect (Fearing, 1998a; Smejkal and Truhlik, 1998).

tween PCAC and the radiative muon capture results could be resolved by a series of small effects in radiative muon capture which happen to add up. Such effects might include, for example, those discussed above or perhaps higher-order loop effects which have not been included, radiative corrections, or variations in some of the parameters. Clearly one cannot test this suggestion without calculating all such effects, which has not been done. We note, however, that insofar as the molecular effects we have discussed are concerned, they all serve to increase the amount of triplet capture, at least for current liquid-H₂ experiments. However in each of these cases, or in some combination of them, as they are somewhat equivalent, it appears that changes sufficient to make radiative muon capture agree, lead to drastic disagreement for ordinary muon capture.

Another particular effect they proposed was an isospin breaking effect. This proposal was based on the observation that the radiative muon capture rate changed quite a bit when the charged pion mass in the pion propagator was replaced by the neutral pion mass, thus supposedly showing a sensitivity to the kinds of presumably electromagnetic isospin breaking effects responsible for the pion mass splitting. This sensitivity clearly originates in the fact that some of the momentum transfers in radiative muon capture can get quite close to the pion pole. Thus changing the position of the pole, even by a few MeV, can change the results significantly. One should note, however, that the pion exchanged is in fact a charged one. Thus in an ideal theory which properly incorporated all electromagnetic effects, after all the renormalizations, and after all the terms which lead to mass splittings were included, the pion mass appearing in the propagator would in fact be the physical charged pion mass, not the neutral one. Thus this particular argument for sensitivity to isospin effects is spurious. In such a complete theory one would probably expect terms in the numerator of the amplitude proportional to the pion mass splitting, and likewise the neutron-proton mass splitting. But the scale in the denominator would likely be something like the pion mass, so these terms should be small. Nevertheless, there could be accidental enhancements, so this is a calculation which should be done.

One might also want to consider radiative corrections to both ordinary and radiative muon capture. Typically these might be expected to be $\mathcal{O}(\alpha/\pi)$, and this was what was found by the one such calculation we are aware of (Goldman, 1972). This is too small an effect to be relevant now, but might be important in the interpretation of future, high precision, ordinary muon capture experiments.

F. Summary and outlook for hydrogen

It is thus possible to summarize the situation in hydrogen as follows. From the theory side, all calculations of ordinary muon capture in hydrogen are in essential agreement, as they must be as all couplings and form factors except g_p are fixed by generally well-accepted principles such as CVC or by other experiments. The several calculations of radiative muon capture, which in principle could differ, e.g., via the extra loop contribu-

tions included in the ChPT calculation relative to the standard diagrammatic calculation, are in fact in general agreement at the few percent level.

On the experimental side, all modern ordinary muon capture experiments now generally lead to values of g_p which are consistent with each other within the errors. The perception that ordinary muon capture agrees with PCAC has changed somewhat, however, with updates to the theoretical calculations and to the μ^+ lifetime. These updates have increased the world average from ordinary muon capture by only about one standard deviation, but result in a value which is now higher than the PCAC value by about 1.3 standard deviations and which is in fact in better agreement with the radiative muon capture result than with PCAC. The one existing radiative muon capture experiment gives a value of g_p which is 50% larger than the PCAC prediction and with uncertainties small enough that it is in clear disagreement with that prediction. Though there have been a number of suggestions and attempts to explain the discrepancy indicated by the radiative muon capture result, none so far have been successful, and the difference remains a puzzle.

So what needs to be done next to resolve this situation? Specifically a high precision measurement of the ordinary muon capture rate in gaseous hydrogen would be very helpful. By using gas rather than liquid the muon chemistry uncertainties are greatly reduced. Indeed a new measurement of the singlet capture rate for ordinary muon capture in H_2 gas at $P \approx 10$ bars using the lifetime method is currently under way at PSI (Kammel *et al.*, 2000; Kammel, 2003). The goal is a precision of about 1% in the singlet rate and about 6% in the coupling g_p . Note that the experiment will use a novel hydrogen time projection chamber that enables direct monitoring of muon stops, muon transfer, and μ -atom diffusion.

Also useful would be a new measurement of ordinary muon capture in liquid hydrogen with significantly improved uncertainties. Such a measurement might distinguish between two possible scenarios. In one, both ordinary and radiative muon capture may give values of g_p which are too high and inconsistent with PCAC, which would suggest that the problem is something common to ordinary muon capture and radiative muon capture, perhaps some difficulty with our understanding of the molecular or atomic effects. In the other ordinary muon capture might clearly agree with PCAC and disagree with radiative muon capture, which would suggest that the problem is something wrong with our understanding of radiative muon capture.

It would also help to confirm some aspects of the muon chemistry, particularly the value of Λ_{op} which is important in determining the initial muonic state and for which the existing experimental (Bardin *et al.*, 1981b; Bardin, 1982) and theoretical (Bakalov *et al.*, 1982) values differ by almost a factor of 2. Such an experiment is under way (Armstrong *et al.*, 1995) and should have results soon.

Another alternative is to try to measure some other quantity which is especially sensitive to g_p . One such quantity is the triplet capture rate for ordinary muon capture in H_2 . Here the central problem is that the triplet rate is about 30 times smaller than the singlet rate. Further, during the time evolution of the μp system following atomic capture, the singlet state is always present, so the singlet capture dominates the ordinary muon capture rate at all times. However, some suggestions have surfaced for isolating the triplet capture from the much larger singlet capture. One possibility suggested by Deutsch (1983) is to measure the time dependence of the neutron polarization. Neutrons following capture from the singlet state have polarization -1 , while those from the triplet state have a polarization depending on the weak dynamics and g_p . Measuring as a function of time allows one to determine a relative neutron polarization, rather than an absolute one, which is more difficult. Such a measurement of the neutron polarization could, in principle, help in identifying the triplet capture and isolating the g_p contribution. Another suggestion (Bailey *et al.*, 1983) notes that the triplet μp atoms, unlike the singlet μp atoms, will precess in a magnetic field. Consequently the time spectra of decay electrons or capture neutrons will be modulated by this precession when muons are stopped in H_2 gas at low pressures, where triplet atoms are relatively long-lived, thus enabling isolation of triplet capture. While interesting and worth reconsidering, such experiments are of course extremely difficult.

For radiative muon capture, it is clear that a new experiment in liquid hydrogen, where triplet capture is largest, would also be both interesting and useful to check the TRIUMF result. Further a new radiative muon capture experiment in gaseous hydrogen, where singlet capture is largest, would be very interesting. However, a radiative muon capture experiment in gaseous hydrogen is extraordinarily difficult since the muon stopping rate is much less and the singlet radiative muon capture rate is much smaller than the triplet radiative muon capture rate.

Since for radiative muon capture the triplet rate is by far the largest, it is possible, by utilizing both a gas target, where capture is primarily from the singlet state, and a liquid target, where there can be significant captures from the triplet state, to obtain as the dominant contribution to the radiative muon capture rate either singlet capture or triplet capture. This is different from the situation for ordinary muon capture since there the singlet rate is the largest and so in both gas and liquid experiments the singlet capture will dominate the total rate.

In principle it is possible to measure spin degrees of freedom in radiative muon capture as well and a suggestion of this type has also been made recently by Ando, Fearing, and Min (2002). Such experiments would be extremely difficult because of the low rates and the necessity of either starting with a polarized muonic atom or measuring the polarization of the outgoing photon, but they are more sensitive to g_p than the rate and are

sensitive to a different combination of amplitudes and so give independent information on the process (Fearing, 1975).

VI. MUON CAPTURE IN DEUTERIUM

We next want to consider ordinary muon capture on deuterium, i.e., the reaction $\mu + d \rightarrow n + n + \nu$, which involves many of the same ingredients as ordinary muon capture on the proton, but also some additional complications.

A. Theory of muon capture in deuterium

Since there are now two nucleons involved in the capture process, several new ingredients appear which were not relevant for capture on the proton. In particular the process now depends on the two nucleon interaction, which is reflected in the properties of the initial state deuteron, such as the wave function, percentage D state, etc., and also in the final-state interaction between the two outgoing neutrons. Furthermore now meson exchange corrections (MEC's) can contribute.

There have been many calculations of the ordinary muon capture rate in deuterium.¹² Some of the more recent ones include Adam *et al.* (1990), Doi *et al.* (1990, 1991), Tatara *et al.* (1990), Morita and Morita (1992), Hwang and Lin (1999), and Ando, Park, *et al.* (2002). Originally the main emphasis was on using this process to extract the neutron-neutron scattering length a_{nn} . In the kinematics in which the two neutrons have low relative momentum, the neutron spectrum peaks at a value several orders of magnitude larger than that for kinematics with large relative momentum. Such a measurement of this low-energy neutron spectrum, while extremely difficult, is still interesting, but perhaps less so than originally in view of the advances in our knowledge of the nucleon-nucleon force from other sources. However, the sensitivity to a_{nn} means that it must be well known to have any hope of using this process to extract g_p , at least if one focuses on the region of low relative neutron momentum where the rate is largest.

Furthermore the total ordinary muon capture rate, which is dominated by the doublet rate, is only moderately sensitive to g_p . A 50% change in g_p produces only about a 10% change in the rate (Doi *et al.*, 1991).

The total rate is also affected by MEC's which have been calculated using specific diagrams involving pion or rho exchange (Doi *et al.*, 1990) or using a more elaborate hard pion Lagrangian involving π 's, ρ 's, ω 's, and a_1 's (Ivanov and Truhlik, 1979b; Adam *et al.*, 1990; Tatara *et al.*, 1990). Generally these MEC's are about a 10% correction to the total rate.

¹²Some representative earlier ones include those of Wang (1965b), Pascual *et al.* (1972), Truhlik (1972), Mintz (1973, 1983), Sotona and Truhlik (1974), Nguyen (1975), Dautry *et al.* (1976), Ho-Kim *et al.* (1976), Švarc *et al.* (1978, 1979), Dogotar *et al.* (1979), Ivanov and Truhlik (1979b), Švarc and Bajzer (1980), and Goulard *et al.* (1982).

The results of modern calculations now generally agree. For example, the doublet capture rate obtained by Tatara *et al.* (1990) is $398\text{--}400\text{ s}^{-1}$ of which $31\text{--}33\text{ s}^{-1}$ comes from MEC's and where the range corresponds to different nucleon-nucleon potentials. Doi *et al.* (1990) obtained 402 s^{-1} and Adam *et al.* (1990) found $416 \pm 7\text{ s}^{-1}$.

It is interesting to note that, since this is a three body final state just like radiative muon capture in the proton case, it is possible to get timelike momentum transfers approaching $+m_\mu^2$ and thus get near the pion pole, where in principle the sensitivity to g_p is enhanced. To our knowledge sensitivity to g_p in that region has not been investigated, although Mintz (1983) considered some effects of timelike form factors and Doi *et al.* (1990) and Goulard *et al.* (1982) showed that meson exchange currents are an important effect there. Unfortunately this kinematic region occurs when the two neutrons go out back to back and the ν has relatively low energy, which is a region which is strongly suppressed relative to the region where the neutron-neutron final state scattering is important, thus making experiments difficult.

There is a very strong hyperfine effect in the capture rate on deuterium. The quartet rate is only $10\text{--}15\text{ s}^{-1}$ (Sotona and Truhlik, 1974; Ho-Kim *et al.*, 1976; Doi *et al.*, 1990). It has been suggested (Dogotar *et al.*, 1979; Doi *et al.*, 1991; Morita and Morita, 1992; Morita *et al.*, 1993) that the ratio of quartet to doublet rate is much more sensitive to g_p than the doublet rate and thus that a measurement of the quartet rate, or directly of the ratio, would give a better value of g_p .

In principle radiative muon capture in deuterium should also be an interesting process, giving information on g_p . However, one might expect that MEC's would be even more important here, since at the least the photon would have to couple to all of the intermediate states which generate the MEC's in ordinary muon capture. To our knowledge there have not been calculations of radiative muon capture in deuterium.

B. Experiments on muon capture in deuterium

A summary of available data for μd total capture rates is given in Table III. It lists experiments with mixed H_2/D_2 targets by Wang *et al.* (1965) and Bertin *et al.* (1973) and pure D_2 targets by Bardin *et al.* (1986) and Cargnelli *et al.* (1989). A H_2/D_2 target is helpful in reducing the neutron background from $d\mu d$ fusion. The Bardin *et al.* (1986) result was obtained using the lifetime method (see Sec. V.C.2) and the other results were obtained using the neutron method (see Sec. V.C.3). Note that the neutron measurements give partial rates for muon capture with neutron energies $> E_{thres}$ and require some input from theory to determine the total rate of μd capture.

The measurement by Wang *et al.* (1965) used a liquid- H_2 target with a 0.32% D_2 admixture. Under these conditions the μ capture is dominantly from $p\mu d$ molecules, since muon transfer yields μd atoms in roughly 20 ns

TABLE III. Summary of world data for the μd doublet capture rate. The columns correspond to the target density in units of liquid-hydrogen density n_o , target temperature, the time delay between μ stop and start of counting, the neutron energy threshold, the deuterium concentration, and the doublet capture rate.

Ref.	n/n_o	T (K)	Δt (μs)	E_n (MeV)	c_d	Rate (s^{-1})
Wang <i>et al.</i> (1965)	1.0	18	0.8	1.4	0.0032	365 ± 96
Bertin <i>et al.</i> (1973)	0.013	293	0.5	1.5	0.05	445 ± 60^a
Bardin <i>et al.</i> (1986)	1.0	18	2.5		1.00	470 ± 29
Cargnelli <i>et al.</i> (1989)	0.04	40	1.9	1.5, 2.5	1.00	409 ± 40

^aNote that the Bertin *et al.* (1973) doublet capture rate was obtained assuming a much faster hyperfine depopulation rate than is consistent with our current understanding of muon chemistry in H_2/D_2 mixtures; see text for details.

and proton capture yields $p\mu d$ molecules in roughly 200 ns. See Sec. IV.C for details. Consequently the neutron signal in Wang *et al.* (1965) involves a superposition of capture on protons, deuterons, and ^3He , the latter being produced via pd fusion in $p\mu d$ molecules. Note that in analyzing their results the authors assumed a statistical mixture of the μd spin states in the $p\mu d$ molecules, as would be expected if hyperfine depopulation by spin-flip collisions is much slower than $p\mu d$ formation. Also the different time dependence of $\mu^3\text{He}$ neutrons and μd neutrons was employed in separating their contributions.¹³ Their final result for doublet capture was $\Lambda_{1/2} = 365 \pm 96 \text{ s}^{-1}$.

The measurement by Bertin *et al.* (1973) used a 7.6-bar H_2 gas target with a 5% D_2 admixture. Under these conditions the μd atom formation is rapid but $p\mu d$ molecule formation is negligible, thus avoiding the complication of contributions from protons, deuterons, and ^3He . Strangely they found that under the assumption of a statistical mix of the μd spin states their extracted rate for doublet capture was 1100–1500 s^{-1} , i.e., three times the theoretical value. Therefore, in order to understand their results, they postulated a much faster hyperfine depopulation rate than assumed by Wang *et al.* (1965). Thus assuming a pure doublet mix of μd spin states the authors obtained a doublet rate of $445 \pm 60 \text{ s}^{-1}$. However, the subsequent studies of hyperfine depopulation in H_2/D_2 systems, e.g., Breunlich (1981), have failed to support this claim and therefore the Bertin *et al.* (1973) result is extremely puzzling.

The more recent experiments of Bardin *et al.* (1986) and Cargnelli *et al.* (1989) were conducted in pure deuterium. In these circumstances the $\mu d + d$ collision rate is sufficient to fully depopulate the F_+ state. Note that any $d\mu d$ formation is followed by prompt fusion and muon recycling into μd atoms. The resulting rates for doublet capture were $\Lambda_{1/2} = 409 \pm 40 \text{ s}^{-1}$ from Cargnelli *et al.* (1989), using a gas target and the neutron method, and $\Lambda_{1/2} = 470 \pm 29 \text{ s}^{-1}$ from Bardin *et al.* (1986), using a

liquid target and the lifetime method. Using the calculation of Doi *et al.* (1991), the Cargnelli *et al.* (1989) result implies $g_p = 8 \pm 4$ and the Bardin *et al.* (1986) result implies $g_p = 2 \pm 3$, which are in disagreement at the level of about 1–1.5 σ . Although one experiment used a gas target and the other experiment used a liquid target, in both cases it is believed that capture is from the doublet atomic state, so that muon chemistry in pure deuterium is unlikely to account for the different results. However, both experiments were challenging and faced different experimental difficulties. Therefore at present we conclude the two results simply indicate a rather large uncertainty in the value of the coupling g_p extracted from the μd system.

There has also been one measurement of the high-energy neutron spectrum following muon capture in deuterium (Lee *et al.*, 1987) using neutron time-of-flight methods. In this kinematic situation the neutrons come out back to back, so the direction is well defined, but there is no start signal for time-of-flight measurements. This group used a novel technique to overcome this, by using the detection of one of the neutrons in a counter placed close to the target as a start signal for the time-of-flight measurement of the other neutron in a counter placed further away from the target. The results suggest the enhancement due to meson exchange corrections found by Goulard *et al.* (1982) and are in qualitative agreement with the calculations of Doi *et al.* (1990) at least as far as the shape of the spectrum is concerned, but are not precise enough to give any real information on g_p . In view of the potentially increased sensitivity to g_p , however, such a measurement of high-energy neutrons is worth reexamining.

A new higher precision measurement of the μd doublet capture rate would be useful in resolving the possible discrepancy between the current results of Bardin *et al.* (1986) and Cargnelli *et al.* (1989). However, in deuterium, unlike in hydrogen, the uncertainties in calculating the contributions of exchange currents may ultimately limit the achievable accuracy in extracting g_p . We also remark that in pure deuterium and hydrogen-deuterium mixtures the hyperfine depopulation rate is much slower than in pure hydrogen. Consequently measuring either the quartet rate or hyperfine dependence in μd capture, which are strongly dependent on g_p , may

¹³The neutrons from μd capture build up quickly with the nanosecond time scale of the μ transfer process. The neutrons from $\mu^3\text{He}$ capture build up slowly with the microsecond time scale of the pd fusion process.

be experimentally easier in μd . It would be worthwhile to reconsider this source of information on g_p , as has been suggested by Doi *et al.* (1991) and Morita and Morita (1992).

VII. MUON CAPTURE IN ${}^3\text{He}$

We now want to consider both ordinary and radiative muon capture on ${}^3\text{He}$. Since it is possible to break up the final state there are several processes possible,

$$\mu^- + {}^3\text{He} \rightarrow {}^3\text{H} + \nu, \quad (26)$$

$$\mu^- + {}^3\text{He} \rightarrow {}^2\text{H} + n + \nu, \quad (27)$$

$$\mu^- + {}^3\text{He} \rightarrow p + n + n + \nu, \quad (28)$$

with analogous processes involving a photon in the case of radiative muon capture.

Of these, most work has been done on the triton final state, Eq. (26). Like the deuteron, since there is more than one nucleon, the complications of exchange currents must be addressed. Additionally three-body forces are now possible. However, there has been a tremendous amount of work done on three-body wave functions in recent years and these wave functions are now extremely well known. Thus the wave function complications which plague interpretation of capture in heavier nuclei really do not enter here. Furthermore, the rate is significantly higher than in capture on protons and deuterons and the atomic and molecular processes which make the interpretation of capture in hydrogen or deuterium difficult are not present here. Thus ${}^3\text{He}$ is an ideal compromise, and we will see that one of the best measurements of g_p to date comes from ordinary muon capture in ${}^3\text{He}$.

A. Theory of ordinary muon capture in ${}^3\text{He}$

There have been two major approaches to the theory of muon capture in ${}^3\text{He}$, the elementary-particle model (EPM) and the impulse approximation (IA), supplemented by explicit calculations of meson exchange corrections. The elementary-particle model exploits the fact that the ${}^3\text{He}$ - ${}^3\text{H}$ system is a spin-1/2 isodoublet just like the proton-neutron system. Thus one can carry over directly the calculations done for capture on the proton. The couplings and form factors now apply to the three-body system as a whole, rather than the nucleon. However, they can be obtained in many cases directly from other processes such as electron scattering on ${}^3\text{He}$ or tritium β decay or from theory, i.e., by applying PCAC to the nuclear pseudoscalar form factor. This approach has the advantage that it already includes effects of MEC's, which are buried in the form factors, and that it can be done relativistically. However, it is difficult to relate the nuclear form factors to the fundamental couplings and form factors of the weak current, e.g., g_p . Some sort of microscopic model is necessary to make this connection.

One of the first such elementary-particle model calculations was that of Kim and Primakoff (1965). The idea

was later applied to ${}^3\text{He}$ by Beder (1976), Fearing (1980), Klieb and Rood (1981), and Klieb (1982). A more modern and very careful calculation with particular attention to the form factors and the various uncertainties was carried out by Congleton and Fearing (1993), and their results were confirmed by Govaerts and Lucio-Martinez (2000) and by Ho *et al.* (2002). The final result is a prediction from the elementary-particle model for the statistical capture rate of $1497 \pm 21 \text{ s}^{-1}$ (Congleton and Fearing, 1993) using the standard PCAC value for g_p .

The impulse approximation, on the other hand, treats the capture process as capture on an essentially free proton. This one nucleon interaction is then expanded in powers of $1/m$ and used as an effective interaction in a matrix element between nuclear wave functions. The information specific to the nucleus comes in only via the nuclear wave functions. Early applications of this approach applied to ${}^3\text{He}$ include Peterson (1968), Phillips *et al.* (1975), Klieb and Rood (1981), and Klieb (1982). Again a very careful calculation was done by Congleton and Fearing (1993) using the variational wave functions of Kameyama *et al.* (1989) with the result for the rate 1304 s^{-1} . This was essentially confirmed by Ho *et al.* (2002) using for the wave functions momentum space Faddeev solutions for a variety of potentials. They found, however, about a $\pm 3\%$ spread among the results using the various wave functions. The fact that the impulse approximation result is about 15% lower than the elementary-particle model is characteristic of the impulse approximation and indicates the effect of the MEC's. Congleton and Truhlik (1996) refined these impulse approximation calculations by including explicitly the MEC's, based on a specific Lagrangian involving π, ρ, a_1, Δ couplings. The end result, which also included some effects of three-body forces, was $1502 \pm 32 \text{ s}^{-1}$. This is in excellent agreement with the elementary-particle model result. Finally, very recently Marcucci *et al.* (2002) repeated the calculation of Congleton and Truhlik (1996) using wave functions arising from the Argonne v_{14} or v_{18} potentials with some three-body forces. They also made some refinements to the weak current and reduced the size of the uncertainty by fixing the Δ contribution to the exchange current corrections via a fit to tritium beta decay. They obtained $1494 \pm 9 \text{ s}^{-1}$. The reduction in the estimated error as compared to Congleton and Truhlik (1996) is apparently primarily due to the fact that they fixed the Δ couplings, whereas Congleton and Truhlik (1996) included in their error estimate an uncertainty in these couplings.

Thus to summarize, the capture rate for ordinary muon capture on ${}^3\text{He}$ is well determined by both elementary-particle model and impulse approximation + MEC calculations with an accuracy of 1–3%. We note that at this level of accuracy radiative corrections might be important and should be evaluated.

Finally it is worth mentioning that there have also been calculations of various spin correlations in ordinary muon capture (Congleton and Fearing, 1993; Congleton, 1994; Congleton and Truhlik, 1996; Govaerts and Lucio-

Martinez, 2000; Marcucci *et al.*, 2002). Generally these correlations are more sensitive to g_p and less sensitive to the MEC's than the rate is. There have also been calculations of some breakup channels (Wang, 1965a; Phillips *et al.*, 1975; Skibinski *et al.*, 1999).

B. Experiments on ordinary muon capture in ^3He

The ^3H channel in ordinary muon capture on ^3He yields a muon neutrino with momentum 100 MeV/c and triton recoil with energy 1.9 MeV. The triton yield per μ stop is roughly 0.3%. Contrary to muon capture on complex nuclei, the recoil triton has a relatively high energy and a relatively small charge, and is therefore directly detectable. In Sec. VII.B.1 below we discuss the current status of the $^3\text{He}\rightarrow^3\text{H}$ capture rate experiments and in Sec. VII.B.2 the $^3\text{He}\rightarrow^3\text{H}$ recoil asymmetry experiments.

1. ^3He capture rate experiments

So far several measurements of the $^3\text{He}\rightarrow^3\text{H}$ rate have been performed. They comprise the early work of Falomkin *et al.* (1963), Zaimidoroga *et al.* (1963), Auerbach *et al.* (1965), Clay *et al.* (1965), and recent work of Ackerbauer *et al.* (1998).

The basic method involves counting the numbers of μ stops and ^3He recoils when a beam of muons is stopped in ^3He . In Auerbach *et al.* (1965) and Ackerbauer *et al.* (1998) a ^3He gas ionization chamber was used whereas in Falomkin *et al.* (1963) and Clay *et al.* (1965) a ^3He liquid scintillator was used. One advantage of a liquid scintillation counter is the higher muon stopping rate in the liquid-helium target. However, one advantage of a gas ionization chamber is the better separation of the μ and ^3He signals via its tracking capabilities.

The recent experiment of Ackerbauer *et al.* (1998) employed an ^3He ionization chamber with a 15-cm³ active volume and a 120-bar gas pressure. The anode plane was segmented to permit the tracking of the incoming muons, the isolation of the recoil tritons, and the definition of the fiducial volume. The anode strips were read out into flash analog-to-digital converters (ADC's) for measurement of the drift time and the energy loss. Separate triggers were employed to count the incoming muons or recoil tritons with full efficiency.

One experimental difficulty is muon-triton pileup, i.e., overlapping of the prompt μ^- ionization and the delayed ^3He ionization. Ackerbauer *et al.* (1998) addressed this problem by both (i) ignoring pileup events and extrapolating to $t=0$ the nonpileup $\mu^-^3\text{H}$ time spectrum, and (ii) keeping pileup events and using the anode pulse shapes for computing $\mu^-^3\text{H}$ time differences. The consistency of (i) and (ii) was helpful in demonstrating the correct treatment of pulse pileup.

Another experimental difficulty is background processes. The 1.9-MeV triton energy-loss peak is superimposed on backgrounds that include ^3H breakup channels, thermal neutron capture, and μ -decay electrons. Ackerbauer *et al.* (1998) employed various fitting procedures in order to separate the triton peak and con-

tinuum background and estimate the uncertainties. Their signal-to-background ratio was roughly 20:1.

The Ackerbauer *et al.* (1998) experiment yielded a $^3\text{He}\rightarrow^3\text{H}$ rate, corresponding to a statistical hyperfine initial population, of $1496.0\pm 4.0\text{ s}^{-1}$, with the largest systematic uncertainty being the subtraction of the background. The $\pm 0.2\%$ accuracy is a tenfold improvement over the earlier experiments of Falomkin *et al.* (1963), $1410\pm 140\text{ s}^{-1}$, Clay *et al.* (1965), $1467\pm 67\text{ s}^{-1}$, and Auerbach *et al.* (1965), $1505\pm 40\text{ s}^{-1}$. In addition, Ackerbauer *et al.* (1998) utilized their time spectrum to establish that transfer from the F_- to the F_+ hyperfine state as well as capture from the $2S$ metastable state can be safely neglected.¹⁴

Taken together the measurement of Ackerbauer *et al.* (1998) and the calculation of Congleton and Truhlik (1996) give $g_p(-0.954m_\mu^2)=8.53\pm 1.54$ which implies $g_p(-0.88m_\mu^2)=8.77\pm 1.58=(1.01\pm 0.18)g_p^{PCAC}$, or $(1.07\pm 0.19)g_p^{PCAC}$ if we use the value of g_p^{PCAC} which includes the constant term. These results are in nice agreement with the PCAC prediction for the coupling g_p . Here the dominant uncertainty originates from the theoretical calculation and not the experimental data. Clearly the key question is the exact size of the theoretical uncertainty. We have quoted the theoretical error of Congleton and Truhlik (1996) which originates mainly from the Δ contribution to the exchange currents. Subsequently, Marcucci *et al.* (2002) have suggested this uncertainty can be reduced by fixing some of the parameters using results from exchange current effects in tritium beta decay. However, Ho *et al.* (2002) found significant theoretical uncertainty arising from different choices of the nuclear wave functions, though some of this may be due to the fact that three-body forces were not included and tuned to give the same binding energies for all choices. Further efforts on establishing and reducing the theoretical uncertainty in calculating the rate for $^3\text{He}\rightarrow^3\text{H}$ capture are definitely worthwhile.

Last we note that there have been some recent measurements of partial capture rates and energy spectra for the break-up channels following muon capture in ^3He (Cummings *et al.*, 1992; Kuhn *et al.*, 1994; Maev *et al.*, 1996). Comparisons with a recent calculation (Skibinski *et al.*, 1999) indicate that a good treatment of final-state effects is necessary to describe the data. However, at the present stage these channels give no information on g_p .

2. ^3He recoil asymmetry experiments

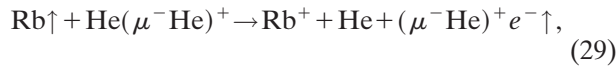
As discussed for nuclei in general in Sec. IX.B.2 below, the recoil asymmetry in muon capture can be very sensitive to the coupling g_p . Unfortunately, production

¹⁴For the hyperfine transition rate Ackerbauer *et al.* (1998) obtained $(0.006\pm 0.008)\mu\text{s}^{-1}$ and for the $2S$ state lifetime they obtained $<50\text{ ns}$.

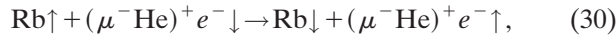
of a measurable ${}^3\text{H}$ asymmetry requires production of a large $\mu^{-3}\text{He}$ polarization, which has proven to be difficult.

Early attempts to polarize $\mu^{-3}\text{He}$, using a polarized beam on an unpolarized target and an unpolarized beam on a polarized target, were unsuccessful. For example, Souder *et al.* (1975) obtained a μ^{-} polarization of only $\sim 6\%$ when stopping polarized muons in unpolarized ${}^3\text{He}$ gas and Newbury *et al.* (1991) obtained a μ^{-} polarization of only $\sim 7\%$ when stopping unpolarized muons in polarized ${}^3\text{He}$ gas.¹⁵ The breakthrough was made at LAMPF by Barton *et al.* (1993) by repolarizing the $\mu^{-3}\text{He}$ system with a laser-pumped Rb vapor after the atomic cascade.

How does repolarization work? Following the $\mu^{-3}\text{He}$ atomic cascade a $(\mu^{-3}\text{He})^{+}$ positive ion is produced. However, the $(\mu^{-3}\text{He})^{+}$ ion is short lived, forming either $(\mu^{-3}\text{He})^{+3}\text{He}$ molecules via collisions with surrounding He atoms or $(\mu^{-3}\text{He})^{+}e^{-}$ atoms after collisions with electron-donor impurities. The repolarization technique developed by Barton *et al.* (1993) employs both spin transfer in the dissociation of the $(\mu^{-3}\text{He})^{+3}\text{He}$ molecules,



and spin transfer in the collisions of the $(\mu^{-3}\text{He})^{+}e^{-}$ atoms,



where the arrows denote the polarization state of transferred electrons. Following the dissociation process of Eq. (29) and collision process of Eq. (30) the polarization of the electron is shared with the muon via their spin-spin interaction. Barton *et al.* (1993) discovered at high Rb \uparrow densities both processes contributed to muon repolarization on the time scale of the muon lifetime, and produced a μ^{-} polarization in ${}^3\text{He}$ gas of 26%.

Recently the first measurement of the recoil asymmetry in the ${}^3\text{He} \rightarrow {}^3\text{H}$ transition was accomplished by Souder *et al.* (1998) at TRIUMF. The experiment utilized a ${}^3\text{He}$ ionization chamber to stop the incoming muons, repolarize the $\mu^{-3}\text{He}$ system, and track the triton recoils. For experimental details, see Bogorad *et al.* (1997) and Souder *et al.* (1998). The chamber had an instrumented volume of 140 cm^3 and a gas pressure of 8 bars. Anode segmentation assisted the definition of the fiducial volume and pulse-shape readout assisted the separation of the $\mu/{}^3\text{He}$ pulses. Running the chamber at high voltage, high temperature, and high Rb density was a great achievement.

Souder *et al.* (1998) employed an interesting approach in determining $\cos\theta$, the direction between the ${}^3\text{H}$ recoil and $\mu^{-3}\text{He}$ polarization. First the magnitude of $\cos\theta$ was determined from the anode signal width. If the recoil travels perpendicular to the anode plane the drift time

range and anode pulse width are large. If the recoil travels parallel to the anode plane the drift time range and anode pulse width are small. Second the sign of $\cos\theta$ was determined from the anode pulse shape. For a recoil traveling towards the anode the early arriving Bragg peak yields a fast rise time pulse. For a recoil traveling away from the anode the late arriving Bragg peak yields a slow rise time pulse.

The $\mu^{-3}\text{He}$ polarization was determined by detecting the μ -decay electrons and using the well-known correlation between the electron momentum and the muon spin in the $\mu \rightarrow e\nu\bar{\nu}$ decay. The electrons were detected using a telescope consisting of wire chambers and plastic scintillators, which permitted ray tracing into the ionization chamber. The asymmetry in the electron counts, on reversing the laser polarization, gave P_{μ} .

Souder *et al.* (1998) achieved a muon polarization of $P_{\mu} = 30 \pm 4\%$. By normalizing the observed triton asymmetry using the measured muon polarization the authors obtained a preliminary value for the vector asymmetry for ${}^3\text{He} \rightarrow {}^3\text{H}$ capture of $A_v = 0.63 \pm 0.09(\text{stat.})_{-0.14}^{+0.11}(\text{syst.})$. The largest uncertainty was the systematic error in the experimental determination of the muon polarization.

Taking the preliminary result of Souder *et al.* (1998) and the model calculation of Congleton and Truhlik (1996) we obtain, at $q^2 = -0.954m_{\mu}^2$, $g_p/g_p^{PCAC} = 0.40_{-0.73}^{+0.89}$, which implies that $g_p(-0.88m_{\mu}^2) = 3.3_{-6.1}^{+7.4}$. This result is consistent with PCAC and the $\mu^{-3}\text{He}$ capture data, but the experimental uncertainties are quite large.

C. Radiative muon capture in ${}^3\text{He}$

1. Theoretical calculations

Much less has been done on radiative muon capture in ${}^3\text{He}$ than on ordinary muon capture, though there have been calculations of the exclusive rate both in impulse approximation and elementary-particle model. Calculations in the elementary-particle model were made by Hwang and Primakoff (1978), who, however, made an incorrect assumption, and thus obtained incorrect results, and also by Fearing (1980), Klieb and Rood (1981), Klieb (1982), and Ho *et al.* (2002). For radiative muon capture, however, the elementary-particle model seems to be less reliable than for ordinary muon capture. The nuclear form factors are more rapidly varying than the nucleon form factors so that the gauge terms involving derivatives of the form factors (Adler and Dothan, 1966; Christillin and Servadio, 1977; Klieb, 1985; Ho *et al.*, 2002) are somewhat larger. Furthermore, as emphasized by Klieb and Rood (1984a, 1984b), some important terms involving intermediate state excitations are missed in the elementary-particle model.

The radiative muon capture rate has also been calculated in impulse approximation by Klieb and Rood (1981), Klieb (1982), and Ho *et al.* (2002). The earlier calculations used wave functions from the Reid soft core potential and made a number of approximations in evaluating the nuclear matrix elements. The later calcu-

¹⁵In both cases the polarizations were smaller than expected from atomic cascade calculations (Reifenröther *et al.*, 1987).

lation of Ho *et al.* (2002) improved on a number of these approximations, kept some additional terms, and used a variety of nuclear wave functions obtained from modern momentum space Faddeev calculations. The end results for the photon spectrum, however, were about the same as those of Klieb (1982), though the photon polarization was somewhat different, apparently because of the higher-order terms kept.

Typical results for the radiative muon capture statistical capture rate for photons with energies greater than 57 MeV are 0.17 s^{-1} in the impulse approximation and 0.25 s^{-1} in the elementary-particle model (Ho *et al.*, 2002). Just as for ordinary muon capture, the impulse approximation result is significantly below that obtained in the elementary-particle model, and presumably the difference is again at least partially explained by MEC's, which will be much more complicated here than they were for ordinary muon capture, and have not yet been calculated in detail. In view, however, of the problems with the elementary-particle model applied to ${}^3\text{He}$, as noted above, it is not possible to simply ascribe the difference just to MEC's. Such corrections will have to be calculated explicitly to finally obtain a reliable rate.

In principle the various breakup channels would give additional information, but to our knowledge there have not been any calculations of such channels for radiative muon capture.

2. Experimental results

In ${}^3\text{He}$ radiative muon capture the ${}^3\text{H}$ channel has a strong peaking at the recoil energy corresponding to the kinematic limit 1.9 MeV. In contrast, the energy spectra of charged particles from breakup channels are a broad continua reaching to 53 MeV and therefore are straightforwardly distinguished from ${}^3\text{He} \rightarrow {}^3\text{H}$.

While the ${}^3\text{He} \rightarrow {}^3\text{H}$ transition following ${}^3\text{He}$ radiative muon capture and the $p \rightarrow n$ transition following ${}^1\text{H}$ radiative muon capture are spin-isospin analogs, the ${}^3\text{He} \rightarrow {}^3\text{H}$ process is experimentally easier. First, the ${}^3\text{He}$ rate is much larger and consequently the background difficulties are greatly reduced. Second, the $\mu^3\text{He}$ atom circumvents the various chemical processes that confound muonic hydrogen. Of course, for ${}^3\text{He}$ radiative muon capture the presence of exchange currents and the contribution of breakup channels have to be considered.

The ${}^3\text{H}$ channel in ${}^3\text{He}$ radiative muon capture has recently been measured by Wright *et al.* (2000) at TRIUMF. In the experiment a μ^- beam was stopped in liquid ${}^3\text{He}$ and gamma-triton coincidences recorded. The photons were detected using a pair spectrometer and the tritons were detected via their scintillation light in the liquid helium. Pulse-shape readout permitted the discrimination of the incoming muon from the recoil triton. The detection efficiency was calibrated via π stops in liquid ${}^3\text{He}$, i.e., with the well-known branching ratios for $\pi^- {}^3\text{He} \rightarrow \gamma {}^3\text{H}$ and $\pi^- {}^3\text{He} \rightarrow \pi^0 {}^3\text{H}$.

In the ${}^3\text{He}$ radiative muon capture experiment the major photon backgrounds originate from muon decay in the target material, muon capture in the nearby ma-

terials, and pion contamination in the muon beam. However, energy cuts, i.e., $E_\gamma > 57 \text{ MeV}$, and timing cuts, i.e., $t_\gamma > 440 \text{ ns}$, together with the gamma-triton coincidence requirement, were effective in discriminating the ${}^3\text{He}$ signal from background processes. Note that the potential background from random coincidences of photons from radiative muon capture and tritons from ordinary muon capture was negligible.

Only preliminary results are presently available for the ${}^3\text{He}$ radiative muon capture experiment (Wright *et al.*, 2000). The results indicate that the shape of the measured ${}^3\text{He}$ radiative muon capture energy spectrum is consistent with the theoretical prediction of Klieb and Rood (1981), but that the overall magnitude is 20–30 % smaller than the impulse approximation prediction. To get agreement in magnitude Wright *et al.* (2000) stated that one needs $g_p = 3.4$, which is much smaller than the PCAC value.

We stress that the ${}^3\text{He} \rightarrow {}^3\text{H}$ radiative capture rate is potentially a very valuable data-point for the determination of g_p . We therefore urge the publication of the final result from the TRIUMF experiment and the undertaking of a modern impulse approximation plus exchange current calculation for the process.

VIII. OTHER FEW BODY PROCESSES

There have also been attempts to extract g_p from other processes, notably pion electroproduction. To do this Choi *et al.* (1993) measured the near threshold π^+ electroproduction at several momentum transfers. The connection to g_p was made via a low-energy theorem described by Vainshtein and Zakharov (1972) and reviewed by Dombey and Read (1973), Scherer and Koch (1991), and Drechsel and Tiator (1992). The theorem is valid in the limit of vanishing pion mass, so it had to be assumed that higher-order corrections were in fact small. Nevertheless, Choi *et al.* (1993) obtained results which they interpreted as $g_p(t)$ over a range of four-momentum transfer squared $0.07 < t < 0.18 \text{ GeV}^2$. These results agreed quite well with the predicted pion pole dominance and with the PCAC value near $t=0$.

It is clear that such an approach to “measuring” g_p is quite different than that described for ordinary and radiative muon capture above. In fact, there has been some disagreement over the question of whether or not pion electroproduction does in fact give new information about either g_p or g_a (Haberzettl, 2000, 2001; Bernard, Kaiser, and Meissner, 2001; Guichon, 2001; Truhlik, 2001; Fuchs and Scherer, 2003). While the consensus now seems to be that g_a is directly measurable, there is still disagreement as to what extent g_p can be obtained from electroproduction, with Bernard *et al.* (2002) claiming that g_p appears and Truhlik (2001) claiming that at least the g_p coupling arising directly from the axial current cancels.

In ordinary muon capture g_p is defined as a parameter in the most general form of the amplitude, so that a measurement of the rate gives directly information about g_p . In radiative muon capture this same ampli-

tude appears directly, albeit with one leg off shell and with additional gauge terms, some of which probe the interior structure of the amplitude. To the extent these are small, one again in radiative muon capture has an almost direct measurement of g_p .

In other processes, however, such as pion electroproduction, one needs to make a number of theoretical assumptions in order to make the connection to g_p . For example, both the low-energy theorem approach and detailed ChPT calculations (Bernard, Kaiser, Lee, and Meissner, 1994) are based on chiral symmetry, which implies the usual PCAC relation between g_a and g_p . Such a relation, at least in principle, allows one to eliminate or partially eliminate in a nonunique way one or the other of these couplings from the expressions for the amplitude. Alternatively in a Born approximation diagram approach, which is often used, a pion pole diagram is included. Within a theoretical framework such as ChPT this diagram is responsible for g_p . But the question still arises in what sense is a measurement of the importance of this pion exchange diagram an independent measurement of g_p , given that the relation between the two depends on the theory?

Truhlik (2001) has analyzed the problem, separating the direct contribution of g_p originating from the axial current from the contribution of the pion pole diagram. He finds, as found by two earlier calculations (Dombey and Read, 1973; Drechsel and Tiator, 1992) that the contributions arising from the g_p appearing in the axial current cancel, leaving just a pion pole contribution. He thus argues that electroproduction does not allow a measurement of g_p . In contrast in a ChPT approach such as (Bernard, Kaiser, Lee, and Meissner (1994); Bernard *et al.* (2002) the relation between the pion pole contribution and g_p is inherent in the theory, and so one naturally identifies a measurement of pion pole diagram with a measurement of g_p .

In any case, however, it is clear that the extraction of g_p from pion electroproduction is not as straightforward as in the ordinary muon capture case. To make a comparison with data, one has to assume a theoretical structure based on chiral symmetry which contains something equivalent to the PCAC relation between g_a and g_p , which is what is being tested. If the data agree with the prediction then one confirms the underlying theoretical framework and its prediction for g_p . If, however, the data disagree then it is not clear how one can logically extract a different value of g_p . This is in marked contrast to ordinary muon capture where a value of g_p can logically be extracted from essentially any experimental result.

In our view then processes such as pion electroproduction are very interesting, and very worth measuring. However, they provide primarily a consistency check on our understanding of the full underlying theory, rather than the kind of direct, independent measurement of g_p possible from ordinary muon capture.

It has been suggested also (Tkebuchava, 1978; Blokhintseva *et al.*, 1998) that the closely related process $\pi p \rightarrow ne^+e^-$ is also particularly sensitive to g_p .

Finally one should note that in the context of ChPT the calculations of ordinary muon capture give a relation between g_p and some of the low-energy constants (Fearing *et al.*, 1997; Bernard *et al.*, 1998; Ando *et al.*, 2000). Thus any process which contains these same low energy constants could be considered as a way of “measuring” g_p , but only within the context of ChPT.

IX. EXCLUSIVE ORDINARY MUON CAPTURE ON COMPLEX NUCLEI

Determining g_p from exclusive ordinary muon capture on complex nuclei is not easy. First, the reaction products are a ~ 100 -MeV neutrino and a ~ 0.1 -MeV recoil, and therefore the β rays or γ rays from the recoil’s decay must be detected. Second, the effects of g_p in ordinary muon capture are small and subtle, and therefore measurements of spin observables are usually required. Last, the observables are functions of both the weak couplings and the nuclear wave functions, and disentangling these contributions is unavoidably model dependent.

In allowed transitions on $J_i=0$ targets the $0p$ transition $^{12}\text{C}(0^+,0) \rightarrow ^{12}\text{B}(1^+,0)$ and $1s-0d$ transition $^{28}\text{Si}(0^+,0) \rightarrow ^{28}\text{Al}(1^+,2201)$ have attracted the most attention. In order to isolate the coupling g_p , the ^{12}C experiments have measured recoil polarizations via the ^{12}B β -decay and the ^{28}Si experiments have measured γ -ray correlations via the ^{28}Al γ decay. In allowed transitions on $J_i \neq 0$ targets the $0p$ nucleus ^{11}B and $1s-0d$ nucleus ^{23}Na have been studied. These experiments measured the hyperfine effect in $3/2^+ \rightarrow 1/2^+$ transitions to extract the coupling g_p . Last, the capture rate of the $^{16}\text{O}(0^+,0) \rightarrow ^{16}\text{N}(0^-,120)$ transition has been measured by several groups; since the $0^+ \rightarrow 0^-$ spin sequence offers special sensitivity to g_p .

The material on exclusive ordinary muon capture is organized as follows. In Sec. IX.B we describe the physical observables in partial transitions. In Sec. IX.C we discuss the dynamical content of the physical observables in ordinary muon capture and in Sec. IX.D we describe the specific manifestations of the coupling g_p in ordinary muon capture. The experimental work on exclusive transitions is covered in Sec. IX.E. In Secs. IX.F and IX.G, respectively, we review the theoretical framework and nuclear models for exclusive ordinary muon capture on complex nuclei. In Sec. IX.H we discuss the results for g_p .

One goal is a unified discussion and comparison of the different experiments and calculations. Another goal is a critical assessment of the current “best values” and model uncertainties in the extraction of the coupling g_p .

We do not discuss the related topic of total ordinary muon capture rates on complex nuclei. Although a large body of accurate data is nowadays available on total ordinary muon capture rates, because the total rate is weakly dependent on g_p and the model uncertainties in total rates are large, extracting g_p is not feasible. We point out though that total ordinary muon capture rates

are employed in analyzing the total rate of radiative capture on complex nuclei (see Sec. X).

A. Free couplings versus effective couplings

We first comment on the meaning of the coupling g_p that is extracted from partial transitions on complex nuclei, and specifically the issue of free nucleon coupling constants versus effective nucleon coupling constants.

Suppose one performed an exact calculation of the nuclear wave functions and the weak nuclear transition, i.e., incorporating every component that contributes significantly to the wave functions and every current that contributes significantly to the weak transition. Naturally the calculation would require a large number of states, a realistic interaction between nucleons, and inclusion of contributions from meson exchange and nucleon excitations. However, the calculation would involve the free values of weak couplings g_a , g_p , etc.

Unfortunately such calculations are feasible for few body systems only. In complex nuclei one considers only a limited number of active nucleons and a restricted set of basis states, and either completely neglects the non-nucleonic effects or includes the dominant contributions such as pion exchange and Δ excitation via perturbative techniques. In such calculations the various weak coupling constants are effective weak coupling constants, with their renormalization accounting for the missing components of the nuclear model. The use of effective proton and neutron charges is an example of this approach.

Herein our interest is the coupling g_p of the free proton. We therefore have tried to use the most realistic nuclear models available in order to extract the induced pseudoscalar coupling constant. For almost all cases we discuss there are complete $0p$, $1s-0d$ shell model calculations that include treatments of core polarization effects (i.e., the effects of truncating the model space) and non-nucleonic effects (e.g., the effects of pion exchange and Δ excitation). In this manner we have strived to come as close as possible to extracting from nuclear muon capture the free nucleon value g_p .

While outside this article's scope we briefly note a number of articles are available on the in-medium renormalization of the effective coupling g_p .¹⁶ Their approach involves embedding the non-nucleonic effects, e.g., pion exchange and Δ excitations, into the in-medium values of the weak couplings. For g_p the renormalization is attributed to modifications of the pion-nucleon coupling, the pion decay constant, and the pion propagator. In the earlier work of Ohta and Wakamatsu (1974), Delorme *et al.* (1976), Nyman and Rho (1977), Ericson (1978), and Rho (1978), the authors had focused on effects of the attractive p -wave part of the pion-

nucleon interaction and the resulting Δ -hole excitations. The calculations yielded a striking result, with a quenching of the coupling by factors of 2–3. Subsequently, however, Delorme and Ericson (1994) have claimed the effects from the attractive p -wave πN interaction are compensated by the repulsive s -wave πN interaction, and therefore the medium modification of the effective coupling g_p is much less. Further, Kirchbach and Riska (1994) have stressed the importance of considering the different renormalizations of g_p 's contributions to the space and time components of the weak current and the $\sigma \cdot \nu$ and $\sigma \cdot q$ terms in the weak Hamiltonian.

B. Physical observables

In muon capture the initial state is the $1S$ ground state of the muonic atom. Capture then yields a muon neutrino with momentum $\vec{\nu}$ and recoil nucleus with momentum $-\vec{\nu}$, i.e.,

$$\mu^- + [A, Z] \rightarrow [A, Z-1] + \nu. \quad (31)$$

For $J_i=0$ targets the total spin of the μ -atom is $F=1/2$, and for $J_i>0$ targets the possible spins of the μ atom are $F_{\pm}=J_i \pm 1/2$. On $J_i=0$ targets the necessary variables for describing capture are the μ -atom orientation, the recoil orientation and the neutrino direction. On $J_i>0$ targets the capture process is further dependent on the F state.

1. Capture rates

The easiest observable to experimentally determine is the capture rate of the partial transition. For $J_i=0$ targets we shall denote the capture rate by Λ and for $J_i>0$ targets we shall denote the hyperfine rates by Λ_{\pm} . In addition on $J_i>0$ targets it is useful to define the statistical rate,

$$\Lambda_S = \left(\frac{J_i+1}{2J_i+1} \right) \Lambda_+ + \left(\frac{J_i}{2J_i+1} \right) \Lambda_-, \quad (32)$$

where $(J_i+1)/(2J_i+1)$ and $J_i/(2J_i+1)$ are the statistical populations of the F_{\pm} hyperfine states.

2. Recoil asymmetries

Generally the direction of emission of recoils after capture is anisotropic about the μ -atom orientation axis.¹⁷ For $J_i=0$ targets the angular distribution for recoil emission is (Bernabeu, 1975; Mukhopadhyay, 1977; Ciechanowicz and Oziewicz, 1984)

$$\frac{d\Lambda}{d\Omega} = \frac{\Lambda}{4\pi} [1 + \alpha |\vec{P}_{\mu}| P_1(\hat{P}_{\mu} \cdot \hat{\nu})], \quad (33)$$

where \vec{P}_{μ} is the muon polarization, $\hat{\nu}$ is the neutrino direction, P_1 is the $\ell=1$ Legendre polynomial, and α is the asymmetry coefficient. Note that the recoil asymme-

¹⁶For example, see Ohta and Wakamatsu (1974), Delorme *et al.* (1976), Nyman and Rho (1977), Ericson (1978), Rho (1978), Bentz, Arima, and Baier (1990), Delorme and Ericson (1994), and Kirchbach and Riska (1994).

¹⁷An exception is the isotropic distribution of the recoil emission from a $F=0$ μ atom.

try is a pseudoscalar quantity, and therefore an example of parity violation in muon capture.

For $J_i > 0$ targets the angular distribution for recoil emission is generally more complicated. For example, a $F=1$ μ atom may possess both a vector polarization, i.e., nonstatistical populations of the $m_F = +1$ and $m_F = -1$ substates, and a tensor polarization, i.e., nonstatistical populations of the $|m_F|=1$ and $m_F=0$ substates. Consequently, for $F=1$ capture the angular distribution of recoil emission is (Galindo and Pascual, 1968; Ciechanowicz and Oziewicz, 1984; Congleton and Fearing, 1993)

$$\frac{d\Lambda}{d\Omega} = \frac{\Lambda}{4\pi} [1 + A_v |\vec{P}_\mu| P_1(\hat{P}_\mu \cdot \hat{\nu}) + A_t |\vec{P}_\mu| P_2(\hat{P}_\mu \cdot \hat{\nu})], \quad (34)$$

where A_v is the vector asymmetry coefficient and A_t is the tensor asymmetry coefficient. Note that for $F > 1$ atoms even higher ranks of μ -atom orientation are possible in principle.

We stress that \vec{P}_μ in Eq. (33) and Eq. (34) is the muon's residual polarization in the μ -atom ground state. Unfortunately in all targets the muon-nucleus spin-orbit interaction leads to substantial depolarization during the atomic cascade. For example, for $J_i = 0$ targets the residual polarization is typically 17%. Further in $J \neq 0$ targets the muon-nucleus spin-spin interaction leads to additional depolarization during the atomic cascade. The degree of depolarization is dependent on J_i and F . For further details, see Favart *et al.* (1970), Hambro and Mukhopadhyay (1975, 1977), Kadono *et al.* (1986), and Kuno *et al.* (1987).

3. Recoil orientations

Generally after muon capture the recoil nucleus is oriented, where orientation along both the ν -momentum axis and the μ -spin axis is possible. For a $J_f = 1/2$ recoil the orientation is described by its recoil polarization P , where $P = (p_{+1/2} - p_{-1/2}) / \sum p_m$ with p_m denoting the population of each magnetic substate m . For a $J_f = 1$ recoil the orientation is described by its polarization P and its alignment A , where $A = (p_{+1} + p_{-1} - 2p_0) / \sum p_m$. For $J_f > 1$ recoils even higher ranks of orientation are possible in principle. Conventionally the recoil orientation along the ν -momentum axis is designated the longitudinal polarization P_L and longitudinal alignment A_L , and the recoil orientation along the μ -spin axis is designated the average polarization P_{av} and average alignment A_{av} . The recoil polarizations, i.e., P_L and P_{av} , are pseudoscalar quantities and additional examples of parity violation in muon capture. For further details, see Devanathan *et al.* (1972), Bernabeu (1975), Subramanian *et al.* (1976), Mukhopadhyay (1977), and Subramanian and Devanathan (1979).

Additionally triple correlations of the recoil orientation with the μ -spin direction and the ν -momentum direction are possible. Of experimental importance are the so-called forward hemisphere and backward hemisphere polarizations. Defining the hemispheres relative to the μ -spin axis, P_F is the polarization along the μ axis for

the ‘‘forward hemisphere’’ recoils, and P_B is the polarization along the μ axis for the ‘‘backward hemisphere’’ recoils. Note that P_F and P_B are related to P_L and P_{av} via

$$P_F = \frac{1}{2} \left(P_{av} + \frac{1}{2} P_L \right), \quad (35)$$

$$P_B = \frac{1}{2} \left(P_{av} - \frac{1}{2} P_L \right), \quad (36)$$

which demonstrates their dependence on both the μ -spin direction and the ν -momentum direction.

4. Gamma-ray correlations

Gamma-ray directional correlations with the ν -momentum axis and the μ -spin axis in the sequence

$$\mu^- + [Z, A] \rightarrow [Z-1, A]^* + \nu \rightarrow [Z-1, A]^{**} + \gamma \quad (37)$$

are additional observables in partial transitions. Such correlations originate from the recoil orientation and the recoil asymmetry in the capture process. For unpolarized muons a γ - ν directional correlation is possible and for polarized muons a γ - ν - μ triple correlation is also possible. In discussing the correlations we shall denote the spin sequence in Eq. (37) by $J_i \rightarrow J_f \rightarrow j$ where J_i , J_f , and j are the angular momenta of the three nuclear states. Note that below we consider only unpolarized targets and $J_f \leq 1$ recoils. For further details, see Ciechanowicz and Oziewicz (1984).

For unpolarized muons $\vec{P}_\mu = 0$ the γ - ν directional correlation is given by¹⁸

$$W = 1 + a_2 P_2(\hat{k} \cdot \hat{\nu}), \quad (38)$$

where \hat{k} is the γ -ray direction, $\hat{\nu}$ is the neutrino direction, P_2 is the $\ell=2$ Legendre polynomial, and a_2 is the γ - ν correlation coefficient. Note that this directional correlation a_2 is a consequence of the longitudinal alignment A_L of the recoil nucleus in the capture process.

For polarized muons $\vec{P}_\mu \neq 0$ the γ - ν - μ triple correlation is given by

$$W = 1 + \left(\alpha + \frac{2}{3} c_1 \right) \vec{P}_\mu \cdot \hat{\nu} \hat{k} \cdot \hat{\nu} + (a_2 + b_2 \vec{P}_\mu \cdot \hat{\nu} \hat{k} \cdot \hat{\nu}) P_2(\hat{k} \cdot \hat{\nu}) \quad (39)$$

and contains three distinct correlation terms involving $(\alpha + \frac{2}{3} c_1)$, a_2 , and b_2 . Note in Eq. (39) that (i) \hat{k} enters only quadratically because of parity conservation in γ decays, (ii) \vec{P}_μ enters only linearly because the muon is spin 1/2, and (iii) $\hat{\nu}$ enters in powers of 2 or less for $J_f \leq 1$. In Eq. (39) the correlation involving α is a conse-

¹⁸The theory of γ -ray correlations was developed by Popov and co-workers in Popov (1963); Bukat and Popov (1964); Oziewicz and Popov (1965); Bukhvostov and Popov (1967a, 1967b, 1967c, 1970). See also Parthasarathy and Sridhar (1978) and Ciechanowicz and Oziewicz (1984).

quence of the recoil asymmetry and the correlation involving a_2 is a consequence of the longitudinal alignment. The remaining terms, i.e., c_1 and b_2 , originate from the triple correlation of the recoil alignment with \vec{P}_μ and $\hat{\nu}$. If either unpolarized muons, i.e., $\vec{P}_\mu=0$, or perpendicular geometry, i.e., $\vec{P}_\mu \cdot \hat{k}=0$, is employed the only nonvanishing correlation is a_2 , and Eq. (39) becomes Eq. (38).

It is important to recognize that c_1 , a_2 , and b_2 are functions of both the μ -capture process and the γ -decay process. For example, the coefficient a_2 may be written in the form of a product $A_L B_2$, where the alignment A_L is governed by the μ -capture process and the parameter B_2 is governed by the γ -decay process. A handy compilation of the coefficients B_2 for various $J_f \rightarrow j$ spin-parities, multipolarities, and mixing ratios is given in Table 1 of Ciechanowicz and Oziewicz (1984). Note that in certain cases, e.g., for $M1$ emission in a $1^+ \rightarrow 0^+$ decay, B_2 is large, but in other cases, e.g., for $M1$ emission in a $1^+ \rightarrow 2^+$ decay, B_2 is small. This makes the former $1^+ \rightarrow 0^+$ case more favorable, and the latter $1^+ \rightarrow 2^+$ case less favorable, for γ -ray correlation experiments.

C. Helicity representation

Herein we consider the overall dynamical content of exclusive ordinary muon capture. Utilizing the helicity representation we discuss the constraints imposed on μ capture by ν handedness and T invariance. We shall denote the corresponding helicity amplitudes by T_λ^F , where λ is the recoil helicity and F is the μ -atom hyperfine state. We use the superscript “+” for $F=J_i+1/2$ capture, the superscript “-” for $F=J_i-1/2$ capture, and no superscript for $J_i=0$ atoms. Assuming the absence of T violation in μ capture the helicity amplitudes are real numbers.

Further details on the helicity representation in the (μ, ν) reaction are given in Bernabeu (1975), Mukhopadhyay (1977), and Ciechanowicz and Oziewicz (1984).

1. Capture on zero-spin targets

For $J_i=0$ targets the helicity representation depicts muon capture as the two-body decay of a spin-1/2 μ atom into a left-handed neutrino and a spin- J_f recoil. Choosing the z axis along the ν axis, the definite neutrino helicity of $\lambda_\nu=-1/2$ means the allowable recoil helicities are $\lambda_f=0, +1$. The corresponding helicity amplitudes, denoted by T_0 and T_1 , are the underlying dynamical variables in μ capture on $J_i=0$ targets.

In Table IV we compile explicit formulas for various physical observables in $0 \rightarrow J_f$ transitions in terms of T_0 , T_1 and their ratio $X=\sqrt{2}T_0/T_1$. The γ -ray correlation coefficients also involve the quantity B_2 that is governed by the γ decay. With the exception of Λ , the reaction dynamics are completely determined by X , and consequently there exist numerous relations between observables in $0 \rightarrow J_f$ transitions; see, for example, Bernabeu (1975) and Mukhopadhyay (1977). Clearly although different observables offer alternative possibilities for ex-

TABLE IV. Helicity decomposition of physical observables in $0 \rightarrow 1$ transitions. We give the capture rate Λ , recoil asymmetry α , longitudinal polarization and alignment P_L and A_L , average polarization and alignment P_{av} and A_{av} , and γ -ray correlation coefficients a_2 , b_2 , and $(\alpha + \frac{2}{3}c_1)$. The helicity amplitudes for recoil helicities of $\lambda_f=0, +1$ are denoted by T_0 and T_1 and $X=\sqrt{2}T_0/T_1$. The parameter B_2 involved in the γ -ray correlations depends on the spin parities of the initial-final states and the multipolarity of the gamma radiation in the γ decay.

Observable	Helicity decomposition
Λ	$ T_1 ^2(2+X^2)$
α	$(X^2-2)/(X^2+2)$
P_L	$-2/(2+X^2)$
A_L	$2(1-X^2)/(2+X^2)$
P_{av}	$2/3(1+2X)/(2+X^2)$
A_{av}	0
$\alpha + \frac{2}{3}c_1$	$B_2\sqrt{2}(2+2X-X^2)/(2+X^2)$
a_2	$B_2\sqrt{2}(1-X^2)/(2+X^2)$
b_2	$B_2\sqrt{2}(1-2X+X^2)/(2+X^2)$

perimental measurements, the dynamical content of $0 \rightarrow J_f$ transitions is somewhat limited.

Note that the $0 \rightarrow 0$ sequence is a special case. Compared to $J_f > 0$, where the $\lambda_f=0, +1$ helicity states are allowable, for $J_f=0$, only the $\lambda_f=0$ helicity state is possible. Consequently a single amplitude T_0 is the sole dynamical quantity for physical observables in $0 \rightarrow 0$ transitions.

2. Capture on nonzero-spin targets

For $J_i > 0$ targets the helicity representation depicts capture as a two-body decay of the $F=J_i \pm 1/2$ μ atom. Based on definite neutrino handedness and angular momentum coupling the total number of recoil helicity states λ_f and contributing helicity amplitudes T_λ^F is the lesser of either $2J_f+1$ or $2F+1$ (Mukhopadhyay, 1977; Ciechanowicz and Oziewicz, 1984).

For concreteness let us consider the example of a $1/2 \rightarrow 1/2$ transition, where the μ -atom spin is either $F=0$ or $F=1$. For $F=1$ both the $\lambda_f=-1/2, +1/2$ recoil helicity states are populated, but for $F=0$ only the $\lambda_f=+1/2$ recoil helicity state is populated because of the single magnetic substate of the $F=0$ μ atom. Consequently, one helicity amplitude governs the $F=0$ capture, two helicity amplitudes govern the $F=1$ capture, and three dynamical variables underlie $1/2 \rightarrow 1/2$ transitions. By comparison in $3/2 \rightarrow 1/2$ transitions a total of four helicity amplitudes contribute, two for F_+ capture and two for F_- capture.

In summary for $J_i > 0$ targets many independent quantities are experimentally accessible. In principle the increased number of variables allows an increased number of cross checks on model calculations for $J_i > 0$ transitions.

D. Induced currents

Most often in partial transitions the leading contributions originate from the axial coupling g_a . This subsection concerns “where to find the coupling g_p .”

To answer this question we shall examine capture in (i) the $q/M \rightarrow 0$ limit, where q is the three-momentum transfer and M is the nucleon mass, and (ii) in the Fujii-Primakoff (FP) approximation (Fujii and Primakoff, 1959). In the $q/M \rightarrow 0$ limit the effects of g_p are absent. However, in the Fujii-Primakoff approximation, which keeps q/M terms involving allowed operators, but drops ℓ -forbidden and gradient operators, the leading effects of induced currents are present. Therefore comparison of the capture process in the $q/M \rightarrow 0$ limit and the Fujii-Primakoff approximation is helpful in understanding the manifestation of g_p in capture.

At this point it is helpful to recall the Fujii-Primakoff effective Hamiltonian for muon capture (Fujii and Primakoff, 1959; Primakoff, 1959). Its form is

$$\tau^+ \frac{\mathbf{1} - \boldsymbol{\sigma} \cdot \hat{\boldsymbol{\nu}}}{2} \sum_{i=1}^A \tau_i^- (G_V \mathbf{1} \cdot \mathbf{1}_i + G_A \boldsymbol{\sigma} \cdot \boldsymbol{\sigma}_i + G_P \boldsymbol{\sigma} \cdot \hat{\boldsymbol{\nu}} \boldsymbol{\sigma}_i \cdot \hat{\boldsymbol{\nu}}) \delta(\mathbf{r} - \mathbf{r}_i), \quad (40)$$

where $\mathbf{1}$, $\mathbf{1}_i$, $\boldsymbol{\sigma}$, and $\boldsymbol{\sigma}_i$ are the 2×2 unit and spin matrices and \mathbf{r} and \mathbf{r}_i are the spatial coordinates of the lepton and the i th nucleon, respectively, $\hat{\boldsymbol{\nu}}$ is the ν -momentum unit vector, and τ^+ , τ_i^- convert the muon into a neutrino and a proton into a neutron. Last, G_V , G_A , and G_P are the so-called Fujii-Primakoff effective couplings,

$$G_V = g_v \left(1 + \frac{q}{2M} \right), \quad (41)$$

$$G_A = - \left(g_a + \frac{q}{2M} (g_v + g_m) \right), \quad (42)$$

$$G_P = - \frac{q}{2M} (g_p - g_a + g_v + g_m). \quad (43)$$

Note that when $q/M \rightarrow 0$ the coupling G_P vanishes and G_V and G_A are determined by g_v and g_a , respectively. Furthermore, the induced currents are order q/M , and g_p appears in G_P only. For the canonical values of the weak couplings, as given in Table I (see Sec. II), $G_V = 1.00$, $G_A = -1.27$, and $G_P = 0.00$ in the $q/M \rightarrow 0$ limit, and $G_V = 1.03$, $G_A = -1.52$, and $G_P = -0.62$ in the Fujii-Primakoff approximation and with $q = 100$ MeV/ c .

1. Asymmetries, orientations, and correlations

To understand the g_p sensitivity of orientations, correlations, etc., we compare the terms with G_A and G_P in Eq. (40). Observe that the operator corresponding to the G_P term, i.e., $(\mathbf{1} - \boldsymbol{\sigma} \cdot \hat{\boldsymbol{\nu}}) \boldsymbol{\sigma} \cdot \hat{\boldsymbol{\nu}} \boldsymbol{\sigma}_i \cdot \hat{\boldsymbol{\nu}}$, cannot change the spin projection of either the lepton or the nucleon along the ν -momentum axis. However, this limitation does not apply to the G_A term and the operator $(\mathbf{1} - \boldsymbol{\sigma} \cdot \hat{\boldsymbol{\nu}}) \boldsymbol{\sigma} \cdot \boldsymbol{\sigma}_i$. Consequently in Eq. (40) the G_P term admits only a longitudinal coupling of the weak currents whereas the G_A term admits also a transverse coupling of the weak

TABLE V. Expressions and values of observables for $0^+ \rightarrow 1^+$ transitions in the $q/M \rightarrow 0$ limit and the Fujii-Primakoff approximation (FPA). G_A and G_P are the Fujii-Primakoff effective constants defined in Eqs. (42) and (43) and the common denominator is $\Gamma = (3G_A^2 + G_P^2 - 2G_A G_P)$. We tabulate the γ -ray directional correlations for the $0^+ \rightarrow 1^+ \rightarrow 0^+$ sequence.

Observable	FPA expression	$q/M \rightarrow 0$ value	FPA value
α	$(3G_A^2 + G_P^2 - 2G_A G_P)/\Gamma$	-0.33	-0.70
P_L	$-2G_A^2/\Gamma$	-0.67	-0.85
A_L	$(-2G_P^2 + 4G_A G_P)/\Gamma$	0.00	-0.55
P_{av}	$(2G_A^2 - \frac{4}{3} G_A G_P)/\Gamma$	0.67	0.61
A_{av}	0	0	0
$\alpha + \frac{2}{3} c_1$	$(3G_A^2 - G_P^2)/\Gamma$	1.0	1.21
a_2	$(-G_P^2 + 2G_P G_A)/\Gamma$	0.00	0.28
b_2	G_P^2/Γ	0.00	0.07

currents. This makes correlations, orientations, etc., sensitive to g_p/g_a . For further details, see Grenacs (1985).

To further illustrate the g_p sensitivity we consider the example of a $0^+ \rightarrow 1^+$ transition. In the $q/M \rightarrow 0$ limit the two helicity amplitudes, i.e., T_0 and T_1 , are both determined by the product of the coupling g_a and the allowed Gamow-Teller operator, and $X=1$. However in the Fujii-Primakoff approximation, the amplitude T_0 is proportional to $(G_A - G_P)$ and involves a longitudinal coupling of the weak currents, and the amplitude T_1 is proportional to G_A and involves a transverse coupling of the weak currents, and $X = (G_A - G_P)/G_A = 0.59$ for $q = 100$ MeV/ c . Therefore the asymmetries, correlations, and orientations, which are governed by X , permit the determination of g_p/g_a . For further details, see Mukhopadhyay (1977).

In Table V we compile Fujii-Primakoff approximation expressions for physical observables in $0^+ \rightarrow 1^+$ transitions in terms of G_A and G_P . Note that in the $q/M \rightarrow 0$ limit the recoil polarizations are $P_L = -2/3$ and $P_{av} = +2/3$ and the recoil alignments are $A_L = 0$ and $A_{av} = 0$, thus indicating that the recoil is “highly polarized” but “not aligned.” Most strikingly, in the Fujii-Primakoff approximation the longitudinal alignment $A_L = +0.55$ is very large and highly sensitive to g_p/g_a . This occurs because the alignment measures the difference in population of the $\lambda_f = 0$ recoil substate, which is populated by G_P , and the $\lambda_f = 1$ recoil substate, which is not populated by G_P . It therefore represents a golden observable for the spin structure of the induced coupling g_p .

2. Hyperfine dependences

The hyperfine dependence Λ_+/Λ_- of $\Delta J^\pi = J_f - J_i = \pm 1^+$ transitions in muon capture on $J_i \neq 0$ targets is also sensitive to the coupling g_p . Specifically in the multipole expansion of the Fujii-Primakoff Hamiltonian the G_A term makes allowed contributions to neutrino waves with total angular momentum $j^\pi = 1/2^+$ only, whereas

TABLE VI. Equations and values for selected observables in $3/2^+ \rightarrow 1/2^+$ transitions in the $q/M \rightarrow 0$ limit and Fujii-Primakoff approximation (FPA). The common denominator is $\Gamma = (24G_A^2 - 16G_A G_P + 3G_P^2)$.

Observable	FPA expression	$q/M \rightarrow 0$ value	FPA value
Λ_+/Λ_-	$3G_P^2/\Gamma$	0.00	0.027
α^-	$-\frac{1}{3}(4G_A - G_P)^2/\Gamma$	-0.22	-0.24
α^+	$\frac{2}{5}$	0.60	0.60
P_L^-	$(8G_A^2 - G_P^2)/\Gamma$	0.33	0.44
P_L^+	$\frac{1}{5}$	0.20	0.20

the G_P term makes allowed contributions to neutrino waves with total angular momentum $j^\pi = 3/2^+$ also. This difference is because of $\hat{\nu}$ in Eq. (40). In $\Delta J^\pi = +1^+$ transitions, neutrinos with $j = 1/2^+$ may be emitted in F_+ capture, but neutrinos with $j = 3/2^+$ must be emitted in F_- capture. This makes $\Lambda_+/\Lambda_- \gg 1$ and a strong function of the ratio g_p/g_a . However, in $\Delta J^\pi = -1^+$ transitions, neutrinos with $j = 1/2^+$ may be emitted in F_- capture, but neutrinos with $j = 3/2^+$ must be emitted in F_+ capture. This makes $\Lambda_+/\Lambda_- \ll 1$ and a strong function of the ratio g_p/g_a .

For example, we consider the important case of $3/2^+ \rightarrow 1/2^+$ transitions. In the $q/M \rightarrow 0$ limit, capture from the $F_- = 1$ hyperfine state is governed by g_a but capture from the $F_+ = 2$ hyperfine state is forbidden. Therefore $\Lambda_+/\Lambda_- = 0$. However, in the Fujii-Primakoff approximation, the two F_+ helicity amplitudes are proportional to G_P while the two F_- helicity amplitudes are proportional to either $(4G_A - G_P)$ or $(2G_A - G_P)$. Consequently the hyperfine dependence Λ_+/Λ_- is highly dependent on g_p/g_a .

The Fujii-Primakoff approximation expressions for various observables in $3/2^+ \rightarrow 1/2^+$ transitions are given in Table VI. In passing we mention that the asymmetries, correlations, and orientations in F_- capture for $3/2^+ \rightarrow 1/2^+$ transitions are also sensitive to the coupling g_p , for the same reasons as described for the $0^+ \rightarrow 1^+$ transitions in the preceding section, Sec. IX.D.1. This is not true for the case of asymmetries, correlations, and orientations for F_+ capture in $3/2^+ \rightarrow 1/2^+$ transitions, because only $j^\pi = 3/2^+$ neutrino emission is possible.

Related Fujii-Primakoff approximation expressions for other $\Delta J^\pi = \pm 1^+$ transitions are given, for example, by Mukhopadhyay (1977) and Ciechanowicz and Oziewicz (1984).

3. Capture rates

In general, in μ capture the rate Λ has a fairly weak dependence on the coupling g_p . For example, in $0^+ \rightarrow 1^+$ transitions the contribution of g_p is typically 10%. However, an exception is the capture rate of the first-forbidden $0^+ \leftrightarrow 0^-$ transition.

To understand the sensitivity it is instructive to assume the dominance of the $\ell = 1$ retarded Gamow-Teller operator in the first-forbidden $0^+ \rightarrow 0^-$ transition, i.e.,

ignoring the contribution from the axial charge operator. For details, see Towner and Khanna (1981). The capture rate in $0^+ \rightarrow 0^-$ transitions is then governed by the coupling constant combination $(G_A - G_P)$, which is strongly dependent on g_p . For example, in going from $g_p = 0$ to $g_p = 6.7g_a$ the rate is increased by roughly 50%. In short, the quantum numbers of the $\Delta J^\pi = 0^-$ multipole are effective in isolating the longitudinal contributions to weak currents, such as g_p .

E. Experimental studies of partial transitions

This subsection concerns the experimental work on exclusive ordinary muon capture. We discuss two allowed transitions on $J_i = 0$ targets, $^{12}\text{C}(0^+, 0) \rightarrow ^{12}\text{B}(1^+, 0)$ and $^{28}\text{Si}(0^+, 0) \rightarrow ^{28}\text{Al}(0^+, 2201)$, two allowed transitions on $J_i \neq 0$ targets, $^{11}\text{B}(3/2^-, 0) \rightarrow ^{11}\text{Be}(1/2^-, 320)$ and $^{23}\text{Na}(3/2^+, 0) \rightarrow ^{23}\text{Ne}(1/2^+, 3458)$, and the first-forbidden transition $^{16}\text{O}(0^+, 0) \rightarrow ^{16}\text{N}(0^-, 120)$. The experiments include measurements of capture rates, recoil orientations, γ -ray correlations, and hyperfine dependences.

1. $^{12}\text{C}(0^+, 0) \rightarrow ^{12}\text{B}(1^+, 0)$

The $^{12}\text{C}(0^+, 0) \rightarrow ^{12}\text{B}(1^+, 0)$ reaction is an allowed Gamow-Teller transition between the spin-0 isoscalar ^{12}C ground state and the spin-1 isovector ^{12}B ground state. The transition was first observed in cosmic-ray data by Godfrey (1953) via the identification of the Godfrey-Tiomino cycle, i.e., μ capture on ^{12}C followed by β decay of ^{12}B .

The first investigation of the recoil polarization in the $^{12}\text{C}(0^+, 0) \rightarrow ^{12}\text{B}(1^+, 0)$ transition was conducted by Love *et al.* (1959) in order to measure the μ^- helicity in π^- decay. The application of polarization measurements to induced currents was pioneered by Possoz *et al.* (1977, 1974) at Saclay and extended by Roesch, Schlumof, *et al.* (1981), Roesch, Telegdi, *et al.* (1981), and Truttman *et al.* (1979) at PSI. Using ingenious techniques these researchers have amassed impressive data on several polarization observables in $^{12}\text{C}(0^+, 0) \rightarrow ^{12}\text{B}(1^+, 0)$ capture. More recently Kuno *et al.* (1984, 1986) at the BOOM facility have polished some techniques and remeasured the polarization P_{av} .

The procedure for measuring the polarization P_{av} of ^{12}B recoils from ^{12}C capture is straightforward in principle. First one makes polarized $\mu^-^{12}\text{C}$ atoms by stopping polarized muons in carbon-containing material. Next the polarized $\mu^{12}\text{C}$ atoms produce the polarized ^{12}B recoils via muon capture. Then one measures the ^{12}B β -ray asymmetry to determine the recoil polarization P_{av} . Note that the method relies on the known correlation of the ejected β rays with the ^{12}B orientation. Also note that this method gives the average polarization P_{av} , i.e., along the μ axis, not the longitudinal polarization P_L , i.e., along the ν axis.

Unfortunately, the measurement of P_{av} is difficult in practice. First, the muon polarization is largely destroyed via the spin-orbit interaction in the atomic cas-

cade. Second, the ^{12}B polarization is easily destroyed by the spin-spin interaction in the host material. Third, only about 1% of μ stops in ^{12}C undergo the $^{12}\text{C}(0^+,0) \rightarrow ^{12}\text{B}(1^+,0)$ transition (Reynolds *et al.*, 1963; Maier *et al.*, 1964). Consequently, the beta-ray asymmetries are small, the target choices are limited, and backgrounds are troublesome. Fortunately the short 29-ms lifetime and high 15-MeV end point for ^{12}B beta decay are ideally suited to a measurement of the polarization.

Average polarization measurements have been performed by Possoz *et al.* (1974, 1977) at Saclay and Kuno *et al.* (1984, 1986) at BOOM. The basic setup comprises a beam telescope for detecting incoming muons, beta-ray counters for detecting ^{12}B decays, and Michel counters for detecting μ decays. Possoz *et al.* (1974, 1977) found that a ≥ 0.3 -kG longitudinal B field and a graphite target were sufficient to preserve the ^{12}B polarization for $t > 29$ ms. Note that the distinctive lifetime/end point are used to identify the ^{12}B β rays and their forward/backward count rates are used to determine the ^{12}B β asymmetry. Pulsed-beam operation allows beta-ray detection under beam-off conditions and reduces the backgrounds. Transverse-field precession of the μ spin is used to measure the muon polarization P_μ .

One challenge is the experimental determination of a small β -ray asymmetry ($\sim 3\%$) with a reasonable accuracy ($\pm 10\%$). Consequently false asymmetries, such as geometrical and instrumental effects, must be minimized and then measured. Possoz *et al.* (1974, 1977) used a polarization preserving target material (graphite) and a polarization destroying target (polyethylene) to determine false asymmetries. Kuno *et al.* (1984, 1986) used a novel magnetic resonance technique to periodically destroy the muon polarization.

In summary, the resulting values of the average polarization were $P_{av} = 0.38 \pm 0.07$ from Possoz *et al.* (1974), $P_{av} = 0.452 \pm 0.042$ from Possoz *et al.* (1977), $P_{av} = 0.462 \pm 0.053$ from Kuno *et al.* (1984, 1986). We discuss the extraction of g_p from P_{av} in Sec. IX.H.1.

Additionally the forward (P_F) and backward (P_B) polarizations, defined in Eqs. (35) and (36), for the $^{12}\text{C}(0^+,0) \rightarrow ^{12}\text{B}(1^+,0)$ transition have been measured by Truttman *et al.* (1979) and Roesch, Telegdi, *et al.* (1981). These experiments are masterpieces of ingenuity and technique.

The experiments employed a novel target with recoil direction sensitivity. The targets comprised a multilayer sandwich of "triple foils" with each triple foil comprising a carbon target foil (C), a polarization preserving foil (P), and a polarization destroying foil (D). Arranging the P foil upstream and D foil downstream of the carbon foil, i.e., DCP, permits selective retention of the forward hemisphere recoil polarization. Arranging the D foil upstream and P foil downstream of the carbon foil, i.e., PCD, permits selective retention of the backward hemisphere recoil polarization. Thereby β -ray asymmetry measurements for the DCP configuration yield P_F and the PCD configuration yield P_B . Additionally a PCP

sandwich enables the measurement of the average polarization and a DCD sandwich enables the measurement of the false asymmetries.

One advantage of measuring $P_{F/B}$ is a larger recoil polarization and a larger beta-ray asymmetry.¹⁹ Another advantage is that combining both P_F and P_B to deduce P_{av}/P_L via

$$\frac{P_{av}}{P_L} = 2 \frac{P_F + P_B}{P_F - P_B} \quad (44)$$

reduces the sensitivity to false asymmetries and systematic uncertainties. Note that the measurements of P_F and P_B are achieved by simply rotating the multilayer target by 180° .

However, a major challenge in measuring $P_{F/B}$ is the small quantity of the ^{12}C material in the multilayer target, since the carbon foils must be thin enough for recoils to emerge and the P/D foils must be thick enough for recoils to stop. Consequently, any ^{12}B background from μ^- stops in nearby carbon is especially perilous. Therefore Truttman *et al.* (1979) and Roesch, Telegdi, *et al.* (1981) took great care to avoid using any carbon-containing materials in the neighborhood of the experiment. Based on these data the authors obtained $P_{av}/P_L = -0.516 \pm 0.041$.

In Table VII we summarize the various measurements of recoil polarizations in $^{12}\text{C}(0^+,0) \rightarrow ^{12}\text{B}(1^+,0)$. Note we quote all results in terms of the helicity amplitude ratio X so as to facilitate their comparison. The experimental results are mutually consistent.

We stress the experimental results for P_{av} and $P_{F/B}$ are for muon capture to all bound states in the ^{12}B nucleus. Therefore a correction is necessary to obtain the interesting ground-state polarization from the observed bound-state polarization. Measurements of the total rate to bound states (Reynolds *et al.*, 1963; Maier *et al.*, 1964) and the individual rates to excited states (Budyashov *et al.*, 1970; Miller *et al.*, 1972a; Giffon *et al.*, 1981; Roesch, Schlumpf, *et al.*, 1981) are employed to determine this correction.

Unfortunately, the γ -ray measurements of μ capture to individual ^{12}B excited states are complicated by near equal energies of several Doppler broadened γ rays.²⁰ Furthermore, the latest results of Roesch, Schlumpf, *et al.* (1981) and earlier results of Budyashov *et al.* (1970), Miller *et al.* (1972a), and Giffon *et al.* (1981) are in disagreement, and consequently there exists some uncertainty in the correction for the capture to the ^{12}B excited states. For a detailed discussion of the experimental data, see Measday (2001). Using the γ -ray yields from Giffon *et al.* (1981) and the model calculations of Fukui *et al.* (1987), the world average for X in

¹⁹Recall from Sec. IX.B.3 that $P_{F/B}$ have contributions from both P_{av} , which is decreased by μ depolarization, and from P_L , which is unchanged by μ depolarization.

²⁰Specifically (i) the 947-keV ($2620 \rightarrow 1674$) and 953-keV ($953 \rightarrow 0$) gamma-ray lines and (ii) the 1668-keV ($2620 \rightarrow 953$) and 1674-keV ($1674 \rightarrow 0$) gamma-ray lines.

TABLE VII. Compilation of results from the recoil polarization experiments for the transition $^{12}\text{C}(0^+,0) \rightarrow ^{12}\text{B}(1^+,0)$. The results are presented in terms of the dynamical parameter $X = \sqrt{2}T_0/T_1$. They incorporate the corrections for capture to ^{12}B bound excited states using the γ -ray data from Giffon *et al.* (1981) in column 3 and Roesch, Schlumpf, *et al.* (1981) in column 4. The experimental observables are listed in the second column and the Fujii-Primakoff estimate for X is given in the last row.

Ref.	Obs.	X using Giffon <i>et al.</i> (1981)	X using Roesch, Schlumpf, <i>et al.</i> (1981)
Possoz <i>et al.</i> (1974)	P_{av}	0.10 ± 0.11	0.08 ± 0.11
Possoz <i>et al.</i> (1977)	P_{av}	0.22 ± 0.07	0.20 ± 0.07
Roesch, Telegdi, <i>et al.</i> (1981)	$P_{F/B}$	0.27 ± 0.07	0.24 ± 0.07
Kuno <i>et al.</i> (1984)	P_{av}	$0.23^{+0.10}_{-0.08}$	$0.21^{+0.10}_{-0.08}$
FPA		0.59	0.59

$^{12}\text{C}(0^+,0) \rightarrow ^{12}\text{B}(1^+,0)$ is 0.23 ± 0.06 . However, using the γ -ray yields from Roesch, Schlumpf, *et al.* (1981) and the model calculations of Fukui *et al.* (1987), the world average for X in $^{12}\text{C}(0^+,0) \rightarrow ^{12}\text{B}(1^+,0)$ is 0.20 ± 0.06 . Fortunately the corrections are not too large.

2. $^{11}\text{B} \rightarrow ^{11}\text{Be}$ and $^{23}\text{Na} \rightarrow ^{23}\text{Ne}$

Historically studies of the hyperfine effect in nuclear muon capture reaction were important in demonstrating the V - A structure of weak interactions. These experiments were performed in muonic ^{19}F by Culligan *et al.* (1961) and Winston (1963). The first application of the hyperfine effect to the induced coupling g_p was conducted by Deutsch, Grenacs, Lehmann, *et al.* (1968) in muonic ^{11}B . Recently Wiaux *et al.* (2002) at PSI have improved the data on ^{11}B , and Johnson *et al.* (1996) at TRIUMF have extended the data to ^{23}Na .

Recall from Sec. IX.B.1 that the $1S$ ground state of a $J_i \neq 0$ μ atom is a hyperfine doublet with a spin $F_{\pm} = J_i \pm 1/2$. These states are split by the spin-spin interaction of the muon-nucleus magnetic moments. For a positive nuclear magnetic moment the F_- state is the true atomic ground state and for a negative nuclear magnetic moment the F_+ state is the true atomic ground state.

The two hyperfine states are initially populated with statistical weights, i.e., $n_+ = (J_i + 1)/(2J_i + 1)$ and $n_- = J_i/(2J_i + 1)$.²¹ Thereafter hyperfine transitions from the upper F state to the lower F state occur by $M1$ -Auger emission, changing the relative occupancies of the hyperfine states. The rate Λ_h of hyperfine conversion by Auger emission is governed by (i) the wave-function overlap of the electron and the μ atom, and (ii) the relative sizes of the electron binding and the hyperfine splitting. The wave-function overlap leads to a systematic increase in Λ_h with Z whereas the electron binding leads to sudden decreases in Λ_h at $Z \sim 6$, where K -shell emission is forbidden, and $Z \sim 18$, where L -shell emission is forbidden. A detailed account of hyperfine

conversion by Auger emission is given by Winston (1963) and experimental determinations of conversion rates have generally confirmed the calculated rates (Suzuki *et al.*, 1987; Gorringer *et al.*, 1993; Measday, 2001). Most importantly for investigating g_p , there exist a handful of μ atoms with comparable hyperfine transition and muon disappearance rates, e.g., ^{11}B , ^{19}F , ^{23}Na , and ^{35}Cl .

Telegdi (1959) was first to recognize that the hyperfine conversion during the μ -atom lifetime would alter the muon occupancy of the F states, and modify the time spectrum of the capture products, and thus permit the determination of the hyperfine dependence Λ_+/Λ_- . Formulas for the time evolution of capture products in the presence of hyperfine conversion have been published by several authors. For the case of a positive nuclear magnetic moment, e.g., ^{11}B and ^{23}Na ,

$$\frac{dN}{dt} \propto e^{-\Lambda_D^- t} \left[\left(\frac{n_-}{n_+} + \frac{\Lambda_h}{\Lambda_h + \Delta\Lambda_D} \right) + \left(\frac{\Lambda_+}{\Lambda_-} - \frac{\Lambda_h}{\Lambda_h - \Delta\Lambda_D} \right) e^{-(\Lambda_h + \Delta\Lambda_D)t} \right], \quad (45)$$

where n_+, n_- and Λ_+, Λ_- are the initial populations and the capture rates of the F_+, F_- hyperfine states, Λ_D^- is the F_- state disappearance rate, $\Delta\Lambda_D = \Lambda_D^+ - \Lambda_D^-$ is the hyperfine disappearance increment, and Λ_h the hyperfine conversion rate. In almost all cases of interest $\Lambda_h \gg \Delta\Lambda_D$ and therefore the factor $\Lambda_h/(\Lambda_h \pm \Delta\Lambda_D)$ is close to unity.

As discussed in Sec. IX.D.2 the hyperfine dependence Λ_+/Λ_- of partial transitions with $\Delta J^\pi = \pm 1^+$ spin sequences is especially sensitive to g_p . Equation (45) demonstrates clearly that the hyperfine dependence Λ_+/Λ_- in such capture is encoded in the time spectrum of the reaction products.

The $^{11}\text{B}(3/2^-,0) \rightarrow ^{11}\text{Be}(1/2^-,320)$ reaction is a $\Delta J^\pi = 1^+$ allowed transition from the ^{11}B ground state to the 320-keV ^{11}B first-excited state. The 320-keV, $1/2^-$ ^{11}Be excited state decays by γ emission ($\tau = 115 \pm 10$ fs) to the ^{11}Be ground state, and the ^{11}Be $1/2^+$ ground state decays by β emission ($\tau = 13.81 \pm 0.08$ s) to the ^{11}B ground state. For reference, the ^{11}B disappearance rate is $\Lambda_D = (0.4787 \pm 0.0008) \times 10^6 \text{ s}^{-1}$ (Wiaux *et al.*, 2002) and the

²¹The exception is the use of a polarized target and a polarized beam (Hambro and Mukhopadhyay, 1977; Mukhopadhyay, 1977).

^{11}B hyperfine transition rate is $\Lambda_h = (0.181 \pm 0.016) \times 10^6 \text{ s}^{-1}$ (Wiaux *et al.*, 2002).

One nice feature in the experimental study of the hyperfine effect in the $^{11}\text{B}(3/2^-, 0) \rightarrow ^{11}\text{Be}(1/2^-, 320)$ transition is the level structure of the ^{11}Be nucleus. Since the only particle-stable states are the $1/2^+$ ground state and the $1/2^-$ excited state this minimizes any concerns of cascade feeding from muon capture to higher-lying ^{11}Be states. However, one difficulty is the very low rate for the $^{11}\text{B}(3/2^-, 0) \rightarrow ^{11}\text{Be}(1/2^-, 320)$ transition, with only about 0.2% of μ stops in ^{11}B undergoing this reaction.

Two $^{11}\text{B}(3/2^-, 0) \rightarrow ^{11}\text{Be}(1/2^-, 320)$ measurements, the pioneering work by Deutsch, Grenacs, Lehmann, *et al.* (1968) at CERN and the recent work by Wiaux *et al.* (2002) at PSI, have been performed. Both counted incoming muons in a plastic scintillator beam telescope, detected outgoing γ rays in a high-resolution Ge detector, and used a natural isotopic abundance boron target. The 320-keV γ -ray signal-to-noise ratio was 1:2 in the earlier Deutsch, Grenacs, Lehmann, *et al.* (1968) experiment and 5:1 in the later Wiaux *et al.* (2002) experiment.

Both experiments fit their 320-keV γ -ray time spectra to the time dependence of Eq. (45) in order to extract Λ_+/Λ_- . The instrumental time resolutions were determined via muonic x rays and the continuum backgrounds were subtracted via neighboring energy windows. Wiaux *et al.* (2002) analyzed both the 320-keV γ -ray time spectrum and the Michel time spectrum in order to reduce the correlations between Λ_D , Λ_h , and Λ_+/Λ_- . For $^{11}\text{B}(3/2^-, 0) \rightarrow ^{11}\text{Be}(1/2^-, 320)$ the Deutsch, Grenacs, Lehmann, *et al.* (1968) experiment yielded $\Lambda_+/\Lambda_- < 0.26$ and the Wiaux *et al.* (2002) experiment yielded $\Lambda_+/\Lambda_- = 0.028 \pm 0.021$. These experiments clearly demonstrate the strong dependence of the capture process on the hyperfine state.

In allowed capture on ^{23}Na nuclei a large fraction of Gamow-Teller strength is to several levels in the energy region 1–4 MeV (Siebels *et al.*, 1995). In particular two $\Delta J^\pi = -1^+$ reactions, $^{23}\text{Na}(3/2^+, 0) \rightarrow ^{23}\text{Ne}(1/2^+, 1017)$ and $^{23}\text{Na}(3/2^+, 0) \rightarrow ^{23}\text{Ne}(1/2^+, 3458)$, exhaust a sizable fraction of Gamow-Teller strength. For reference, the ^{23}Na disappearance rate is $\Lambda_D = (0.831 \pm 0.002) \times 10^6 \text{ s}^{-1}$ (Suzuki *et al.*, 1987) and the ^{23}Na hyperfine conversion rate is $\Lambda_h = (15.5 \pm 1.1) \times 10^6 \text{ s}^{-1}$ (Gorringer *et al.*, 1994).

Compared to ^{11}B , in ^{23}Na (i) the capture rates are considerably larger, and (ii) the hyperfine rate and disappearance rate are more readily distinguished, thus making the measurement more straightforward. However, the large number of ^{23}Ne states, and greater fragmentation of Gamow-Teller strength, means that cascade feeding from higher-lying levels to lower-lying levels is a worry.

The study of the hyperfine effect in the $\mu^{23}\text{Na}$ atoms was conducted at TRIUMF (Gorringer *et al.*, 1994; Johnson *et al.*, 1996). Incident muons were counted in a plastic scintillator telescope and stopped in a sodium metal target. Emerging γ rays were detected in high-purity Ge detectors with surrounding NaI Compton suppressors. For $^{23}\text{Na}(3/2^+, 0) \rightarrow ^{23}\text{Ne}(1/2^+, 1017)$ and

$^{23}\text{Na}(3/2^+, 0) \rightarrow ^{23}\text{Ne}(1/2^+, 3458)$ the measurement yielded $\Lambda_+/\Lambda_- = 0.18 \pm 0.03$ and $\Lambda_+/\Lambda_- \leq 0.19$ and revealed a very large hyperfine effect. Note that in analyzing their data the authors had to account for the direct production and the indirect production of the 1017-keV γ rays. For more details on the interpretation of their data, see Johnson *et al.* (1996).

3. $^{16}\text{O}(0^+, 0) \rightarrow ^{16}\text{N}(0^-, 120)$

The $^{16}\text{O}(0^+, 0) \rightarrow ^{16}\text{N}(0^-, 120)$ transition is a first forbidden transition from the $J_i^\pi = 0^+$, ^{16}O ground state to the $J_f^\pi = 0^-$, ^{16}N metastable state. As discussed in Sec. IX.D.3 the capture rates of $\Delta J^\pi = 0^-$ transitions are especially sensitive to the longitudinal component of the axial current, and hence to g_p . The ^{16}N level structure comprises four particle-stable bound states: the $(2^-, 0)$ ground state and $(0^-, 120)$, $(3^-, 298)$, and $(1^-, 397)$ excited states. Note that the $^{16}\text{N}(0^-, 120)$ state decays, with a half-life $t_{1/2} = 5.25 \mu\text{s}$, both by γ -ray emission to the $^{16}\text{N}(2^-, 0)$ ground state and by β -ray emission to the $^{16}\text{O}(0^+, 0)$ ground state. Also note that the dominant decay of the 1^- , ^{16}N state is via γ -ray cascade through the 0^- , ^{16}N state.

One experimental difficulty is the low rate of the $^{16}\text{O}(0^+, 0) \rightarrow ^{16}\text{N}(0^-, 120)$ transition. This difficulty is compounded by the low energy of the deexcitation γ ray, resulting in large backgrounds from Michel bremsstrahlung and Compton scattering. Furthermore, because of the metastability of the $^{16}\text{N}(0^-, 120)$ state, the 120-keV γ -ray time spectrum is a convolution of the $1.8\text{-}\mu\text{s}$ ^{16}O lifetime and the $5.2\text{-}\mu\text{s}$ $^{16}\text{N}(0^-, 120)$ lifetime. Consequently, some care is needed in applying μ -stop timing gates as the 120-keV ^{16}N γ ray and other ^{16}N γ rays are impacted differently. Last, the feeding of the $^{16}\text{N}(0^-, 120)$ level from the $^{16}\text{N}(1^-, 398)$ level also complicates the extraction of Λ .

The first experimental studies of $^{16}\text{O} \rightarrow ^{16}\text{N}$ partial transitions were conducted by Cohen *et al.* (1963, 1964) and Astbury *et al.* (1964) in the early 1960s. The experiments detected the deexcitation γ rays from ^{16}N excited states using NaI detectors. Unfortunately, because of the limited resolution of the NaI detectors, they suffered from poor signal-to-noise and unidentified background lines. Consequently, from the late 1960s to the late 1970s a further series of γ -ray experiments were conducted using Ge detectors by Deutsch *et al.* (1969), Kane *et al.* (1973), and Guichon *et al.* (1979).

The experimental results for μ capture rates to ^{16}N bound states are summarized in Table VIII. All experiments indicate substantial capture to the 2^- ground state, some capture to the 0^- and 1^- excited states, and negligible capture to the 3^- excited state. Unfortunately, measurement-to-measurement discrepancies of a factor of 2 are apparent for $^{16}\text{O}(0^+, 0) \rightarrow ^{16}\text{N}(0^-, 120)$. Probably one should reject the early measurements with NaI detectors due to poor resolution and thus uncertain backgrounds. Further, the peculiar time dependence of the interesting 120-keV γ ray is probably the origin of

TABLE VIII. Muon capture rates in ^{16}O to the $(0^-, 120)$ and $(1^-, 397)$ excited states of ^{16}N from the published results of Cohen *et al.* (1963), Astbury *et al.* (1964), Deutsch *et al.* (1969), Kane *et al.* (1973), and Guichon *et al.* (1979) in units of $\times 10^3 \text{ s}^{-1}$. No evidence was found for production of the $^{16}\text{N}(3^-, 298)$ excited state.

Ref.	$0^+ \rightarrow 0^-$	$0^+ \rightarrow 1^-$
Cohen <i>et al.</i> (1963)	1.1 ± 0.2	1.7 ± 0.1
Astbury <i>et al.</i> (1964)	1.6 ± 0.2	1.4 ± 0.2
Deutsch <i>et al.</i> (1969)	$0.85^{+0.15}_{-0.060}$	$1.85^{+0.36}_{-0.17}$
Kane <i>et al.</i> (1973)	1.56 ± 0.18	1.31 ± 0.11
Guichon <i>et al.</i> (1979)	1.50 ± 0.11	1.27 ± 0.09

disagreement between the early studies of Deutsch *et al.* (1969) and later studies of Kane *et al.* (1973) and Guichon *et al.* (1979). In the later experiments special efforts were made to tackle this difficulty. Kane *et al.* (1973) employed a continuous beam without a μ -stop time gate and Guichon *et al.* (1979) employed a pulsed beam with a long μ -stop time gate. These experiments, using different timing techniques and yielding consistent results, give a mean value for the $^{16}\text{O}(0^+, 0) \rightarrow ^{16}\text{N}(0^-, 0)$ rate of $\Lambda = 1520 \pm 100 \text{ s}^{-1}$.

4. $^{28}\text{Si}(0^+, 0) \rightarrow ^{28}\text{Al}(1^+, 2201)$

The study of g_p by measurement of γ -ray angular correlations in $\mu^- [A, Z] \rightarrow \nu [A, Z-1]^* \rightarrow \gamma [A, Z-1]**$ transitions was originally proposed by Popov and co-workers.²² The authors examined γ -ray correlations in allowed and forbidden transitions on $J=0$ and $J \neq 0$ targets, and emphasized the g_p sensitivity of the $0^+ \rightarrow 1^+ \rightarrow 0^+$ spin sequence.

An experimental method for γ -ray correlation measurements was subsequently suggested by Grenacs *et al.* (1968). The method exploits the Doppler energy shift of nuclear γ ray from in-flight decay. To illustrate the method we consider a recoil nucleus with a γ -decay lifetime denoted by τ and a stopping time denoted by τ_S (the stopping time is typically ~ 0.5 ps in medium-weight nuclei). If $\tau \ll \tau_S$ the recoil is in motion as it decays and consequently the γ -ray energy is Doppler shifted by

$$\frac{\Delta E}{E_o} = \frac{E - E_o}{E_o} = \beta \cos \theta, \quad (46)$$

where E_o is the γ -ray energy in the recoil reference frame, E is the γ -ray energy in the laboratory reference frame, $\beta = v/c$ is the velocity of the recoil in the laboratory, and θ is the angle between the γ ray and the recoil momentum. As a consequence of Eq. (46) the energy spectra of nuclear γ rays from muon capture are Doppler broadened when $\tau \ll \tau_S$. Further, the exact line shape of the Doppler spectrum is a function of the cor-

relations between the γ ray, recoil, and μ -spin directions. As recognized by Grenacs *et al.* (1968), this permits a determination of the γ -ray correlation coefficients by measurement of the γ -ray Doppler energy spectrum.

Two experimental configurations for correlation measurements have special significance. In the first arrangement, the γ - ν configuration, the experiment is conducted with either unpolarized muons or perpendicular geometry, so that $\vec{P}_\mu \cdot \hat{k} = 0$ where \hat{k} is the γ -ray direction. From Eq. (39) this configuration yields sensitivity to the correlation coefficient a_2 only. In the second arrangement, the γ - ν - μ configuration, the experiment is conducted with both polarized muons and nonperpendicular geometry, so that $\vec{P}_\mu \cdot \hat{k} \neq 0$. From Eq. (39) this configuration yields sensitivity to the correlation coefficients $\alpha + \frac{2}{3}c_1$ and b_2 also. Note that, due to different powers of \hat{k} in Eq. (39), the Doppler line shape arising from a_2 is symmetric about E_o whereas the Doppler line shapes arising from $\alpha + \frac{2}{3}c_1$ and b_2 are asymmetric about E_o .

Measurements of γ - ν and γ - ν - μ correlations have pros and cons. One disadvantage of γ - ν - μ correlation measurements is the small μ polarization in the μ -atom ground state. However, one advantage is that the Doppler line shape may be manipulated by varying the μ -spin direction or γ -detector position, which is helpful in separating the Doppler signal from the continuum background. Furthermore, distortion of the γ -ray line shape due to slowing down of the recoil nucleus is more straightforwardly separated from the asymmetric effects of γ - ν - μ correlations than from the symmetric effects of γ - ν correlations.

Two $\mu^- [A, Z] \rightarrow \nu [A, Z-1]^* \rightarrow \gamma [A, Z-1]**$ transitions have attracted the most attention,

$$^{28}\text{Si}(0^+, 0) \rightarrow ^{28}\text{Al}(1^+, 2201) \rightarrow ^{28}\text{Al}(0^+, 973), \quad (47)$$

$$^{28}\text{Si}(0^+, 0) \rightarrow ^{28}\text{Al}(1^+, 2201) \rightarrow ^{28}\text{Al}(2^+, 37). \quad (48)$$

They involve a common Gamow-Teller transition from the $^{28}\text{Si}(0^+, 0)$ ground state to the $^{28}\text{Al}(1^+, 2201)$ excited state. Note that the $0^+ \rightarrow 1^+ \rightarrow 0^+$ sequence involves a pure $M1$ γ decay whereas the $0^+ \rightarrow 1^+ \rightarrow 2^+$ sequence involves a mixed $E2/M1$ γ decay with mixing ratio $\delta(E2/M1) = 0.37 \pm 0.11$ (Kudoyarov *et al.*, 1998). Additionally the 2201-keV state lifetime is 59 ± 6 fs and slowing-down effects are non-negligible. Although at first glance the two sequences involve six correlations, i.e., $(\alpha + \frac{2}{3}c_1)^{1229}$, a_2^{1229} , and b_2^{1229} for the 1229-keV γ ray and $(\alpha + \frac{2}{3}c_1)^{2170}$, a_2^{2170} , and b_2^{2170} for the 2170-keV γ ray, these coefficients are related to a single underlying dynamical parameter, the helicity amplitude ratio X , as described in Sec. IX.C.1.

The ground-breaking work on the γ -ray correlations in these spin sequences was conducted at SREL by Miller *et al.* (1972b). They measured the γ -ray line shapes from μ stops in both natural Si and enriched $^{28}\text{SiO}_2$ targets. Unfortunately, the statistics were limited and the authors were forced to assume the absence of distortions of the Doppler line shape due to slowing down of the recoil ion.

²²See Popov (1963); Bukat and Popov (1964); Oziewicz and Popov (1965); Bukhvostov and Popov (1967a, 1967b, 1967c, 1970).

TABLE IX. Compilation of recent results from the γ -ray correlation experiments for the transition $^{28}\text{Si}(0^+,0) \rightarrow ^{28}\text{Al}(1^+,2201)$. The results are presented in terms of the dynamical parameter $X = \sqrt{2}T_0/T_1$. The analyzed gamma rays are listed in column 2 and the experimental technique is listed in column 3. FPA is the Fujii-Primakoff approximation value.

Ref.	γ -ray trans.	γ -ray corr.	$X = \sqrt{2}T_0/T_1$
Moftah <i>et al.</i> (1997)	1229	" γ - ν "	$0.454^{+0.12}_{-0.11}$
Brudanin <i>et al.</i> (1995)	1229, 2171	" γ - ν - μ "	0.543 ± 0.052
Briançon <i>et al.</i> (2000)	1229, 2171	" γ - ν - μ "	0.566 ± 0.045
FPA			0.59

More recently an improved measurement of the a_2 coefficient was conducted at TRIUMF by Moftah *et al.* (1997). The experiment was performed in perpendicular geometry, i.e., with $\vec{P}_\mu \cdot \hat{k} = 0$, and utilized a coincidence technique with Compton suppression to improve the 1229-keV γ -ray signal-to-noise. In analyzing the data the authors treated the a_2 coefficients for 1229- and 2170-keV γ rays as independent, since the 2170-keV multipolarity was not known at the time. However, they included recoil slowing-down effects in the fit of the line shapes.

Also recently a new measurement of all the coefficients has been performed at the Dubna phasotron by Brudanin *et al.* (1995) and Briançon *et al.* (2000). To identify both $(\alpha + \frac{2}{3}c_1)$ and b_2 the authors recorded the Doppler spectra for different values of $\vec{P}_\mu \cdot \hat{k}$. In Brudanin *et al.* (1995) they used forward/backward positioned Ge detectors to vary $\vec{P}_\mu \cdot \hat{k}$ and in Briançon *et al.* (2000) they used muon spin precession to vary $\vec{P}_\mu \cdot \hat{k}$. In analyzing their data the authors enforced the dynamical relations between correlation coefficients and fit the 2201-keV lifetime and 2170-keV mixing ratio.

Note that a concern in all experiments is the production of the $^{28}\text{Al}(1^+,2201)$ state by either (i) $(\mu, n\nu)$ or $(\mu, nn\nu)$ capture on ^{29}Si or ^{30}Si isotopes, or (ii) (μ, ν) capture to higher-lying ^{28}Si levels. Such contributions would distort the line shapes and impact the extraction of $(\alpha + \frac{2}{3}c_1)$, a_2 , and b_2 . Note that Miller *et al.* (1972a) obtained constraints on contributions from $^{29}\text{Si}(\mu, n\nu)$ and Moftah *et al.* (1997) and Briançon *et al.* (2000) obtained limits on cascade feeding from higher levels. However, a small contribution from (i) or (ii) is not completely excluded.

In Table IX we summarize the various measurements of γ -ray correlations for $^{28}\text{Si}(0^+,0) \rightarrow ^{28}\text{Al}(1^+,2201)$. The experimental configurations are denoted by $\vec{P}_\mu \cdot \hat{k} = 0$ or $\vec{P}_\mu \cdot \hat{k} \neq 0$ and indicate the absence or presence of sensitivity to $(\alpha + \frac{2}{3}c_1)$ and b_2 . To assist the comparison of experiments we quote all results in terms of the helicity amplitude ratio X . The "world data" weighted mean is $X = 0.554 \pm 0.042$.

F. Theoretical framework for exclusive ordinary muon capture

Herein we describe the theoretical treatment of physical observables in (μ, ν) reactions. Our main goals are to

outline the steps and assumptions in calculating the observables and provide some details of work on ^{11}B , ^{12}C , ^{16}O , ^{23}Na , and ^{28}Si . In Sec. IX.F.1 we describe the operators that contribute to μ capture. In Sec. IX.F.2 we discuss the application of the impulse approximation and in Sec. IX.F.3 we discuss the effects due to exchange currents. The detailed discussion of nuclear models is left to Sec. IX.G.

Prior to considering the case of muon capture it is helpful to introduce a set of multipole operators (labeled by their total angular momentum J and orbital angular momentum L). Using the notation of Walecka (1975) they are $M_J(qx)$, $\mathbf{M}_{JL}(qx) \cdot \boldsymbol{\sigma}$, $\mathbf{M}_{JL}(qx) \cdot \nabla$, and $M_J(qx) \boldsymbol{\sigma} \cdot \nabla$ where

$$M_J^{M_J}(qx) \equiv j_J(qx) Y_J^{M_J}(\Omega_x), \quad (49)$$

$$\mathbf{M}_{JL}^{M_J}(qx) \equiv j_L(qx) \mathbf{Y}_{JL}^{M_J}(\Omega_x), \quad (50)$$

and $j_J(qx)$ are spherical Bessel functions, $Y_J^{M_J}(\Omega_x)$ are spherical harmonics, and $\mathbf{Y}_{JL}^{M_J}(\Omega_x)$ are vector spherical harmonics.²³ Note that $M_0(qx)$ is encountered in allowed Fermi transitions via the term $g_v M_0(qx) \tau^\pm$ and $\mathbf{M}_{10}(qx)$ is encountered in allowed Gamow-Teller transitions via the term $g_a \mathbf{M}_{10}(qx) \tau^\pm$.

1. Multipole operators

The model calculation of partial transitions on complex nuclei is generally conducted via a multipole expansion of the Fujii-Primakoff effective Hamiltonian of Eq. (40). We refer the reader who is interested in the details of the formalism to the articles by Primakoff (1959), Morita and Fujii (1960), Luyten *et al.* (1963), Walecka (1975), Mukhopadhyay (1977), and Ciechanowicz and Oziewicz (1984). Below we briefly describe the specific operators that contribute to transitions of interest for g_p , i.e., the spin-parity sequences $0^+ \rightarrow 0^-$, $0^+ \rightarrow 1^+$, and $3/2^\pm \rightarrow 1/2^\pm$.

Using the notation of Walecka (1975) the weak operators that participate in μ capture are $\mathcal{L}_J - \mathcal{M}_J$ and $T_J^{el} - T_J^{mag}$ where \mathcal{M}_J , \mathcal{L}_J , T_J^{el} , and T_J^{mag} are the so-called charge, longitudinal, transverse electric, and transverse magnetic operators. Note that $\mathcal{L}_J - \mathcal{M}_J$ involves a longitudinal coupling to the lepton field and is dependent on g_p while $T_J^{el} - T_J^{mag}$ involves a transverse coupling to the lepton field and is independent of g_p . Also note that \mathcal{M}_J originates from the time component of the weak current and \mathcal{L}_J , T_J^{el} , and T_J^{mag} originate from the space component of the weak current. Often one writes the operators as $\mathcal{M}_J \equiv M_J + M_J^5$, etc., to distinguish the vector current contribution (i.e., M_J) and axial current contribution (i.e., M_J^5). Expressions for $\mathcal{L}_J - \mathcal{M}_J$ and $T_J^{el} - T_J^{mag}$ in

²³Convenient expressions for the matrix elements of these multipole operators are given in Donnelly and Haxton (1979) for harmonic oscillator wave functions and in Donnelly and Haxton (1980) for other radial wave functions.

TABLE X. Compilation of formulas for the weak operators $\mathcal{L}_J - \mathcal{M}_J$ and $T_J^{el} - T_J^{mag}$ with multiplicities $J^\pi = 0^+, 0^-, 1^+, \text{ and } 2^+$ that contribute to partial transitions with spin-parity sequences $0^+ \rightarrow 0^-, 0^+ \rightarrow 1^+, 1/2^+ \rightarrow 1/2^+, \text{ and } 3/2^+ \rightarrow 1/2^+$. The basic multipole operators $M_J(qx)$, $\mathbf{M}_{JL}(qx) \cdot \boldsymbol{\sigma}$, $\mathbf{M}_{JL}(qx) \cdot \nabla$ and $M_J(qx) \boldsymbol{\sigma} \cdot \nabla$ are defined in Eqs. (49) and (50).

J^π	Weak operator	Multipole operator decomposition
0^+	$L_0 - M_0$	$-g_v M_0 \tau^\pm$
0^-	$L_0^5 - M_0^5$	$i \left[\left(g_a + \frac{q}{2M} (g_a - g_p) \right) \mathbf{M}_{01} \cdot \boldsymbol{\sigma} + \frac{q}{M} g_a M_0 \boldsymbol{\sigma} \cdot \nabla \right] \tau^\pm$
1^+	$L_1^5 - M_1^5$	$i \left[\left(g_a + \frac{q}{2M} (g_a - g_p) \right) \left(\sqrt{\frac{1}{3}} \mathbf{M}_{10} \cdot \boldsymbol{\sigma} + \sqrt{\frac{2}{3}} \mathbf{M}_{12} \cdot \boldsymbol{\sigma} \right) + \frac{q}{M} g_a M_1 \boldsymbol{\sigma} \cdot \nabla \right] \tau^\pm$
1^+	$T_1^{el5} - T_1^{mag}$	$i \left[\left(g_a - \frac{q}{2M} (g_v - g_m) \right) \left(\sqrt{\frac{2}{3}} \mathbf{M}_{10} \cdot \boldsymbol{\sigma} - \sqrt{\frac{1}{3}} \mathbf{M}_{12} \cdot \boldsymbol{\sigma} \right) + \frac{q}{M} g_v \mathbf{M}_{11} \cdot \nabla \right] \tau^\pm$
2^+	$L_2 - M_2$	$-g_v M_2 \tau^\pm$
2^+	$T_2^{el} - T_2^{mag5}$	$i \left[\left(-g_a + \frac{q}{2M} (g_v + g_m) \right) \mathbf{M}_{22} \cdot \boldsymbol{\sigma} + \frac{q}{M} g_v \left(\sqrt{\frac{3}{5}} \mathbf{M}_{21} \cdot \nabla - \sqrt{\frac{2}{5}} \mathbf{M}_{23} \cdot \nabla \right) \right] \tau^\pm$

terms of the basic multipole operators [$M_J(qx)$, $\mathbf{M}_{JL}(qx) \cdot \boldsymbol{\sigma}$, $\mathbf{M}_{JL}(qx) \cdot \nabla$, and $M_J(qx) \boldsymbol{\sigma} \cdot \nabla$] and the weak-coupling constants (g_v , g_m , g_a and g_p) are given in Walecka (1975) and Donnelly and Haxton (1979, 1980). For the $J^\pi = 0^-, 0^+, 1^+, \text{ and } 2^+$ multipoles that are relevant to the ^{11}B , ^{12}C , ^{16}O , ^{23}Na , and ^{28}Si transitions the expressions are reproduced in Table X.

$0^+ \rightarrow 0^-$ transitions, e.g., ^{16}O , involve a unique $J^\pi = 0^-$ multipole, a single electroweak weak operator, $L_0^5 - M_0^5$, and two multipole operators, $\mathbf{M}_{01} \cdot \boldsymbol{\sigma}$ and $M_0 \boldsymbol{\sigma} \cdot \nabla$. The $\mathbf{M}_{01} \cdot \boldsymbol{\sigma}$ operator is the $\ell=1$ retarded Gamow-Teller operator originating from the space component of the axial current. The $M_0 \boldsymbol{\sigma} \cdot \nabla$ operator is the axial charge operator originating from the time component of the axial current. Note that the contribution of g_p in $0^+ \rightarrow 0^-$ transitions is via $\mathbf{M}_{01} \cdot \boldsymbol{\sigma}$.

$0^+ \rightarrow 1^+$ transitions, e.g., ^{12}C and ^{28}Si , involve a unique $J^\pi = 1^+$ multipole, two electroweak weak operators, $L_1^5 - M_1^5$ and $T_1^{el5} - T_1^{mag}$, and four multipole operators, $\mathbf{M}_{10} \cdot \boldsymbol{\sigma}$, $\mathbf{M}_{12} \cdot \boldsymbol{\sigma}$, $M_1 \boldsymbol{\sigma} \cdot \nabla$, and $\mathbf{M}_{11} \cdot \nabla$. The $\mathbf{M}_{10} \cdot \boldsymbol{\sigma}$ operator is the allowed Gamow-Teller operator. The remaining contributions include the axial current's time component, i.e., $M_1 \boldsymbol{\sigma} \cdot \nabla$, and second-forbidden corrections, i.e., $\mathbf{M}_{12} \cdot \boldsymbol{\sigma}$. Note that the leading contribution of g_p in $0^+ \rightarrow 1^+$ transitions is via $\mathbf{M}_{10} \cdot \boldsymbol{\sigma}$.

For transitions on $J_i \neq 0$ targets a range of multipoles are involved, i.e., $|J_i - J_f|$ to $(J_i + J_f)$. For example, a $1/2^+ \rightarrow 1/2^+$ transition, e.g., ^1H or ^3He , involves $J^\pi = 0^+, 1^+$ multipoles and a $3/2^+ \rightarrow 1/2^+$ transition, e.g., ^{11}B or ^{23}Na , involves $J^\pi = 1^+, 2^+$ multipoles. For $1/2^+ \rightarrow 1/2^+$ transitions the $L_0 - M_0$ operator yields an additional contribution from the allowed Fermi operator. For $3/2^+ \rightarrow 1/2^+$ transitions the $L_2 - M_2$ and $T_2^{el} - T_2^{mag5}$ operators yield additional contributions from the ℓ -forbidden multipole operators M_2 and $\mathbf{M}_{22} \cdot \boldsymbol{\sigma}$ and the gradient multipole operators $\mathbf{M}_{21} \cdot \nabla$ and $\mathbf{M}_{23} \cdot \nabla$. However, the leading contribution of g_p in $1/2^+ \rightarrow 1/2^+$ transitions and $3/2^+ \rightarrow 1/2^+$ transitions is still via $\mathbf{M}_{10} \cdot \boldsymbol{\sigma}$. Note that the multipoles with $J^\pi = 0^+$ and $J^\pi = 2^+$ are independent of g_p .

2. Impulse approximation

In principle the weak amplitudes in muon capture have one-, two-, and many-body contributions. However, in practice the starting point for most calculations is to approximate the weak nuclear amplitude by a summation of A one-body amplitudes, i.e., the impulse approximation. This amounts to ignoring the effects of pion exchange currents, Δ -hole excitations, etc.

Assuming a one-body form for nuclear currents, the required multiparticle weak matrix elements $\langle J_f | O^J | J_i \rangle$ between an initial state $|J_i\rangle$ and final state $|J_f\rangle$ may be written in terms of single-particle weak matrix elements $\langle \alpha' | O^J | \alpha \rangle$ between single-particle states labeled by $|\alpha\rangle$ and $|\alpha'\rangle$ as (Donnelly and Haxton, 1979)

$$\langle J_f | O^J | J_i \rangle = \sum_{\alpha, \alpha'} C(J, \alpha, \alpha', J_f, J_i) \langle \alpha' | O^J | \alpha \rangle, \quad (51)$$

where the states $\alpha \equiv [n, j, \ell]$ and $\alpha' \equiv [n', j', \ell']$ and in μ capture the operator O^J is $\mathcal{M}_J - \mathcal{L}_J$ or $T_J^{el} - T_J^{mag}$. The coefficients $C(J, \alpha, \alpha', J_f, J_i)$ are called one-body transition densities and determine the contributions of each single-particle matrix element $\langle \alpha' | O^J | \alpha \rangle$ to the multiparticle matrix element $\langle J_f | O^J | J_i \rangle$. Note that the one-body transition densities are determined by the nuclear structure while the single-particle matrix elements are functions of the weak couplings. Equation (51) therefore represents a convenient separation of nuclear structure and weak dynamics.²⁴ We stress that in practice in applying Eq. (51) the summation is truncated to a finite number of the single-particle transitions.

3. Exchange currents

At some level the impulse approximation will break down, and consequently the evaluation of contributions

²⁴Strictly the radial form of the nuclear wave functions also enters the computation of the single-particle matrix elements.

from pion exchange, delta excitation, etc., is important in extracting g_p . One approach to computing exchange currents is to use low-energy theorems to constrain soft pion contributions. Another approach involves enumerating a plausible set of Feynman diagrams that incorporate π 's, Δ 's, etc. We shall not attempt to cover in detail the broad topic of exchange currents, but rather we summarize their application to muon capture on complex nuclei.

The work of Kubodera *et al.* (1978) was pivotal in establishing the importance of soft pion exchange currents in various electroweak processes. The authors observed that soft pions produce large effects in the time component of the axial current and the space component of the vector current. Further, they recognized that arguments based on chiral symmetry fix the size of these effects, yielding a powerful tool in determining the corrections from two-body currents. In particular for muon capture the soft-pion corrections to axial charge operators, while substantial, are reasonably well determined. Such $M_J \boldsymbol{\sigma} \cdot \nabla$ operators compete with the leading contributions of g_p in both allowed and $0^+ \rightarrow 0^-$ transitions. For further details see Guichon *et al.* (1978), Guichon and Samour (1979), and Towner (1986).

Unfortunately, for the space component of the axial current and the time component of the vector current the constraints dictated by chiral symmetry are ineffective in determining the contributions of two-body currents. For example, for the allowed Gamow-Teller operator and the allowed Fermi operator this approach is not helpful. Instead the modifying effects of exchange currents must be addressed by explicitly evaluating a specific set of Feynman graphs. An example of such an approach is the $N\pi\rho A_1$ phenomenological Lagrangian model of Ivanov and Truhlik (1979a). Note that the Feynman graphs and corresponding operators are obviously not unique and the coupling constants and form factors are frequently not well known. Consequently the calculation of two-body corrections to Gamow-Teller matrix elements and Fermi matrix elements have significant uncertainties. In particular the Δ 's contribution is poorly determined. For examples of applications to muon capture, see Adam *et al.* (1990).

G. Nuclear models for partial transitions

Next we consider the specific structure and nuclear models for partial transitions on $A=11, 12, 16, 23,$ and 28 nuclei. Our focus is on the elements of the models that impact the determination of g_p .

Nowadays full-space shell model calculations are routinely performed for $4 < A < 16$, i.e., $0p$ shell nuclei, and $16 < A < 40$, i.e., $1s-0d$ shell nuclei, and the empirical determination of effective interactions from least-squares fits to nuclear data is well established. For example, the parameters of the $0p$ shell interaction were obtained by Cohen and Kurath (1967) by fitting $4 < A < 16$ level energies and the parameters of the $1s-0d$ interaction were obtained by Wildenthal (1984) by fitting $16 < A < 40$ level energies. In addition semiempirical in-

teractions, which incorporate assumptions for the particular form of the effective interaction, are available (Brown *et al.*, 1988). Both empirical and semiempirical interactions are capable of reproducing many features and phenomena in $0p$ and $1s-0d$ nuclei.

Note that an alternative approach is the microscopic derivation of the effective nucleon-nucleon (NN) interaction from the free nucleon-nucleon interaction. The derivation involves a power series relating the effective interaction and free interaction, but unfortunately the question of convergence is tricky. In general, such interactions either give less satisfactory model-data agreement than empirical interactions, e.g., the interaction of Kuo and Brown (1966), or need some *ad hoc* tuning of model parameters, e.g., the interaction of Hauge and Maripuu (1973). However, the comparison of results from empirical interactions and realistic interactions is helpful in understanding and evaluating the model uncertainties.

1. $^{11}\text{B}(3/2^-, 0) \rightarrow ^{11}\text{Be}(1/2^-, 320)$

Several calculations of capture rate and hyperfine dependences have been performed for the $^{11}\text{B}(3/2^-, 0) \rightarrow ^{11}\text{Be}(1/2^-, 320)$ transition (Bernabeu, 1971; Koshigiri *et al.*, 1982, 1984; Kuz'min *et al.*, 1994; Suzuki, 1997). Bernabeu (1971) first discussed the relatively high sensitivity to g_p and relatively low sensitivity to nuclear structure of Λ_+ / Λ_- . More recently Kuz'min *et al.* (1994) assessed the effects of different $0p$ -shell effective interactions while Suzuki (1997) assessed the effects of a ^{11}Be neutron halo.

The simplest picture of $^{11}\text{B}(3/2^-, 0) \rightarrow ^{11}\text{Be}(1/2^-, 320)$ consists of a $0s_{1/2}^4 0p_{3/2}^7$ initial state, $0s_{1/2}^4 0p_{3/2}^6 0p_{1/2}^1$ final state, and $0p_{3/2} \rightarrow 0p_{1/2}$ single-particle transition. However, in reality the $^{11}\text{B}(3/2^-, 0)$ initial state has substantial contributions from both $0s_{1/2}^4 0p_{3/2}^5 0p_{1/2}^2$ and $0s_{1/2}^4 0p_{3/2}^3 0p_{1/2}^4$ configurations, and interference between the $0p_{1/2} \rightarrow 0p_{3/2}$ single-particle transition and the $0p_{3/2} \rightarrow 0p_{1/2}$ single-particle transition is important. For example, the capture rate is grossly overestimated in a simple $0p_{3/2} \rightarrow 0p_{1/2}$ picture.

Full $0p$ -shell model calculations for $^{11}\text{B}(3/2^-, 0) \rightarrow ^{11}\text{Be}(1/2^-, 320)$ with well-established effective interactions confirm the leading transition is $0p_{3/2} \rightarrow 0p_{1/2}$, with a substantial contribution from $0p_{1/2} \rightarrow 0p_{3/2}$ and a significant contribution from $0p_{3/2} \rightarrow 0p_{3/2}$. Since the Gamow-Teller matrix elements for $0p_{3/2} \rightarrow 0p_{1/2}$ and $0p_{1/2} \rightarrow 0p_{3/2}$ have opposite signs they interfere destructively and dramatically decrease both Λ_+ and Λ_- . Typical model-to-model variations in the $0p_{3/2} \rightarrow 0p_{1/2}$ and $0p_{1/2} \rightarrow 0p_{3/2}$ densities are roughly $\pm 10\%$. Note that the remaining $0p_{1/2} \rightarrow 0p_{1/2}$ and $0p_{3/2} \rightarrow 0p_{3/2}$ densities show larger model-to-model variations, however, their contributions to capture are smaller.

A unique complication for the $^{11}\text{B}(3/2^-, 0) \rightarrow ^{11}\text{Be}(1/2^-, 320)$ transition is the ^{11}Be neutron halo. The halo is interesting in the context of nuclear structure studies but worrisome in the context of extracting g_p . Recently Suzuki (1997) has assessed the impact of the

neutron halo on the capture rate and its hyperfine dependence. Suzuki (1997) reported it tends to reduce both Λ_+ and Λ_- but barely changes Λ_+/Λ_- .

2. $^{12}\text{C}(0^+,0) \rightarrow ^{12}\text{B}(1^+,0)$

A large number of model calculation are available for $^{12}\text{C}(0^+,0) \rightarrow ^{12}\text{B}(1^+,0)$. Early studies of μ capture rates and β -decay rates were performed by Flamard and Ford (1959), Mukhopadhyay and Macfarlane (1971), O'Connell *et al.* (1972), Immele and Mukhopadhyay (1975), and Mukhopadhyay and Martorell (1978). More comprehensive studies of rates and polarizations in μ capture were published by Morita and co-workers,²⁵ and by Subramanian *et al.* (1976), Rosenfelder (1979), Ciechanowicz (1981), Hayes and Towner (2000), and Auerbach and Brown (2002). They include investigations of two-body currents and core polarization effects.

The simplest picture of $^{12}\text{C}(0^+,0) \rightarrow ^{12}\text{B}(1^+,0)$ consists of a $0s_{1/2}^4 0p_{3/2}^8$ initial state, $0s_{1/2}^4 0p_{3/2}^7 0p_{1/2}^1$ final state, and a $0p_{3/2} \rightarrow 0p_{1/2}$ single-particle transition. Like the ^{11}B ground state (g.s.), the ^{12}C ground state has substantial contributions from both $0s_{1/2}^4 0p_{3/2}^6 0p_{1/2}^2$ and $0s_{1/2}^4 0p_{3/2}^4 0p_{1/2}^4$ configurations, and the interference of amplitudes from $0p_{3/2} \rightarrow 0p_{3/2}$ transitions and $0p_{1/2} \rightarrow 0p_{3/2}$ transitions is important. Again the capture rate is grossly overestimated by a simple $0p_{3/2} \rightarrow 0p_{1/2}$ picture.

Note that the overall pattern of the transition densities obtained from full $0p$ -shell model calculations with well-established effective interactions is quite similar for $^{11}\text{B}(3/2^-,0) \rightarrow ^{11}\text{Be}(1/2^-,320)$ and $^{12}\text{C}(0^+,0) \rightarrow ^{12}\text{B}(1^+,0)$. Specifically for ^{12}C the largest density is $0p_{3/2} \rightarrow 0p_{1/2}$, the next-to-largest density is $0p_{1/2} \rightarrow 0p_{3/2}$, and the contributions from $0p_{3/2} \rightarrow 0p_{3/2}$ and $0p_{1/2} \rightarrow 0p_{1/2}$ are small. As in ^{11}B , in ^{12}C the interference of $0p_{3/2} \rightarrow 0p_{1/2}$ with $0p_{1/2} \rightarrow 0p_{3/2}$ is important in reducing the Gamow-Teller matrix element.

A nice feature of $^{12}\text{C}(0^+,0) \rightarrow ^{12}\text{B}(1^+,0)$ is that related data on other electroweak processes are available, e.g., ^{12}B β decay, $^{12}\text{C}(e,e')$ scattering, and $^{12}\text{C}(1^+,15.1 \text{ MeV})$ γ decay, and are helpful in testing the model calculations. For example, the one-body transition densities have been extracted from these data by Haxton (1978) and Doyle and Mukhopadhyay (1995) and generally support the model calculations.

3. $^{23}\text{Na}(3/2^+,0) \rightarrow ^{23}\text{Ne}(1/2^+,3458)$

Calculations of capture rates and hyperfine dependencies in $^{23}\text{Na} \rightarrow ^{23}\text{Ne}$ transitions have been performed by Johnson *et al.* (1996), Koshigiri *et al.* (1997), and Siiskonen *et al.* (1998). The calculations have been conducted in the full $1s$ - $0d$ model space using the Wildenthal empirical interaction (Wildenthal, 1984) and the Kuo-Brown realistic interaction (Kuo and Brown, 1966).

A study of two-body currents and core polarization was made by Koshigiri *et al.* (1997).

The ^{23}Na ground state is $J^\pi = 3/2^+$, indicating that the simplest picture of a single unpaired proton in a $0d_{5/2}$ orbital is wrong. Rather the $A=20$ – 24 mass region is well known for examples of light deformed nuclei and rotational band spectra. Consequently the spherical shell model representation of these nuclei is quite complex, with $A=23$ wave functions having small occupancies for the $(d_{5/2})^7$ configuration and large occupancies of the $1s_{1/2}, 1d_{3/2}$ orbitals.

For concreteness we describe the $^{23}\text{Na}(3/2^+,0) \rightarrow ^{23}\text{Ne}(1/2^+,3458)$ transition, which is the strongest transition in the μ - ^{23}Na experiment. Full $1s$ - $0d$ shell model calculations with well-tested effective interactions show $0d_{5/2} \rightarrow 0d_{3/2}$ is the strongest single-particle transition and $0d_{3/2} \rightarrow 0d_{3/2}$ is the next strongest single-particle transition. Other contributions are typically 10–20% of $0d_{5/2} \rightarrow 0d_{3/2}$. The variations of the one-body transition densities between models are $\leq 10\%$ for $0d_{5/2} \rightarrow 0d_{3/2}$ densities and $\leq 25\%$ for $0d_{3/2} \rightarrow 0d_{3/2}$ densities.

4. $^{28}\text{Si}(0^+,0) \rightarrow ^{28}\text{Al}(1^+,2201)$

Several authors have calculated the rates and correlations for $^{28}\text{Si}(0^+,0) \rightarrow ^{28}\text{Al}(1^+,2201)$. The first efforts were made by Ciechanowicz (1976) and Parthasarathy and Sridhar (1978, 1981), but employed relatively crude nuclear wave functions, the $1p$ - $1h$ wave function of Donnelly and Walker (1970) and the truncated $1s$ - $0d$ wave function of McGrory and Wildenthal (1971). More recently Ciechanowicz *et al.* (1998), Siiskonen *et al.* (1999), Kuz'min and Tetereva (2000), and Kuz'min *et al.* (2001) have conducted full $1s$ - $0d$ calculations. Ciechanowicz *et al.* (1998) and Siiskonen *et al.* (1999) also considered both two-body currents and core polarization in $^{28}\text{Si}(0^+,0) \rightarrow ^{28}\text{Al}(1^+,2201)$.

In the simplest picture $^{28}\text{Si}(0^+,0) \rightarrow ^{28}\text{Al}(1^+,2201)$ consists of a full $0d_{5/2}^{12}$ initial state, $J^\pi = 1^+$ ($0d_{5/2}^{-1}, 0d_{3/2}^1$) final state, and $0d_{5/2} \rightarrow 0d_{3/2}$ single-particle transition. However, the model calculations show that the simple picture is insufficient and configurations with several particles in $1s_{1/2}$ - $0d_{3/2}$ orbitals are important.

A special remark on the one-body transition densities in the $^{28}\text{Si}(0^+,0) \rightarrow ^{28}\text{Al}(1^+,2201)$ transition is worthwhile. Unlike the previous examples of ^{11}B , ^{12}C , and ^{23}Na , in ^{28}Si the variations from model to model are large, e.g., the densities from Kuo and Brown (1966) and Wildenthal (1984) are quite different. Also no particular single-particle transition is dominant, e.g., the interaction of Wildenthal (1984) shows $0d_{5/2} \rightarrow 0d_{3/2}$, $0d_{5/2} \rightarrow 0d_{5/2}$, and $1s_{1/2} \rightarrow 0d_{3/2}$ with similar magnitudes. Therefore, as discussed by Kuz'min and Tetereva (2000), the model calculations are especially sensitive to interference effects.

5. $^{16}\text{O}(0^+,0) \rightarrow ^{16}\text{N}(0^-,120)$

Because the nucleus ^{16}O is doubly magic and the transition $^{16}\text{O}(0^+,0) \rightarrow ^{16}\text{N}(0^-,120)$ is first forbidden this case is special. The simple model for $^{16}\text{O}(0^+,0)$

²⁵See Kobayashi *et al.* (1978); Ami *et al.* (1981); Fukui *et al.* (1983a, 1983b, 1987); Koshigiri *et al.* (1985); Morita *et al.* (1994).

$\rightarrow {}^{16}\text{N}(0^-, 120)$ comprises a $0p$ closed-shell initial state, and a $1p-1h$ $J^\pi=0^-$ final state, and involves $1p_{1/2} \rightarrow 2s_{1/2}$ and $1p_{3/2} \rightarrow 1d_{3/2}$ single-particle transitions. Several authors have computed the rates of μ capture (Λ_μ) and β decay (Λ_β) for ${}^{16}\text{O}(0^+, 0) \leftrightarrow {}^{16}\text{N}(0^-, 120)$ within this scheme; for example, see Guichon *et al.* (1978) and references therein. They found the rates to be strongly dependent on the $0p_{3/2}^{-1}-0d_{3/2}$ admixture in the ${}^{16}\text{N}$ wave function, but the ratio $\Lambda_\mu/\Lambda_\beta$ to be near-model independent.

Since the work of Brown and Green (1966) we know the above picture is not complete, and that $2p-2h$ configurations in the ${}^{16}\text{O}$ ground state are important. The effects of $2p-2h$ configurations on μ capture and β decay were first investigated by Guichon and Samour (1979) who considered $(2s_{1/2})^2(1p_{1/2})^{-2}$ and $(1d_{3/2})^2(1p_{3/2})^{-2}$ admixtures. They found that the effects of $2p-2h$ configurations on the axial charge matrix element $M_0\sigma\cdot\nabla$ and the $\ell=1$ retarded Gamow-Teller matrix element $M_{10}\cdot\sigma$ were opposite in sign, and consequently the near cancellation of model uncertainties in $\Lambda_\mu/\Lambda_\beta$ broke down. Subsequently Towner and Khanna (1981) evaluated the effects of $2p-2h$ configurations in ${}^{16}\text{N}(0^-, 120) \leftrightarrow {}^{16}\text{O}(0^+, 0)$ transitions with more extensive configurations and various effective interactions. They concluded that $2p-2h$ configurations decrease the β -decay rate by factors of 2–4, decrease the μ capture rate by factors of 1.5–2, and increase $\Lambda_\mu/\Lambda_\beta$ by factors of 1.5–2, thus confirming the model dependence observed by Guichon and Samour (1979).

Recently Haxton and Johnson (1990) and Warburton *et al.* (1994) have performed full $4\hbar\omega$ ($3\hbar\omega$) calculation for ${}^{16}\text{O}$ (${}^{16}\text{N}$) low-lying levels. These calculations nicely reproduce the excitation energies of the ${}^{16}\text{O}$ isoscalar positive parity states and the ${}^{16}\text{N}$ isovector negative parity states, and indicate significant $4p-4h$ probabilities in ${}^{16}\text{O}$. In both works the authors stress the large destructive interference between $M_0\sigma\cdot\nabla$ and $M_{10}\cdot\sigma$ in β decay, and therefore substantial model dependences in Λ_β and $\Lambda_\mu/\Lambda_\beta$. Consequently the authors argue that Λ_μ , not $\Lambda_\mu/\Lambda_\beta$, is preferable for extracting the coupling g_p .

The foregoing discussions of ${}^{16}\text{O}(0^+, 0) \leftrightarrow {}^{16}\text{N}(0^-, 120)$ transitions show a worrisome sensitivity to the multiparticle wave functions. In addition the matrix element $M_0\sigma\cdot\nabla$ is modified considerably by two-body currents from soft-pion exchange. These effects are discussed in detail by Guichon *et al.* (1978), Towner and Khanna (1981), Jäger *et al.* (1983), and Nozawa *et al.* (1986). The calculations indicate that they increase the β -decay rate by a factor of about 4 and increase the μ capture rate by a factor of about 2. The contribution of $M_0\sigma\cdot\nabla$ is larger in β decay than μ capture. This further complicates the extraction of g_p from capture on ${}^{16}\text{O}$.

H. The coupling g_p from partial transitions

1. Recommended values of g_p/g_a

In Table XI we list our recommended values for g_p/g_a from exclusive ordinary muon capture on complex nu-

TABLE XI. Recommended values of g_p/g_a from exclusive ordinary muon capture on complex nuclei. The quoted errors are experimental uncertainties, and do not include model uncertainties.

Transition	g_p/g_a
${}^{11}\text{B}(3/2^-, 0) \rightarrow {}^{11}\text{Be}(1/2^-, 320)$	$4.3^{+2.8}_{-4.3}$
${}^{12}\text{C}(0^+, 0) \rightarrow {}^{12}\text{B}(1^+, 0)$	9.8 ± 1.8
${}^{16}\text{O}(0^+, 0) \rightarrow {}^{16}\text{N}(0^-, 120)$	6.0 ± 0.4
${}^{23}\text{Na}(3/2^+, 0) \rightarrow {}^{23}\text{Ne}(1/2^+, 3458)$	$6.6^{+2.6}_{-2.4}$
${}^{28}\text{Si}(0^+, 0) \rightarrow {}^{28}\text{Al}(1^+, 2201)$	$1.0^{+1.1}_{-1.2}$

clei. By “recommended values for g_p/g_a ” we mean our assessment of the best values from the current world experimental data set and the most complete model calculations. In quoting these values we combined the experimental results of Possoz *et al.* (1974, 1977), Roesch, Telegdi, *et al.* (1981), and Kuno *et al.* (1984) to obtain a world average of the helicity amplitude ratio $X=0.23 \pm 0.06$ for ${}^{12}\text{C}(0^+, 0) \rightarrow {}^{12}\text{B}(1^+, 0)$ and combined the experimental results of Brudanin *et al.* (1995), Mofteh *et al.* (1997), and Briançon *et al.* (2000) to obtain a world average of the helicity amplitude ratio $X=0.55 \pm 0.04$ for ${}^{28}\text{Si}(0^+, 0) \rightarrow {}^{28}\text{Al}(1^+, 2201)$.²⁶ For the hyperfine dependence on ${}^{11}\text{B}$ we employ the results of Wiaux *et al.* (2002) and for the hyperfine dependence on ${}^{23}\text{Na}$ we employ the results of Johnson *et al.* (1996). For the capture rate of the ${}^{16}\text{O}(0^+, 0) \rightarrow {}^{16}\text{N}(0^-, 120)$ transition we averaged the experimental results of Kane *et al.* (1973) and Guichon *et al.* (1979). Note that in Table XI the quoted errors include only experimental uncertainties. Also note we quote the results in Table XI in terms of g_p/g_a not g_p . In most cases the measured quantities are recoil polarizations, γ -ray correlations, or hyperfine dependences, and therefore are governed by ratios of nuclear matrix elements and of weak-coupling constants. Consequently quoting g_p/g_a is more natural and more appropriate.

In order to extract the coupling g_p/g_a from experimental data a model is necessary. Our model choices, and arguments for selecting them, are given below.

For ${}^{11}\text{B}$ we took the results of Kuz'min *et al.* (1994) yielding $g_p/g_a=4.3^{+2.8}_{-4.3}$. These authors used the full $0p$ space with Cohen-Kurath interaction but omitted the effects of core polarization and exchange currents. Note that the earlier calculation of Bernabeu (1971) yields a similar value of $g_p/g_a=4^{+3}_{-3}$. According to Suzuki (1997) the effects of the ${}^{11}\text{Be}$ neutron halo on the hyperfine dependence are small.

For ${}^{12}\text{C}$ we used the model calculations of Fukui *et al.* (1987) and excited state yields of Giffon *et al.* (1981) to

²⁶In the literature both the helicity amplitude ratio, denoted X , and the neutrino-wave amplitude ratio, denoted x , have been used in this context. Although both X and x are suitable for representing the dynamical content of $\Delta J^\pi=1^+$ transitions, they are different, i.e., $X=(-2x+\sqrt{2})/(x+\sqrt{2})$. Therefore it is important not to confuse the two variables; see Sec. IX.F.1.

TABLE XII. Comparison of the corrections from the terms involving $M_1 \boldsymbol{\sigma} \cdot \nabla$, $M_{12} \cdot \boldsymbol{\sigma}$, and $M_{11} \cdot \nabla$ to the multipole amplitude of $L_1^5 - M_1^5$ for $A=11, 12, 23$, and 28 and several effective interactions denoted CKPOT (Cohen and Kurath, 1967), PKUO (Kuo and Brown, 1966), USD (Wildenthal, 1984), and KUOSD (Kuo and Brown, 1966). The values in columns 4–6 correspond to the percentage change in the matrix elements as the correction terms are successively included. Note that $M_{11} \cdot \nabla$ does not contribute to $L_1^5 - M_1^5$.

A	Int.	$L_1^5 - M_1^5$	$M_1 \boldsymbol{\sigma} \cdot \nabla$ corr. (%)	$M_{12} \cdot \boldsymbol{\sigma}$ corr. (%)	$M_{11} \cdot \nabla$ corr. (%)
11	CKPOT	-0.103	-30.6	-2.6	0.0
11	PKUO	-0.094	-32.4	0.6	0.0
12	CKPOT	0.107	-34.5	-9.4	0.0
12	PKUO	-0.071	-41.6	-18.4	0.0
23	USD	0.090	-31.8	4.1	0.0
23	KUOSD	-0.071	-44.4	13.1	0.0
28	USD	0.070	-37.2	-27.5	0.0
28	KUOSD	-0.071	-54.5	-18.4	0.0

obtain $g_p/g_a = 9.8 \pm 1.8$. These authors used the full $0p$ space with Hauge-Maripuu interaction and accounted for core polarization and exchange currents. The core polarization effects were computed to second order in perturbation theory and the exchange currents were computed with contributions from pair currents, pionic currents, and Δ excitations. Earlier calculations with more rudimentary wave functions and less sophisticated treatments of core polarization and exchange currents gave similar results.

For ^{16}O a number of determinations of g_p/g_a are published. We took the value $g_p/g_a = 6.0 \pm 0.4$ from Warburton *et al.* (1994), which incorporates both $4p-4h$ ^{16}O configurations and $3p-3h$ ^{16}N configurations and reproduces the ^{16}N β -decay rate. The $4p-4h$ calculation of Haxton and Johnson (1990) yields a similar value of $g_p/g_a = 5-7$. We note, however, that the earlier calculations which omit $4p-4h$ configurations have generally preferred higher values for g_p/g_a .

For ^{23}Na we took the results of Koshigiri *et al.* (1997) yielding $g_p/g_a = 6.6_{-2.4}^{+2.6}$. The authors used the full $1s-0d$ space with the Brown-Wildenthal interaction, and accounted for core polarization to first order and exchange currents from soft pions and Δ excitations. The results of Johnson *et al.* (1996) are similar to Koshigiri *et al.* (1997).

For ^{28}Si we took the results of Siiskonen *et al.* (1999) yielding $g_p/g_a = 1.0_{-1.2}^{+1.1}$. The authors used the full $1s-0d$ space with the Brown-Wildenthal interaction. They included core polarization corrections but omitted exchange current corrections. Note that Ciechanowicz *et al.* (1998) found that the effects of soft-pion exchange were negligible. For comparison, the earlier calculations of Ciechanowicz (1976) and Parthasarathy and Sridhar (1981) gave values for g_p/g_a of 3.3 ± 1.0 and $1.5_{-1.1}^{+0.9}$, respectively.

2. Model sensitivities of g_p/g_a

The interesting observables in allowed transitions are governed by ratios of nuclear matrix elements. More

specifically, in $0^+ \rightarrow 1^+$ transitions the observables are completely determined by, and in $3/2^\pm \rightarrow 1/2^\pm$ transitions the observables are strongly dependent on, the helicity amplitude ratio $X = \sqrt{2}T_0/T_1$.²⁷ Therefore understanding the model uncertainties in computing X is central to tracing the model dependences in recoil polarizations, γ -ray correlations, and hyperfine dependences. For example, see Junker *et al.* (2000).

Tables XII and XIII show the corrections that arise from $M_1 \boldsymbol{\sigma} \cdot \nabla$, $M_{12} \cdot \boldsymbol{\sigma}$, and $M_{11} \cdot \nabla$ to $L_1^5 - M_1^5$ (or T_0) and $T_1^{el5} - M_1^{mag}$ (or T_1) for the relevant transitions.²⁸ The tables show that $T_1^{el5} - M_1^{mag}$ is entirely dominated by $M_{10} \cdot \boldsymbol{\sigma}$. However, while $M_{10} \cdot \boldsymbol{\sigma}$ is the leading piece in the $L_1^5 - M_1^5$ term, the contributions from $M_1 \boldsymbol{\sigma} \cdot \nabla$ of about 30–40% and $M_{12} \cdot \boldsymbol{\sigma}$ of up to 25% are important. Clearly the leading source of model dependence in computing X is therefore uncertainties in the ratios of $M_1 \boldsymbol{\sigma} \cdot \nabla / M_{10} \cdot \boldsymbol{\sigma}$ and $M_{12} \cdot \boldsymbol{\sigma} / M_{10} \cdot \boldsymbol{\sigma}$, i.e., corrections arising from axial charge and second-forbidden effects.

Uncertainties in one-body transition densities are important sources of model dependencies in $M_1 \boldsymbol{\sigma} \cdot \nabla / M_{10} \cdot \boldsymbol{\sigma}$ and $M_{12} \cdot \boldsymbol{\sigma} / M_{10} \cdot \boldsymbol{\sigma}$. For example, let us consider the transitions on boron and carbon which involve the interference of a $0p_{3/2} \rightarrow 0p_{1/2}$ single-particle transition and a $0p_{1/2} \rightarrow 0p_{3/2}$ single-particle transition. Under the interchange of initial and final states the matrix element $M_{10} \cdot \boldsymbol{\sigma}$ changes sign but the matrix element $M_1 \boldsymbol{\sigma} \cdot \nabla$ does not. Consequently $M_1 \boldsymbol{\sigma} \cdot \nabla / M_{10} \cdot \boldsymbol{\sigma}$ is quite sensitive to the $0p_{1/2} \rightarrow 0p_{3/2}$ admixture in these $A = 11, 12$ transitions. Fortunately the destructive interference of $0p_{1/2} \leftrightarrow 0p_{3/2}$ amplitudes is also reflected in, and thus calibrated by, the capture rates of $^{11}\text{B}(3/2^-, 0) \rightarrow ^{11}\text{Be}(1/2^-, 320)$ and $^{12}\text{C}(0^+, 0) \rightarrow ^{12}\text{B}(1^+, 0)$.

²⁷Note that for $\Delta J^\pi = 1^+$ multipoles the helicity amplitude ratio $\sqrt{2}T_0/T_1$ and multipole amplitude ratio $\sqrt{2}(L_1^5 - M_1^5)/(T_1^{el5} - M_1^{mag})$ are identical.

²⁸There is a phase ambiguity in quoting the amplitudes in Tables XII and XIII. Only the relative sign of $L_1^5 - M_1^5$ and $T_1^{el5} - M_1^{mag}$ (i.e., the sign of X) is important in determining the various observables.

TABLE XIII. Comparison of the corrections from the terms involving $M_1\boldsymbol{\sigma}\cdot\nabla$, $M_{12}\cdot\boldsymbol{\sigma}$, and $M_{11}\cdot\nabla$ to the multipole amplitude of $T_1^{el5} - T_1^{mag}$ for $A=11, 12, 23$, and 28 and several effective interactions denoted CKPOT (Cohen and Kurath, 1967), PKUO (Kuo and Brown, 1966), USD (Wildenthal, 1984), and KUOSD (Kuo and Brown, 1966). The values in columns 4–6 correspond to the percentage change in the matrix elements as the correction terms are successively included. Note that $M_1\boldsymbol{\sigma}\cdot\nabla$ does not contribute to $T_1^{el5} - T_1^{mag}$.

A	Int.	$T_1^{el5} - T_1^{mag}$	$M_1\boldsymbol{\sigma}\cdot\nabla$ corr. (%)	$M_{12}\cdot\boldsymbol{\sigma}$ corr. (%)	$M_{11}\cdot\nabla$ corr. (%)
11	CKPOT	-0.243	0.0	0.9	0.6
11	PKUO	-0.222	0.0	-0.2	1.7
12	CKPOT	0.249	0.0	3.1	-0.4
12	PKUO	-0.164	0.0	5.4	2.1
23	USD	0.213	0.0	-1.4	-2.2
23	KUOSD	-0.170	0.0	-3.6	-4.8
28	USD	0.171	0.0	8.6	4.7
28	KUOSD	-0.106	0.0	4.2	0.7

A special comment is worthwhile for $^{28}\text{Si}(0^+, 0) \rightarrow ^{28}\text{Al}(1^+, 2201)$. The calculations indicate this transition involves the destructive interference of numerous single-particle transitions with comparable one-body densities; see Sec. IX.G.4 for details. Consequently, for ^{28}Si the calculation of X may be especially sensitive to the model uncertainties.

The inevitable truncation of model spaces, e.g., $0p$ orbitals for $A=11, 12$ and $1s-0d$ orbitals for $A=23, 28$, is another source of model dependence in $M_1\boldsymbol{\sigma}\cdot\nabla/M_{10}\cdot\boldsymbol{\sigma}$ and $M_{12}\cdot\boldsymbol{\sigma}/M_{10}\cdot\boldsymbol{\sigma}$. Such core polarization effects have been studied by Fukui *et al.* (1987) for ^{12}C , Siiskonen *et al.* (1999) for ^{28}Si , and Koshigiri *et al.* (1997) for ^{23}Na . For ^{12}C Fukui *et al.* (1987) found downward renormalizations of 13% for $M_{10}\cdot\boldsymbol{\sigma}$, 33% for $M_{12}\cdot\boldsymbol{\sigma}$, and 22% for $M_1\boldsymbol{\sigma}\cdot\nabla$, and for ^{28}Si Siiskonen *et al.* (1999) found downward renormalizations of 11% for $M_{10}\cdot\boldsymbol{\sigma}$, 30% for $M_{12}\cdot\boldsymbol{\sigma}$, and 39% for $M_1\boldsymbol{\sigma}\cdot\nabla$. The small effect of core polarization on $M_{10}\cdot\boldsymbol{\sigma}$ is because the model spaces are “complete spaces” for this operator. Note that the renormalization of $M_{10}\cdot\boldsymbol{\sigma}$ has strong support from experimental data on allowed β decay and $(p, n)/(n, p)$ reactions, and the renormalization of $M_{12}\cdot\boldsymbol{\sigma}$ has some support from experimental data on second-forbidden β decay. For example, see Warburton (1992) and Martínez-Pinedo and Vogel (1998).

The contributions arising from exchange currents in allowed transitions have been studied by Fukui *et al.* (1987) for ^{12}C , Ciechanowicz *et al.* (1998) for ^{28}Si , and Koshigiri *et al.* (1997) for ^{23}Na . For ^{12}C Fukui *et al.* (1987) found corrections of -4% to $M_{10}\cdot\boldsymbol{\sigma}$, +10% to $M_{12}\cdot\boldsymbol{\sigma}$, and +41% to $M_1\boldsymbol{\sigma}\cdot\nabla$. Recall that the large renormalization of the axial charge operator $M_1\boldsymbol{\sigma}\cdot\nabla$ arises from large soft-pion contributions in the axial current's time component. This renormalization is supported by experimental data on first-forbidden β decay.

The assumed form for the radial dependence of the nuclear wave functions is another source of model dependence, e.g., at the surface of the nucleus the difference in harmonic oscillator and Wood-Saxon wave functions are large. Such effects were investigated for ^{11}B by

Suzuki (1997) and ^{12}C , ^{23}Na , and ^{28}Si by Kortelainen *et al.* (2000). They found the sensitivity of X to the radial form of the nuclear wave function was typically 5% or less.

Last, we consider the determination of g_p/g_a from the capture rate of the $^{16}\text{O}(0^+, 0) \rightarrow ^{16}\text{N}(0^-, 120)$ transition. Note that this requires knowing the absolute values of $M_{01}\cdot\boldsymbol{\sigma}$ and $M_1\boldsymbol{\sigma}\cdot\nabla$, i.e., not ratios like $M_1\boldsymbol{\sigma}\cdot\nabla/M_{10}\cdot\boldsymbol{\sigma}$. Also the capture rate is highly sensitive to the $2p-2h$, $4p-4h$ structure of the ^{16}O ground state and the two-body contributions due to soft-pion exchange. Consequently, as discussed by Haxton and Johnson (1990) and Warburton *et al.* (1994), the extraction of g_p/g_a from $^{16}\text{O}(0^+, 0) \rightarrow ^{16}\text{N}(0^-, 120)$ is a formidable challenge. Indeed Warburton *et al.* (1994) have cautioned that their result for g_p/g_a is highly model dependent.

3. Conclusions and outlook for g_p/g_a

The results in Table XI are largely consistent with PCAC, ChPT, and $g_p/g_a = 6.50$. Specifically the values obtained from ^{11}B , ^{16}O , and ^{23}Na all support the prediction based on chiral symmetry arguments. The situation for ^{12}C is more borderline, with theory and experiment just under 2σ apart, but not enough to cause concern. In contrast, however, for ^{28}Si the experiment determination and theoretical prediction are in obvious disagreement.

Ignoring the puzzle of ^{28}Si for now, we believe the theoretical uncertainties in extracting g_p/g_a from these data are likely about ± 2 or so. For example, for recoil polarizations and γ -ray correlations the largest contribution to model uncertainties arises via corrections at the 30–40% level from the $M_1\boldsymbol{\sigma}\cdot\nabla$ operator. Although the matrix elements for this gradient operator are rather difficult to compute accurately, we note even a 50% uncertainty in $M_1\boldsymbol{\sigma}\cdot\nabla$ will produce only a 10–20% uncertainty in extracting g_p/g_a . A similar situation arises in extracting the coupling g_p/g_a from hyperfine dependences, although here the additional contributions from $\Delta J=2^+$ multipoles may increase somewhat the model uncertainty. However, the model uncertainty is probably

larger for $^{16}\text{O}(0^+,0) \rightarrow ^{16}\text{N}(0^-,120)$, since absolute values and not ratios of matrix elements are needed, and those required are quite difficult to accurately compute; see Sec. IX.G.5 for details.

The value of $g_p/g_a = 1.0_{-1.2}^{+1.1}$ from ^{28}Si is rather puzzling. Interestingly the experimental results for ^{12}C of $X = 0.26 \pm 0.06$ and ^{28}Si of $X = 0.55 \pm 0.04$ are quite different, while the theoretical predictions for ^{12}C and ^{28}Si are not, i.e., the calculated corrections arising from axial charge and second-forbidden operators are similar in ^{12}C and ^{28}Si . Inspection of the one-body transition densities for ^{12}C and ^{28}Si does indicate a difference in the two cases. Whereas for ^{12}C the transition is mainly $0p_{3/2} \rightarrow 0p_{1/2}$ with some $0p_{1/2} \rightarrow 0p_{3/2}$, for ^{28}Si the transition involves numerous single-particle transitions of similar magnitudes. Therefore sensitivity to the nuclear model for the $^{28}\text{Si}(0^+,0) \rightarrow ^{28}\text{Al}(1^+,2201)$ transition is likely larger. In addition we observe that the agreement of theory and experiment is good for the $^{12}\text{C}(0^+,0) \rightarrow ^{12}\text{B}(1^+,0)$ capture rate but poor for the $^{28}\text{Si}(0^+,0) \rightarrow ^{28}\text{Al}(1^+,2201)$ capture rate, indicating the Gamow-Teller matrix element is reproduced well for ^{12}C but reproduced poorly for ^{28}Si . For further details, see Goringe *et al.* (1999).

What new experimental and theoretical work is worthwhile? For partial transitions on complex nuclei a limiting factor is the small number of the available transitions, i.e., four allowed transitions and one first-forbidden transition. Given the unavoidable sensitivity to nuclear structure a larger data set of partial transitions would be helpful. With more data an improved understanding of contributions from $M_1 \sigma \cdot \nabla$ and $M_{12} \cdot \sigma$ is presumably possible. Unfortunately of course the experimental techniques for measuring recoil polarizations, gamma-ray correlations and hyperfine dependences are often limited to special cases. However, new experimental studies of muon capture on ^{20}Ne , ^{32}S , and ^{35}Cl are under way at TRIUMF and PSI.

Last, we suggest new work on $\mu + ^6\text{Li}(1^+,0) \rightarrow ^6\text{He}(0^+,0) + \nu$. This allowed Gamow-Teller transition, from the 1^+ ground state of ^6Li to the 0^+ ground state of ^6He , was considered theoretically by various authors. Mukhopadhyay (1972) calculated the statistical capture rate within the $0p$ shell model, and evaluated the contributions of the various weak couplings and the different multipole operators. He obtained a rate $\Lambda = 1813 \text{ s}^{-1}$ and observed it was entirely dominated by the Gamow-Teller operator $M_{01} \cdot \sigma$ with a sizable contribution from the coupling g_p . Additionally, Walecka (1976) has studied the capture rate and hyperfine dependence by first fixing the $^6\text{Li} \rightarrow ^6\text{He}$ one-body densities via related $A=6$ electroweak data. He obtained a capture rate $\Lambda = 1380 \text{ s}^{-1}$ and hyperfine dependence $\Lambda_+/\Lambda_- = 0.039$, and observed that Λ_+/Λ_- is strongly dependent on the coupling g_p but weakly dependent on the $M_1 \sigma \cdot \nabla$ operator (the latter in contrast to ^{11}B and ^{23}Na).

Unfortunately, the only $\mu + ^6\text{Li}(1^+,0) \rightarrow ^6\text{He}(0^+,0) + \nu$ data are an early measurement of the capture rate by Deutsch, Grenacs, Igo-Kemenes, *et al.* (1968) at

CERN. The experiment utilized the sequence of $\mu + ^6\text{Li} \rightarrow ^6\text{He} + \nu$ capture and $^6\text{He} \rightarrow ^6\text{Li} + e + \nu$ decay, by repeatedly exposing the ^6Li target to the muon beam and then detecting the ^6He activity in a shielded β -ray counter.²⁹ The authors obtained a capture rate $\Lambda = 1600_{-130}^{+330} \text{ s}^{-1}$, but unfortunately the accuracy was limited by the low signal rate and the large background rates. We encourage both a new measurement of the capture rate and a first measurement of the hyperfine dependence.

X. INCLUSIVE RADIATIVE MUON CAPTURE ON COMPLEX NUCLEI

Several factors have motivated investigations of inclusive radiative muon capture on complex nuclei. First, the radiative rate on complex nuclei is highly sensitive to g_p . Second, the branching ratios for nuclear radiative muon capture are comparatively large, e.g., the ^{12}C rate is about 100 times the ^1H rate and the ^{40}Ca rate is about 1000 times the ^1H rate. Third, the early theoretical studies implied the ratio of radiative capture to ordinary capture was only mildly model dependent.

We note comprehensive reviews that cover nuclear radiative muon capture were published by Mukhopadhyay (1977) and Gmitro and Truöl (1987). These authors have discussed in detail the formalism and methods for radiative muon capture calculations on complex nuclei. Herein we simply outline the major approaches, referring the reader to these reviews for more detail, and focus mainly on recent developments. We update the status of model calculations in Sec. X.A and experimental data in Sec. X.B. We discuss the interpretation of the radiative muon capture branching ratio data in Sec. X.C.

A. Theory of nuclear radiative muon capture

The theory of radiative muon capture in nuclei has a long history, dating back to Rood and Tolhoek (1965). Although they were not the first to consider the problem, they carefully laid out the approach which has become the standard in subsequent calculations. The standard approach to radiative muon capture in nuclei is to develop a nonrelativistic Hamiltonian for the process which is then evaluated in impulse approximation (IA) between nuclear states. There are thus two main ingredients, the Hamiltonian and nuclear structure.

In the usual approach the Hamiltonian is derived from the same five diagrams, Figs. 3(a)–(e), used to describe capture on the nucleon. This Hamiltonian, which originates as a relativistic amplitude, is then expanded in powers of the nucleon momentum either directly, or using a Foldy-Wouthuysen procedure. The leading order is independent of the nucleon momentum and the linear order correction is typically 10–20 % and is neglected in many calculations. The correction to the nonrelativistic

²⁹The ^6He beta decay has a lifetime of 0.8 s and an end-point energy of 3.5 MeV.

Hamiltonian from the terms quadratic in the nucleon momentum was considered by Sloboda and Fearing (1980) and found to be very small.

This single-particle Hamiltonian is then summed over all nucleons and matrix elements of the result are taken between nuclear states. In early calculations very crude nuclear states were used, e.g., a simple Slater determinant of harmonic oscillator wave functions. In recent calculations, however, more modern shell-model wave functions have been used which are derived using more realistic interactions.

The muon deposits a lot of energy in the nucleus and thus there can be many levels excited in the final nucleus. However, all measurements so far are of the inclusive rate, and so a technique must be developed to sum over all final states. In early calculations closure was used. However, this introduces a new parameter k_{\max} corresponding to the average maximum photon energy, or equivalently the average nuclear excitation. Unfortunately the rate is just as sensitive to k_{\max} as to g_p . Furthermore, as pointed out by Christillin (1981), the closure sum includes many excited states which are not allowed in the radiative process due to energy conservation.

There have been several approaches to attempt to bypass this problem. One approach involves obtaining the spectrum of excited states from some other source. Foldy and Walecka (1964) did this for ordinary muon capture, by recognizing that much of the strength went to the giant dipole resonance state and that one could get this strength from empirical photoabsorption cross sections.³⁰ This idea was generalized to radiative muon capture by Fearing (1966) and further generalized by Christillin (1981) who added additional phenomenological components to account for transitions to quadrupole states. This approach lessened the dependence on k_{\max} but did not totally eliminate it, as there were still matrix elements, e.g., the leading p/m corrections which could not be obtained this way.

Another approach involved sum rules, in which various matrix elements were evaluated using energy weighted sum rules. This approach was considered, for example, by Sloboda and Fearing (1978) and more recently applied to ordinary muon capture by Navarro and Krivine (1986). It was developed further and used more recently for radiative muon capture by Roig and Navarro (1990). While still somewhat phenomenological, and still depending to some extent on the closure approximation, this approach is much less sensitive to average excitation energies than the closure approximation.

In principle, the best method is to calculate explicitly transitions to all possible excited states and sum the results. This takes the energy dependence into account properly, which can be important (Fearing and Welsh,

1992). One must always truncate the sum somewhere, however, which, in principle, introduces errors. Modern shell-model codes are good enough, however, to produce enough of the excited states so that for at least some nuclei the important transitions can be calculated and summed. Most recent calculations (Gmitro *et al.*, 1986, 1990, 1991; Eramzhyan *et al.*, 1998) have used this approach.

One can also attempt to modify or improve the basic Hamiltonian. Recall that the standard Hamiltonian (Rood and Tolhoek, 1965) is a single-particle operator coming from the same basic five diagrams, Figs. 3(a)–(e), used for radiative muon capture on the proton. In principle, one should include various meson exchange corrections, which lead to two-body operators, in the same fashion as has been done for ordinary muon capture in light nuclei (see Sec. IX.F.3). To our knowledge this has not been done, at least recently, for heavy nuclei.

An alternative approach is to look at these meson exchange corrections as effects of the intermediate pion rescattering in the nuclear medium. This leads to a renormalization of the effective couplings in the nuclear medium. This approach has a long and involved history, and applies to a number of processes involving axial current matrix elements. It is a bit outside the scope of this review, however. The reader interested in pursuing this further can consider the recent papers of Kirchbach and Riska (1994) or Kolbe *et al.* (2000) or older studies such as that of Akhmedov *et al.* (1985).

Still another attempt to modify the basic Hamiltonian has been proposed by Gmitro *et al.* (1986). The idea here is to use current conservation to evaluate parts of the matrix element. This is analogous to the Siegert theorem approach which has been used for other processes, and originates in the observation that the nuclear matrix element of the impulse approximation Hamiltonian, unlike the nucleon matrix element, does not correspond to a conserved current. An attempt is made to fix this by expanding the photon field and using the continuity equation to eliminate parts of the three-vector current in favor of the charge distribution. This leads to some different terms and to what the authors call a modified impulse approximation (MIA).

Calculations using this modified impulse approximation suggest that it is extremely important (Gmitro *et al.*, 1986, 1990, 1991; Eramzhyan *et al.*, 1998). It reduces the radiative muon capture rate by a factor of 2 or more and thus increases the value of g_p needed to fit a given experimental result rather dramatically. The approach also seems to produce rates which are much less sensitive to g_p than the impulse approximation. It does, however, suppress the usual impulse approximation results so that they are in better agreement with phenomenological approaches. However, there are some caveats. The very fact that what is effectively enforcing gauge invariance makes such a huge difference is worrisome. The results also depend, though not strongly, on an arbitrary choice among various ways to make the original expansion of the photon field. It also appears that one is using the

³⁰Later calculations extended this to consider SU_4 breaking and the excitation of the spin dipole state by the axial current; see, for example, Cannata *et al.* (1970).

continuity equation on only part of the current, still leaving some reference to the three-vector current in the problem. Clearly this needs to be looked at more carefully to determine if it is indeed correct since it makes such a large difference in the final results.

Finally, we should mention one other modern calculation (Fearing and Walker, 1989; Fearing and Welsh, 1992) which uses a relativistic Fermi gas model together with relativistic mean-field theory to examine the A and Z dependence of the radiative and ordinary muon capture rates. The Fermi gas model was used in very early calculations, but is clearly too crude a model to give good results for specific details for individual nuclei. It does, however, allow one to elucidate general trends and select out features which are important. This will be discussed further in the next section.

B. Measurement of nuclear radiative muon capture

The first observation of radiative capture was made at CERN by Conforto *et al.* (1962). Muons were stopped in Fe and photons were detected by gamma-ray conversion in an iron sheet/spark chamber sandwich and energy deposition in a large volume NaI crystal. After subtraction of backgrounds a total of five photons from radiative muon capture on Fe were identified and yielded a Fe radiative muon capture branching ratio of roughly 10^{-4} . During the following ten years a few more studies of nuclear radiative muon capture were conducted by Conversi *et al.* (1964), Chu *et al.* (1965), and Rosenstein and Hammerman (1973). However, the measurements remained extremely difficult because of the low signal rate and the high background rates. In particular undercounted neutron backgrounds most likely corrupted these early experiments.

More recently the availability of higher-quality muon beams and higher performance pair spectrometers has dramatically improved the experimental situation. The new era for nuclear radiative muon capture was pioneered by Hart *et al.* (1977) for radiative muon capture on Ca. Later experimental programs at PSI in the late 1980s and TRIUMF in the early 1990s have produced an extensive body of nuclear radiative muon capture data. Today's beams and detection systems allow data collection on $Z > 12$ targets at count rates of ~ 1000 radiative muon capture photons/day with nearly background-free conditions.

In principle, the method for determining the branching ratio for nuclear radiative muon capture is straightforward. It simply requires counting the incoming muons and outgoing photons and determining their detection efficiencies. However, as discussed in detail in Sec. V.C.4 the small branching ratio means troublesome γ -ray backgrounds arise from μ decay in the target material, radiative μ capture in the neighboring materials, and the pion contamination in the muon beam. Additionally, neutron backgrounds from ordinary capture in the target material and other sources on the accelerator site are dangerous if the n/γ discrimination is not highly effective.

Two basic types of pair spectrometers have been widely employed in the radiative muon capture studies of recent years. In one approach, as used by Frischknecht *et al.* (1988), the photons are converted in a relatively thin passive converter and the e^+e^- pair is tracked in a multiwire chamber arrangement. In another approach, as used by Döbeli *et al.* (1988), the photons are converted in a relatively thick active converter and the e^+e^- pair is measured by combinations of Cherenkov detectors and NaI crystals. The former approach offers good resolution, typically 1–2%, but at the expense of a low efficiency, typically 10^{-5} . The latter approach offers high efficiency, typically 0.5%, but at the expense of a poor resolution, typically 20%. Such experimental setups have yielded excellent n/γ discrimination and provided nearly background-free radiative muon capture spectra.

Most recently a novel large solid-angle pair spectrometer was developed at TRIUMF by Wright *et al.* (1992) for radiative muon capture on ^1H . The spectrometer offers both a relatively high detection efficiency and a relatively good energy resolution. It has permitted quick and straightforward measurements of nuclear radiative muon capture for numerous targets, and significantly extended the radiative muon capture data set (Armstrong *et al.*, 1992; Gorringer *et al.*, 1998; Bergbusch *et al.*, 1999).

C. Interpretation of nuclear radiative muon capture

The world data set³¹ for nuclear radiative muon capture, consisting of targets from carbon to bismuth, is summarized in Table XIV in which we tabulate the ratio R_γ of the $E_\gamma > 57$ MeV partial radiative rate to the total ordinary rate. In addition, we plot the data versus atomic number Z in Fig. 8 and versus neutron excess $\alpha = (A - 2Z)/Z$ in Fig. 9. The figures illustrate some intriguing trends, i.e., that R_γ is observed to decrease from ~ 2 to ~ 0.6 with increasing Z and increasing α .³² Note that the overall trend is somewhat smoother with neutron excess than atomic number. Specifically, the isotope effect in the mass $^{58,60,62}\text{Ni}$ isotopes and the odd/even- A effect in the Al-Si, Ca-Ti pairs fit the α dependence but not the Z dependence. Below we discuss the R_γ data in the context of the determination of the coupling g_p .

For ^{40}Ca the value of R_γ is well established by numerous experiments. The average of those included in Table XIV is $R_\gamma = 2.08 \pm 0.11$. A number of calculations are available including the phenomenological models of Fearing (1966) and Christillin (1981), the microscopic shell-model calculations of Gmitro *et al.* (1986), and the sum-rule calculations of Roig and Navarro (1990). Un-

³¹We omit the results from the early experiments of Conversi *et al.* (1964), Chu *et al.* (1965), and Rosenstein and Hammerman (1973) due to large neutron backgrounds. Also we omit the case of radiative muon capture on ^3He that is discussed in detail in Sec. VII.C.

³²Note that in this section we will quote all values of R_γ in units of 10^{-5} .

fortunately, as discussed earlier, the calculation of inclusive radiative muon capture on complex nuclei is notoriously difficult. It is often difficult to quantify the effect of the various approximations and assumptions and so to set limits on the uncertainty in the theoretical predictions.

The phenomenological calculations of Christillin (1981), based on the giant dipole resonance model (Foldy and Walecka, 1964; Fearing, 1966) with parameters determined from electromagnetic data but including effects of a quadrupole resonance with parameters fit to the ordinary muon capture rate, gave $R_\gamma=2.4$ using the canonical value $g_p/g_a\approx 6.7$. The calculation of Roig and Navarro (1990) used fairly realistic random-phase approximation (RPA) wave functions but with the phenomenological aspects of a sum-rule calculation to obtain $R_\gamma=1.87$. The microscopic shell-model calculation of Gmitro *et al.* (1986) used simple $1p-1h$ wave functions, with some corrections to obtain $R_\gamma=4.25$ in the standard impulse approximation and $R_\gamma=2.28$ in the modified impulse approximation. Thus the modified impulse approximation makes a large difference, and brings the results in closer agreement with the more phenomenological approaches. Note that all of these calculations, except the standard impulse approximation approach, apparently neglected the velocity or p/m terms which could be up to 10–20 %.

On a superficial level all of these results, except perhaps for the standard impulse approximation result, are reasonably consistent with the experimental result. However, if one turns the question around and asks what limits are set on g_p/g_a things become much less clear. A theoretical value of R_γ less than the experiment implies a larger value of g_p/g_a is needed to fit the data. Thus the sum-rule calculation of Roig and Navarro (1990) requires $g_p/g_a\sim 8$. On the other hand, the phenomenological calculations of Christillin (1981) and the modified impulse approximation results of Gmitro *et al.* (1986) require $g_p/g_a\sim 4-5$ and the impulse approximation result implies that g_p/g_a is much smaller. Thus one has to conclude that it is unreasonable to claim that $g_p/g_a\sim 6.7$ is well established by radiative muon capture on ^{40}Ca .

For ^{16}O a number of measurements and calculations are also available. Unfortunately, measurement of radiative muon capture on ^{16}O is more difficult, since the γ -ray yield per μ^- stop is $\sim 2\times 10^{-5}$ for ^{40}Ca and $\sim 0.4\times 10^{-5}$ for ^{16}O , and most probably the earlier experiments have undersubtracted contamination from γ -ray backgrounds. Therefore we employ the recent result from Bergbusch *et al.* (1999) of $R_\gamma=1.67\pm 0.18$. Like ^{40}Ca , both phenomenological calculations and microscopic calculations are available, but similarly the sensitivities of results to approximations are difficult to estimate. Taking $g_p/g_a\approx 6.7$ the phenomenological calculation of Christillin and Gmitro (1985) gave $R_\gamma=2.08$, the shell-model calculation of Gmitro *et al.* (1986) gave $R_\gamma=1.61$ in modified impulse approximation and $R_\gamma=3.10$ in impulse approximation, and sum-rule calculation of Roig and Navarro (1990) gave R_γ

TABLE XIV. Summary of the world data on the quantity R_γ on $A>3$ targets, where R_γ is the ratio of the radiative muon capture rate with $E_\gamma>57$ MeV to the ordinary muon capture rate in units of 10^{-5} . In order to assist comparisons in most cases the quoted results are for the closure approximation spectra shape where the corresponding value of the parameter k_{max} is given in column 4. The quantity α is the neutron excess $(A-2Z)/Z$.

Target	α	$R_\gamma (\times 10^{-5})$	k_{max} (MeV)
Bergbusch <i>et al.</i> (1999)			
$^{16}_8\text{O}$	0.000	1.67 ± 0.18	88.4 ± 2.3
$^{27}_{13}\text{Al}$	0.077	1.43 ± 0.11	90.1 ± 1.8
$^{28}_{14}\text{Si}$	0.000	2.09 ± 0.20	89.4 ± 1.8
$^{nat}_{22}\text{Ti}$	0.173	1.30 ± 0.12	89.2 ± 2.0
$^{nat}_{40}\text{Zr}$	0.280	1.31 ± 0.15	89.2 ± 3.4
$^{nat}_{47}\text{Ag}$	0.296	1.12 ± 0.13	89.0 ± 3.2
Gorringer <i>et al.</i> (1998)			
$^{58}_{28}\text{Ni}$	0.071	1.48 ± 0.08	92.0 ± 2.0
$^{60}_{28}\text{Ni}$	0.143	1.39 ± 0.09	90.0 ± 2.0
$^{62}_{28}\text{Ni}$	0.214	1.05 ± 0.06	89.0 ± 2.0
Armstrong <i>et al.</i> (1992)			
$^{27}_{13}\text{Al}$	0.077	1.43 ± 0.13	90.0 ± 2.0
$^{28}_{14}\text{Si}$	0.000	1.93 ± 0.18	92.0 ± 2.0
$^{40}_{20}\text{Ca}$	0.000	2.09 ± 0.19	93.0 ± 2.0
$^{nat}_{42}\text{Mo}$	0.283	1.11 ± 0.11	90.0 ± 2.0
$^{nat}_{50}\text{Sn}$	0.374	0.98 ± 0.09	87.0 ± 2.0
$^{nat}_{82}\text{Pb}$	0.527	0.60 ± 0.07	84.0 ± 3.0
Armstrong <i>et al.</i> (1991)			
$^{12}_6\text{C}$	0.000	1.98 ± 0.20	
$^{16}_8\text{O}$	0.000	2.18 ± 0.20	
$^{40}_{20}\text{Ca}$	0.000	2.04 ± 0.14	
Frischknecht <i>et al.</i> (1988)			
$^{16}_8\text{O}$	0.000	3.80 ± 0.40	
Döbeli <i>et al.</i> (1986)			
$^{12}_6\text{C}$	0.000	2.70 ± 1.80	
$^{16}_8\text{O}$	0.000	2.44 ± 0.47	89.9 ± 5.0
$^{27}_{13}\text{Al}$	0.077	1.83 ± 0.26	88.8 ± 1.8
$^{40}_{20}\text{Ca}$	0.000	2.30 ± 0.21	92.5 ± 0.7
$^{nat}_{26}\text{Fe}$	0.146	1.71 ± 0.17	90.2 ± 1.1
$^{165}_{67}\text{Ho}$	0.463	0.75 ± 0.13	84.1 ± 5.1
$^{209}_{83}\text{Bi}$	0.518	0.62 ± 0.08	88.2 ± 0.6
Frischknecht <i>et al.</i> (1985)			
$^{40}_{20}\text{Ca}$	0.000	1.92 ± 0.20	90.8 ± 0.9
Hart <i>et al.</i> (1977)			
$^{40}_{20}\text{Ca}$	0.000	2.11 ± 0.14	86.5 ± 1.9

$=1.73$. Again, with the exception of the impulse approximation result, these are reasonably consistent with the experimental result (Bergbusch *et al.*, 1999) $R_\gamma=1.67\pm 0.18$ with the sum rule and modified impulse approximation approaches implying roughly the canonical value of g_p/g_a and the approach of Christillin and Gmitro (1985) requiring a somewhat smaller value. The impulse approximation result would require a significantly smaller value to fit the data. However, like radiative muon capture on ^{40}Ca , due to the approximations in

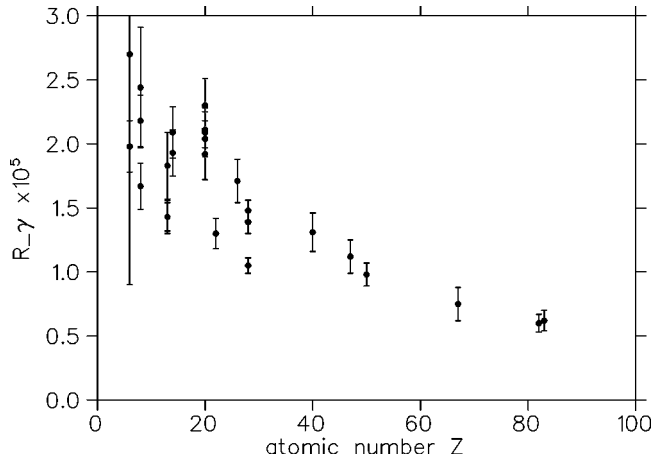


FIG. 8. The world data for R_γ versus Z on $A > 3$ nuclei.

the calculations and the differences among the results of different calculations the case for $g_p/g_a \sim 6.7$ in radiative muon capture on ^{16}O is not firmly established.

There are also both theoretical and experimental results for ^{12}C . The most recent result, and the one with by far the smallest uncertainty, is that of Armstrong *et al.* (1991), $R_\gamma = 1.98 \pm 0.20$. This is to be compared with the sum-rule result (Roig and Navarro, 1990) of $R_\gamma = 1.42$, and the impulse approximation result, $R_\gamma = 3.60$, and the modified impulse approximation result, $R_\gamma = 1.48$ (Gmitro *et al.*, 1990). In this case both modified impulse approximation and sum rule results are too low, implying $g_p/g_a \sim 10$ – 13 , to fit the data whereas the impulse approximation is too high, implying a very low value of g_p/g_a .

Finally we should mention the calculations for $^{58,60,62}\text{Ni}$ of Eramzhyan (1998) carried out in a microscopic model using the quasiparticle RPA. Again the impulse approximation results for R_γ are much higher than those in modified impulse approximation, but even the modified impulse approximation results are significantly higher than the experiment (Gorringer *et al.*, 1998).

Thus by now there have been a number of experiments and enough calculations that we can make comparisons of R_γ for several different nuclei. The situation can only be described as confused. The standard impulse approximation calculations are consistently too high, implying a value of g_p/g_a much smaller than the canonical value. The modified impulse approximation starts out too low for ^{12}C , implying a large value of g_p/g_a , and rises with increasing A to become significantly too high for the Ni isotopes, implying there a small value of g_p/g_a . The phenomenological calculations of Christillin (1981) and Christillin and Gmitro (1985) for ^{16}O and ^{40}Ca are both too high and the sum-rule calculations show no consistent pattern. It appears clear that we are not yet at a stage where theoretical uncertainties are sufficiently under control to consistently reproduce experimental results.

In addition to discussing the detailed calculations for specific nuclei it is worthwhile to consider the systematics of radiative muon capture data versus atomic number

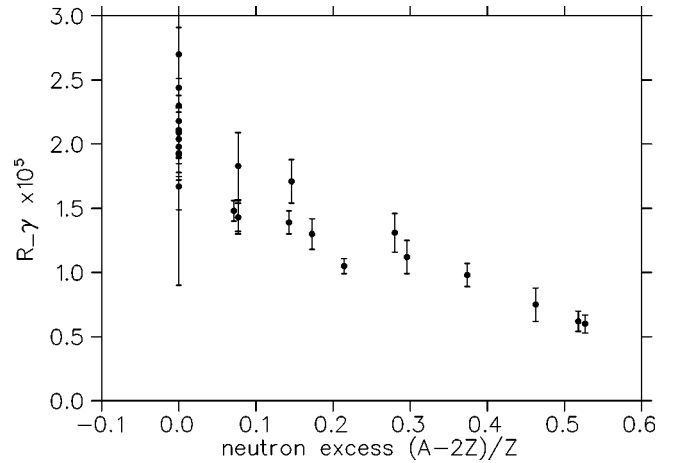


FIG. 9. The world data for R_γ versus $\alpha = (A - 2Z)/Z$ on $A > 3$ nuclei.

and neutron excess. Such systematics were examined in the nonrelativistic Fermi-gas calculation of Christillin *et al.* (1980) and the relativistic Fermi-gas calculation of Fearing and Welsh (1992). These models clearly oversimplify the nuclear structure, for example, omitting the important effects of giant resonances in muon capture, or the effects of shell closures. However, they demonstrate a number of interesting dependences of muon capture on Z and α .

For concreteness we consider the calculation of Fearing and Welsh (1992). These authors have carefully studied the dependence of inclusive ordinary muon capture and inclusive radiative muon capture on the input parameters and the model assumptions. They stress that the ordinary muon capture rate, the radiative muon capture rate, and their ratio, are highly sensitive to phase-space effects, i.e., things that alter the available energy for the neutrino and the photon. For example, including the μ^- atomic binding energy, which increases from ~ 0.1 MeV in light nuclei to ~ 10 MeV in heavy nuclei, decreases the ordinary muon capture rate by a factor of 2 and the radiative muon capture rate by a factor of 8 for the heaviest nuclei. Other parameters, e.g., for Fermi-gas models the Coulomb energy, symmetry energy, etc., also have large effects on the available energy and therefore the rates. Consequently, the authors caution that reliably extracting the coupling g_p from inclusive radiative muon capture on complex nuclei is difficult.

Despite such concerns, the calculation of Fearing and Welsh (1992) does reproduce the overall dependence of R_γ data with Z and α . This model-data agreement, however, suggests no reason to invoke a large-scale medium modification of g_p/g_a to explain the Z dependence of R_γ data.

Earlier suggestions for an A dependence of the coupling g_p , as discussed by Gmitro and Truöl (1987) and Döbeli *et al.* (1988), were largely grounded in large values of g_p/g_a obtained from shell-model calculations on light nuclei and small values of g_p/g_a obtained from Fermi-gas calculations on heavy nuclei. Given the differ-

ent systematics of the various models and the difficulty of all models in consistently fitting the data, such differences do not provide real evidence for an A dependence of the coupling g_p .

In summary, although the radiative muon capture rate on complex nuclei is undoubtedly g_p dependent, the problem of separating the coupling constant and nuclear structure is extraordinarily tricky. While the overall features of nuclear radiative muon capture are generally accommodated by $g_p/g_a=6.7$ there is a model uncertainty of at least 50%. Thus inclusive radiative muon capture on complex nuclei is not competitive with radiative muon capture or ordinary muon capture in hydrogen or few body systems in the determination of the coupling g_p .

For inclusive radiative muon capture on complex nuclei we find the progress on model calculations is lagging the progress on experimental data, and a breakthrough on the theoretical side is needed before this particular tool for studying the coupling is competitive. However, exclusive radiative muon capture on complex nuclei, which is so far unmeasured, might offer interesting possibilities.

XI. OTHER OBSERVABLES IN MUON CAPTURE

A. Neutron asymmetries in nuclear ordinary muon capture

A further topic that attracted some attention as a possible probe of the coupling g_p was the angular distribution of the neutrons emitted in the muon capture process. During the 1960s it generated some excitement with suggestions of a large neutron asymmetry and speculations of an unexpected large induced pseudoscalar coupling. However, with more modern experimental work and more sophisticated theoretical work these puzzles were resolved, and interest in neutron asymmetry measurements for determining the induced pseudoscalar coupling has waned.

Specifically the neutron asymmetry about the μ -spin direction has the form

$$\Lambda(\theta) \propto 1 + \alpha P_\mu \cos \theta, \quad (52)$$

where P_μ is the muon residual polarization, α is the neutron asymmetry coefficient, and θ is the angle between the μ -spin vector and the neutron momentum vector. As such the neutron asymmetry is another manifestation of parity violation in muon capture.

The neutron asymmetry in capture on hydrogen was first calculated by Huang, Yang, and Lee (1957) and Shapiro, Dolinsky, and Blokhintsev (1957). The authors observed the asymmetry coefficient was fairly sensitive to the ratio of the couplings g_p/g_a ; for example, with $g_p/g_a=8$ yielding $\alpha=-0.4$ and with $g_p/g_a=0$ yielding $\alpha=-0.2$. Unfortunately, as discussed in detail in Sec. IV, the muon polarization in muonic hydrogen is completely destroyed by the hyperfine transitions from the μp triplet state to the μp singlet state, a process taking roughly 100 ps in liquid H_2 and roughly 10 ns in 10-bar H_2 gas. Thus emission of neutrons from capture on hydrogen is

isotropic,³³ which precludes the measurement of the asymmetry α in the elementary process.

In contrast, in nuclear muon capture on spin-zero targets a significant fraction ($\sim 15\%$) of the initial polarization of the incident muons is retained (see Sec. IX.B.2), and neutron asymmetry measurements following nuclear muon capture are therefore experimentally feasible. Of course, the emission of neutrons is considerably more complicated in muon capture on complex nuclei, one expecting both relatively high-energy, direct neutrons from the elementary process $\mu p \rightarrow n \nu$ in the nuclear medium and relatively low-energy, indirect neutrons that are “boiled off” in the subsequent decay of the particle unstable capture products. For direct neutrons the neutron asymmetry is expected to reveal the neutron asymmetry of the elementary $\mu p \rightarrow n \nu$ process, whereas for indirect neutrons the neutron asymmetry is expected to vanish as the neutrons have no memory of the elementary $\mu p \rightarrow n \nu$ process. Of course, in reality the division between direct neutron production and indirect neutron production is a very naive picture of a very complex process.

A number of authors have investigated the resulting asymmetry of direct neutrons from muon capture on spin-zero nuclei, and particularly its sensitivity to g_p/g_a . For example, Primakoff (1959) considered a two-step mechanism that involved the recoil nucleus production $\mu + [A, Z] \rightarrow [A, Z-1]^* + \nu$ and its single neutron decay $[A, Z-1]^* \rightarrow [A-1, Z-1]^{**} + n$. Primakoff used the closure approximation to estimate the asymmetry of the recoil nucleus averaged over all final states, and argued that the recoil asymmetry is then translated into the neutron asymmetry for the high-energy neutrons. He thereby predicted a large neutron asymmetry of $\alpha = -0.4$ with significant sensitivity to g_p/g_a . These conclusions were supported by specific calculations of neutron asymmetries in muon capture, e.g., for ^{16}O and ^{40}Ca by Dolinsky and Blokhintsev (1959). Such results thus generated much interest in the use of the neutron asymmetry α as a probe of the induced coupling g_p .

The first measurements of neutron asymmetries in muon capture were made by Baker and Rubbia (1959) on magnesium and Astbury *et al.* (1959) on silicon. However, the experiments were difficult because of the small muon residual polarization and the challenging gamma/neutron discrimination. The results of Astbury *et al.* (1959) favored a negative asymmetry coefficient (consistent with Primakoff’s prediction) whereas the results of Baker and Rubbia (1959) favored a positive asymmetry coefficient (inconsistent with Primakoff’s prediction). Subsequently, an extensive series of asymmetry measurements on various targets was conducted by Evseev and co-workers at JINR [see, for example, Evseev *et al.* (1963, 1967)]. These experiments suggested a negligible asymmetry for low-energy neutrons but a large negative asymmetry for high-energy neutrons. In

³³With the exception of the brief period before the triplet state is fully depopulated.

deed, for neutrons with energies $E > 20$ MeV the authors concluded the asymmetry coefficient approached $\alpha = -1$. Such a large asymmetry was very surprising, and prompted some speculations about either a very large induced pseudoscalar coupling or a nonzero induced tensor coupling (Yovnovich and Evseev, 1963).

Since these early measurements of neutron asymmetries two further studies, one by Sundelin and Edelstein (1973) at Carnegie-Mellon using Si, S, and Ca targets and one by Kozlowski *et al.* (1985) at PSI using O, Si, Ca, and Pb targets, have been published. The authors took advantage of the improved techniques and the modern facilities of the 1970s and 1980s. Incoming muons were counted in a beam telescope and stopped in the target material, and the outgoing neutrons were detected in liquid scintillator counters with n/γ separation based on pulse-shape discrimination. The muon spin was rotated in a transverse magnetic field and the neutron asymmetry was extracted from the resulting precession curve. The experiments found a positive neutron asymmetry, falling from $\alpha \approx +0.3$ for the higher-energy neutrons to $\alpha \approx 0$ for the lower-energy neutrons. The different targets gave similar results.

Paralleling the more modern experimental studies were more modern theoretical studies of neutron asymmetries from muon capture on complex nuclei. As a result it was found that some underlying assumptions of the earlier investigations were either too rough or not valid. First, in the earlier theoretical work the momentum-dependent pieces in the Fujii-Primakoff Hamiltonian were ignored. Bogan (1969) subsequently showed for higher-energy neutrons the momentum-dependent terms are non-negligible, these terms changing the asymmetry's sign. Second, in the earlier theoretical work it was claimed that the effects of the final-state interaction between the ejected neutron and the recoiling nucleus were small. Bouyssy and Vinh Mau (1972) subsequently showed that this conclusion was not correct, with such effects increasing the magnitude of the neutron asymmetry. Also, significant sensitivities to the muonic wave function, nuclear wave functions, and channel coupling effects were uncovered by Kume *et al.* (1975).

The outcome of the various experimental and theoretical efforts on neutron asymmetries is the positive asymmetry for the high-energy neutrons of $\alpha \approx +0.3$ is nowadays both experimentally established and theoretically understood. However, unfortunately, the various sensitivities to momentum dependent terms, final-state interactions, etc., are such to introduce too many uncertainties and too many parameters to permit the determination of g_p from neutron asymmetry measurements on complex nuclei.

B. Photon asymmetries in nuclear radiative muon capture

In radiative muon capture the gamma-ray direction and muon polarization are correlated according to

$$\Lambda(\theta) \propto 1 + \alpha P_\mu \cos \theta, \quad (53)$$

where P_μ is the muon polarization, α is the asymmetry coefficient, and θ is the angle between the μ -spin axis and the γ -ray momentum axis. The left handedness of the neutrino leads to $\alpha \approx +1$, and g_p is manifest as departures of α from unity (Fearing, 1975). The specific dependence of α on g_p/g_a for radiative muon capture on ^{40}Ca was computed by Rood and Tolhoek (1965), Christillin (1981), and Gmitro *et al.* (1981, 1987).

To measure the asymmetry one stops the incoming muons in a suitable target, precesses the muon spin in a magnetic field, and measures the time spectrum of the outgoing photons. The resulting time spectrum consists of an exponential decay with a sinusoidal modulation, where the amplitude of the sine wave is governed by the product $P_\mu \alpha$. Note that the time spectrum of the Michel electrons is employed to measure P_μ and isolate α . In the first measurement by di Lella *et al.* (1971) the authors used a single NaI crystal for γ -ray detection. In the later measurements by Hart *et al.* (1977), Döbeli *et al.* (1986), and Virtue *et al.* (1990) the authors used a separate γ -ray converter and NaI calorimeter. A ^{40}Ca target was used in each experiment.

The experimental difficulties originate from the tiny radiative muon capture branching ratio and the small μ residual polarization. Consequently the backgrounds are severe. They include γ rays from pion capture in the target, γ rays from Michel bremsstrahlung in the target, neutrons from muon capture in the target, and n/γ backgrounds from cosmic-ray and accelerator sources. Note that a prompt cut reduces the γ rays following π capture and a $E > 57$ MeV cut reduces the bremsstrahlung following μ decay. The neutron background is reduced via the converter-calorimeter setup and cosmic-ray background is reduced via combined passive and active shielding.

In Table XV we summarize the results of Hart *et al.* (1977), Döbeli *et al.* (1986), and Virtue *et al.* (1990). We omit the earliest results of di Lella *et al.* (1971), which suffered severe neutron backgrounds. The various experiments are mutually consistent and yield a world average value $\alpha = 1.02 \pm 0.25$.

Unfortunately the effect of g_p on α is (i) not large and (ii) model dependent. For example, with $g_p/g_a \approx 6.7$ the phenomenological model of Christillin (1981) gives $\alpha \approx 0.80$ and the shell model of Gmitro *et al.* (1987) gives $\alpha \approx 0.90$. Conservatively the measurements yield $g_p/g_a < 20$.

XII. SUMMARY

The determination of g_p is important for several reasons. First, whereas the values of the proton's other weak couplings are nowadays well determined, the induced pseudoscalar coupling is still poorly determined. Second, based on chiral symmetry arguments a solid theoretical prediction for g_p with 2–3 % accuracy is available. Third, the prediction is founded on some elementary symmetries of the standard model, and determining the coupling is therefore an important test of quantum chromodynamics at low energies.

TABLE XV. Summary of the world data on the photon asymmetry in radiative capture on calcium.

Ref.	Asymmetry α
Hart <i>et al.</i> (1977)	0.90 ± 0.50
Döbeli <i>et al.</i> (1986)	0.90 ± 0.43
Virtue <i>et al.</i> (1990)	$1.32^{+0.54}_{-0.47}$
World average	1.02 ± 0.25

Since the classic review of Mukhopadhyay (1977) an extensive body of experimental data on the coupling g_p has been accumulated. This work spans the elementary processes of ordinary muon capture and radiative muon capture on hydrogen, muon capture on few body systems, and exclusive ordinary muon capture and inclusive radiative muon capture on complex nuclei. The experimental approaches have ranged from ultrahigh precision measurements to ultrarare process measurements, and include some novel studies of spin phenomena in complex nuclei. The disentangling of the couplings from the physical observables has involved diverse fields from muon chemistry to traditional nuclear structure and modern effective-field theories.

One would expect muon capture on hydrogen to be the most straightforward and most easily interpreted of the muon capture reactions. This is the situation from the nuclear perspective, but unfortunately there exist atomic and molecular complications which also must be thoroughly understood. For ordinary muon capture there are several older experiments together with the most recent and precise measurement of Bardin *et al.* (1981a) whereas for radiative muon capture there is only the TRIUMF experiment (Wright *et al.*, 1998). To extract g_p from these results we updated the theoretical calculations to include the current best values of the other weak couplings and their q^2 dependences. Additionally, we updated the capture rate of Bardin *et al.* (1981a) for the present world average value of the positive muon lifetime. We found, for the standard values of the muon chemistry parameters and specifically with $\Lambda_{op} = 4.1 \times 10^4 \text{ s}^{-1}$, values of $g_p = 12.2 \pm 1.1$ from the TRIUMF radiative muon capture experiment (Wright *et al.*, 1998), $g_p = 10.6 \pm 2.7$ from the Saclay ordinary muon capture experiment (Bardin *et al.*, 1981a), and $g_p = 10.5 \pm 1.8$ for the world average of all ordinary muon capture experiments. These updates increased the value of g_p from ordinary muon capture, as compared to the original analysis, so that now both ordinary muon capture and radiative muon capture give results larger than expected from chiral symmetry based arguments, and in fact agree better with each other than with the theoretical value $g_p = 8.23$. When uncertainties are taken into account, however, only the TRIUMF result is clearly inconsistent with theory, while the ordinary muon capture results are only marginally inconsistent with theory.

Our prejudice that the approximate chiral symmetry of the strong interaction, which leads to the prediction $g_p = 8.23$, is not violated at such a level, makes the situation for μ capture in hydrogen very puzzling. We there-

fore have examined some suggestions for solving the puzzle, such as modifications to the μ chemistry and the role of the Δ resonance. By “tuning parameters” the discrepancy between the hydrogen data and the symmetry-based prediction can be reduced somewhat, but no clear-cut solution, which makes ordinary and radiative muon capture simultaneously agree with theory, has emerged.

New work on μ capture in liquid H_2 and gaseous H_2 is in progress. At TRIUMF an investigation of the μ chemistry in liquid hydrogen has taken data, and at PSI a measurement of μ^- lifetime in gaseous hydrogen is now under way. Hopefully these experiments will help to clarify the situation on g_p . Looking further ahead, perhaps both new facilities, e.g., an intense muon source at a neutrino factory, and new techniques, e.g., neutron polarizations or hyperfine effects, will permit a determination of g_p to an accuracy of 2–3 % or better.

The situation for muon capture on pure deuterium is inconclusive. Recall that in deuterium the g_p sensitivity is smaller than in hydrogen, the neutron experiments are harder, and nuclear models are needed. At present the world data for muon capture in pure deuterium comprises the experiment of Cargnelli *et al.* (1989), which appears consistent with theory, and the experiment of Bardin *et al.* (1986), which may be inconsistent with theory. The results on μd capture by Bertin *et al.* (1973) using a H_2/D_2 target are even more puzzling.

Further studies of μd capture are clearly worthwhile. Obviously resolving the possible discrepancy between the doublet rates obtained by Bardin *et al.* (1986) and Cargnelli *et al.* (1989) is important. Additionally, we note that the chemistry of muons in pure H_2 and pure D_2 is quite different in several ways, including a slower rate for hyperfine depopulation and near absence of muonic molecules in pure D_2 . These features may permit the study of g_p via alternative approaches, such as the hyperfine dependence of the capture reaction.

In $\mu + {}^3\text{He} \rightarrow {}^3\text{H} + \nu$ capture, the recent precision measurement of the statistical capture rate by Ackerbauer *et al.* (1998) and ground-breaking measurement of the recoil angular correlation by Souder *et al.* (1998), were major achievements. Preliminary data on the radiative capture rate in the ${}^3\text{He} \rightarrow {}^3\text{H}$ channel are also available (Wright *et al.*, 2000). Further modern treatments of $A = 3$ wave functions and two-body exchange currents have been applied to the process by Congleton and Truhlik (1996) and others. The ordinary muon capture results for g_p are completely consistent with theory, and the value of $g_p = 8.53 \pm 1.54$ from Ackerbauer *et al.* (1998) is arguably the best individual determination of g_p .

The extraction of the coupling from the measurement of the $\mu + {}^3\text{He} \rightarrow {}^3\text{H} + \nu$ statistical rate is unfortunately limited by theoretical uncertainties in calculating contributions from exchange currents. Further theoretical work is definitely worthwhile to quantify the contributions arising from radiative corrections and nail down the uncertainties arising from exchange currents, etc., but improvements in extracting the coupling may be difficult. A precision measurement of the recoil correlation,

which has enhanced sensitivity to g_p and reduced sensitivity to exchange currents, would be extremely interesting.

A significant body of new data on exclusive transitions in ordinary capture on complex nuclei has been collected recently. This includes the measurement of γ -ray correlations in $\mu^{28}\text{Si}$ and hyperfine dependences in $\mu^{11}\text{B}$ and $\mu^{23}\text{Na}$. These data complement earlier investigations of polarizations in $\mu^{12}\text{C}$ and rates in $\mu^{16}\text{O}$. Furthermore, modern well-tested models of nuclear structure in $0p$, $1s$ - $0d$ nuclei offer improved multiparticle wave functions for interpreting these experiments. In most cases, with the exception of ^{28}Si , the values of g_p that are extracted from the experiments with such wave functions are consistent with the theoretical prediction $g_p=8.23$. Generally, the major uncertainty in extracting g_p originates in the interplay of the contributions from the pseudoscalar coupling, arising from the space part of the axial current, and the axial charge, arising from the time part of the axial current. Unfortunately, it is difficult to precisely quantify such theoretical uncertainties.

Additional experiments on exclusive ordinary muon capture could be helpful to our understanding of the interplay of the induced pseudoscalar contribution and the axial charge contribution. Clearly if a wealth of data were available for nuclear ordinary muon capture a better assessment of model uncertainties would be possible. However, the experiments generally involve the use of methods and observables that cannot be applied to large numbers of exclusive transitions. Alternatively a measurement of observables in a transition such as $^6\text{Li}(1^+,0)\rightarrow^6\text{He}(0^+,0)$, where highly accurate wave functions and related nuclear data are nowadays available, is definitely interesting.

In inclusive radiative muon capture on complex nuclei the application of pair spectrometers has yielded data with good statistics and little background, and enabled the systematics of the radiative muon capture rate across the Periodic Table to be mapped out. Unfortunately, the situation in regards to the model calculation of the inclusive rate is less satisfactory. In general, the models employed for inclusive radiative muon capture have too many assumptions and too many parameters in order to reliably extract the coupling g_p . Furthermore, questions remain regarding the effective Hamiltonian for radiative capture on complex nucleus. Therefore we believe that earlier claims for large renormalizations of g_p in inclusive radiative muon capture on complex nuclei were premature and that, at the level of the uncertainties, the data are consistent with the predicted value $g_p=8.23$.

In conclusion, we hope we have convinced the reader of the importance of the coupling g_p , both as a fundamental parameter in nucleon weak interactions and as an important test of low-energy quantum chromodynamics. In recent years an impressive body of experimental data has been accumulated and most data are consistent, within sometimes large experimental and theoretical uncertainties, with the chiral symmetry based arguments for the induced pseudoscalar coupling. Unfortunately, the results from μ capture in hydrogen,

which should be the simplest and cleanest process, are very puzzling. We believe that the resolution of this puzzle should be a high priority, and that, until the situation is clarified, the accurate determination of g_p , and implied testing of low-energy QCD, remains an important task but an elusive goal.

ACKNOWLEDGMENTS

The authors would like to thank David Armstrong, Jules Deutsch, Mike Hasinoff, and David Measday for valuable discussions and Jean-Michel Poutissou for encouraging us to prepare this review and for supporting the sabbatical at TRIUMF of one of us (T.G.). We would also like to thank David Measday for a careful reading of the manuscript and Emil Truhlik for a number of useful comments. This work was supported in part by grants from the Natural Sciences and Engineering Research Council of Canada and the U.S. National Science Foundation.

REFERENCES

- Abbott, D. J., *et al.*, 1997, "Diffusion of muonic deuterium and hydrogen atoms," *Phys. Rev. A* **55**, 214.
- Ackerbauer, P., *et al.*, 1998, "A precision measurement of nuclear muon capture on ^3He ," *Phys. Lett. B* **417**, 224.
- Adam, J., E. Truhlik, S. Ciechanowicz, and K. M. Schmitt, 1990, "Muon capture in deuterium and the meson exchange current effect," *Nucl. Phys. A* **507**, 675.
- Adamczak, A., C. Chiccoli, V. I. Korobov, V. S. Melezhik, P. Pasini, L. I. Ponomarev, and J. Wozniak, 1992, "Muon transfer rates in hydrogen isotope-mesic atom collisions," preprint JINR-E4-92-140.
- Adler, S. L., and Y. Dothan, 1966, "Low-energy theorem for the weak axial vertex," *Phys. Rev.* **151**, 1267; **164**, 2062(E).
- Ahrens, L. A., *et al.*, 1988, "A study of the axial-vector form factor and second-class currents in antineutrino quasielastic scattering," *Phys. Lett. B* **202**, 284.
- Akhmedov, E. Kh., T. V. Tetereva, and R. A. Eramzhyan, 1985, "Influence of renormalization of weak nucleon form factors on radiative muon capture by nuclei," *Yad. Fiz.* **42**, 67 [*Sov. J. Nucl. Phys.* **42**, 40 (1985)].
- Alberigi-Quaranta, A., A. Bertin, G. Matone, F. Palmonari, G. Torelli, P. Dalpiaz, A. Placci, and E. Zavattini, 1969, "Muon capture in gaseous hydrogen," *Phys. Rev.* **177**, 2118.
- Ami, H., M. Kobayashi, H. Ohtsubo, and M. Morita, 1981, "Longitudinal polarization of ^{12}B in muon capture reaction," *Prog. Theor. Phys.* **65**, 632.
- Ando, S., H. W. Fearing, and D.-P. Min, 2002, "Polarized photons in radiative muon capture," *Phys. Rev. C* **65**, 015502.
- Ando, Shung-ichi, and Dong-Pil Min, 1998, "Radiative muon capture in heavy baryon chiral perturbation theory," *Phys. Lett. B* **417**, 177.
- Ando, Shung-ichi, Fred Myhrer, and Kuniharu Kubodera, 2000, "Capture rate and neutron helicity asymmetry for ordinary muon capture on hydrogen," *Phys. Rev. C* **63**, 015203.
- Ando, Shung-ichi, Fred Myhrer, and Kuniharu Kubodera, 2002, "Ordinary and radiative muon capture in liquid hydrogen re-examined," *Phys. Rev. C* **65**, 048501.

- Ando, S., T. S. Park, K. Kubodera, and F. Myhrer, 2002, “The μ -D capture rate in effective field theory,” *Phys. Lett. B* **533**, 25.
- Armstrong, D. S., *et al.*, 1991, “Radiative muon capture on carbon, oxygen, and calcium,” *Phys. Rev. C* **43**, 1425.
- Armstrong, D. S., *et al.*, 1992, “Radiative muon capture on Al, Si, Ca, Mo, Sn, and Pb,” *Phys. Rev. C* **46**, 1094.
- Armstrong, D. S., *et al.*, 1995, “The ortho-para transition rate in muonic molecular hydrogen,” *TRIUMF Expt.* 766.
- Arndt, Richard A., Igor I. Strakovsky, and Ron L. Workman, 1995, “Extraction of the πNN coupling constant from NN scattering data,” *Phys. Rev. C* **52**, 2246.
- Astbury, A., L. B. Auerbach, D. Cutts, R. J. Esterling, D. A. Jenkins, N. H. Lipman, and R. C. Shafer, 1964, “Muon capture in oxygen,” *Nuovo Cimento* **33**, 1020.
- Astbury, A., I. M. Blair, M. Hussain, M. A. R. Kemp, H. Muirhead, and R. G. P. Voss, 1959, “Angular distribution of neutrons following the nuclear capture of polarized muons,” *Phys. Rev. Lett.* **3**, 476.
- Auerbach, L. B., R. J. Esterling, R. E. Hill, D. A. Jenkins, J. T. Lach, and N. H. Lipman, 1965, “Measurements of the muon capture rate in ^3He and ^4He ,” *Phys. Rev.* **138**, B127.
- Auerbach, N., and B. A. Brown, 2002, “Weak interaction rates involving ^{12}C , ^{14}N , and ^{16}O ,” *Phys. Rev. C* **65**, 024322.
- Bailey, J., C. Oram, G. Azuelos, J. Brewer, K. Erdman, and K. Crowe, 1983, “Triplet μ^-p absorption in H_2 gas,” *TRIUMF Expt. Proposal No.* 273.
- Bakalov, D. D., M. P. Faifman, L. I. Ponomarev, and S. I. Vintitsky, 1982, “ μ capture and ortho-para transitions in the muonic molecule $p\mu p$,” *Nucl. Phys. A* **384**, 302.
- Baker, W. F. and C. Rubbia, 1959, “Neutron asymmetry from μ capture in magnesium,” *Phys. Rev. Lett.* **3**, 179.
- Bardin, G., 1982, “Mesure du taux de transition ortho-para de la molecule p- μ -p: Interpretation des mesures du taux de capture de μ^- sur le proton et deduction de la constante de couplage pseudoscalaire F_p^μ ,” Ph.D. thesis, Univ. Paris Sud (Orsay).
- Bardin, G., J. Duclos, A. Magnon, J. Martino, A. Richter, E. Zavattini, A. Bertin, M. Piccinini, A. Vitale, and D. Measday, 1981a, “A novel measurement of the muon capture rate in liquid hydrogen by the lifetime technique,” *Nucl. Phys. A* **352**, 365.
- Bardin, G., J. Duclos, A. Magnon, J. Martino, A. Richter, E. Zavattini, A. Bertin, M. Piccinini, and A. Vitale, 1981b, “Measurement of the ortho-para transition rate in the $p\mu p$ molecule and deduction of the pseudoscalar coupling constant g_p^μ ,” *Phys. Lett.* **104B**, 320.
- Bardin, G., J. Duclos, J. Martino, A. Bertin, M. Capponi, M. Piccinini, and A. Vitale, 1986, “A measurement of the muon capture rate in liquid deuterium by the lifetime technique,” *Nucl. Phys. A* **453**, 591.
- Barton, A. S., P. Bogorad, G. D. Cates, H. Mabuchi, H. Middleton, N. R. Newbury, R. Holmes, J. McCracken, P. A. Souder, J. Xu, and D. Tupa, 1993, “Highly polarized muonic He produced by collisions with laser optically pumped Rb,” *Phys. Rev. Lett.* **70**, 758.
- Beder, D., 1976, “Radiative μ capture on protons and ^3He ,” *Nucl. Phys. A* **258**, 447.
- Beder, Douglas S., and Harold W. Fearing, 1987, “Contribution of the $\Delta(1232)$ to $\mu^-p \rightarrow n\nu\gamma$,” *Phys. Rev. D* **35**, 2130.
- Beder, Douglas S., and Harold W. Fearing, 1989, “Radiative muon capture in hydrogen and nucleon excitation,” *Phys. Rev. D* **39**, 3493.
- Bentz, W., A. Arima, and H. Baier, 1990, “Chiral symmetry and the axial current in nuclear matter,” *Ann. Phys. (N.Y.)* **200**, 127.
- Bergbusch, P. C., *et al.*, 1999, “Radiative muon capture on O, Al, Si, Ti, Zr, and Ag,” *Phys. Rev. C* **59**, 2853.
- Bernabeu, J., 1971, “Muon capture in ^{11}B ,” *Nuovo Cimento A* **4**, 715.
- Bernabeu, J., 1975, “Restrictions for asymmetry and polarizations of recoil in muon capture,” *Phys. Lett.* **55B**, 313.
- Bernard, V., L. Elouadrhiri, and U.-G. Meissner, 2002, “Axial structure of the nucleon,” *J. Phys. G* **28**, R1.
- Bernard, V., H. W. Fearing, T. R. Hemmert, and Ulf-G. Meissner, 1998, “The form factors of the nucleon at small momentum transfer,” *Nucl. Phys. A* **635**, 121.
- Bernard, V., T. R. Hemmert, and Ulf-G. Meissner, 2001, “Ordinary and radiative muon capture on the proton and the pseudoscalar form factor of the nucleon,” *Nucl. Phys. A* **686**, 290.
- Bernard, V., N. Kaiser, J. Kambor, and U.-G. Meissner, 1992, “Chiral structure of the nucleon,” *Nucl. Phys. B* **388**, 315.
- Bernard, V., N. Kaiser, T.-S. H. Lee, and Ulf G. Meissner, 1994, “Threshold pion electroproduction in chiral perturbation theory,” *Phys. Rep.* **246**, 315.
- Bernard, V., N. Kaiser, and U.-G. Meissner, 1992, “Determining the axial radius of the nucleon from data on pion electroproduction,” *Phys. Rev. Lett.* **69**, 1877.
- Bernard, V., N. Kaiser, and U.-G. Meissner, 1994, “QCD accurately predicts the induced pseudoscalar coupling constant,” *Phys. Rev. D* **50**, 6899.
- Bernard, V., N. Kaiser, and Ulf-G. Meissner, 2001, “Further comment on pion electroproduction and the axial form factor,” e-print hep-ph/0101062.
- Bertin, A., A. Vitale, A. Placci, and E. Zavattini, 1973, “Muon capture in gaseous deuterium,” *Phys. Rev. D* **8**, 3774.
- Bertolini *et al.*, 1962, *Proceedings of the International Conference on High Energy Physics*, CERN, edited by J. Prentki, p. 421.
- Bjorken, J. D., and S. D. Drell, 1964, *Relativistic Quantum Mechanics* (McGraw-Hill, New York).
- Bleser, E., L. Lederman, J. Rosen, J. Rothberg, and E. Zavattini, 1962, “Muon capture in liquid hydrogen,” *Phys. Rev. Lett.* **8**, 288.
- Blokhintseva, T. D., Yu. S. Surovtsev, and M. Nagy, 1998, “Nucleon structure from the quasithreshold inverse pion electroproduction,” e-print hep-ph/9812241.
- Bogan, A., 1969, “Spectrum and asymmetry of high energy neutrons emitted in the absorption of polarized muons,” *Nucl. Phys. B* **12**, 89.
- Bogorad, P., *et al.*, 1997, “A combined polarized target/ionization chamber for measuring the spin dependence of nuclear muon capture in laser polarized muonic ^3He ,” *Nucl. Instrum. Methods Phys. Res. A* **398**, 211.
- Bouyssi, A., and N. Vinh Mau, 1972, “Spectrum and asymmetry of neutrons emitted after polarized muon capture by ^{16}O and ^{40}Ca ,” *Nucl. Phys. A* **185**, 32.
- Bracci, L., and G. Fiorentini, 1982, “Mesic molecules and muon catalyzed fusion,” *Phys. Rep.* **86**, 169.
- Breunlich, W. H., 1981, “Muon capture in hydrogen isotopes,” *Nucl. Phys. A* **353**, 201c.

- Breunlich, W. H., P. Kammel, J. S. Cohen, and M. Leon, 1989, "Muon catalyzed fusion," *Annu. Rev. Nucl. Sci.* **39**, 311.
- Briançon, Ch., *et al.*, 2000, "The spin-neutrino correlation revisited in ^{28}Si muon capture: A new determination of the induced pseudoscalar coupling g_p/g_a ," *Nucl. Phys. A* **671**, 647.
- Brown, B. A., W. A. Richter, R. E. Julies, and B. H. Wil-denthal, 1988, "Semi-empirical effective interactions for the 1s-0d shell," *Ann. Phys. (N.Y.)* **182**, 191.
- Brown, G. E., and A. M. Green, 1966, "Even parity states of ^{16}O and ^{17}O ," *Nucl. Phys. A* **75**, 401.
- Brudanin, V., *et al.*, 1995, "Measurement of the induced pseudoscalar form factor in the capture of polarized muons by Si nuclei," *Nucl. Phys. A* **587**, 577.
- Budyashov, Yu. G., V. G. Zinov, A. D. Konin, S. V. Medved, A. I. Mukhin, E. B. Ozerov, A. M. Chatrchyn, and R. A. Eramzhyan, 1970, "Excited nuclear states during capture of negative muons by carbon and oxygen," *Zh. Eksp. Teor. Fiz.* **58**, 1211 [*Sov. Phys. JETP* **31**, 651 (1970)].
- Bukat, G. M., and N. P. Popov, 1964, "Capture of μ -mesons by the ^{10}B nucleus," *Zh. Eksp. Teor. Fiz.* **46**, 1782 [*Sov. Phys. JETP* **19**, 1200 (1964)].
- Bukhvostov, A. P., and N. P. Popov, 1967a, " γ -neutrino correlations in allowed nuclear μ -meson capture," *Phys. Lett.* **24B**, 497.
- Bukhvostov, A. P., and N. P. Popov, 1967b, "Correlation of neutrino and γ -quantum in allowed capture of a polarized muon," *Yad. Fiz.* **6**, 1241 [*Sov. J. Nucl. Phys.* **6**, 903 (1968)].
- Bukhvostov, A. P., and N. P. Popov, 1967c, "Correlations of neutrino and gamma quanta in nuclear muon capture," *Yad. Fiz.* **6**, 809 [*Sov. J. Nucl. Phys.* **6**, 589 (1968)].
- Bukhvostov, A. P., and N. P. Popov, 1970, "Time dependence of particle correlations in muon capture," *Nucl. Phys. A* **147**, 385.
- Bystritski, V. M., *et al.*, 1974, "Measurement of muon capture rate in gaseous hydrogen," *Zh. Eksp. Teor. Fiz.* **66**, 43 [*Sov. Phys. JETP* **39**, 19 (1974)].
- Cannata, F., R. Leonardi, and M. Rosa Clot, 1970, "Break-down of SU_4 invariance and total muon capture rates: ^4He , ^{12}C , ^{16}O , ^{40}Ca ," *Phys. Lett.* **32B**, 6.
- Cargnelli, M., W. Breunlich, H. Fuhrmann, P. Kammel, J. Marton, P. Pawlek, J. Werner, J. Zmeskal, W. Bertl, and C. Petitjean, 1989, "Measurement of the muon capture rate in gaseous deuterium," *Nuclear Weak Process and Nuclear Structure, Yamada Conference XXIII*, edited by M. Morita, H. Ejiri, H. Ohtsubo, and T. Sato (World Scientific, Singapore), p. 115.
- Cheon, I.-T., and M. K. Cheoun, 1998, "Induced pseudoscalar coupling constant," e-print nucl-th/9811009 v2.
- Cheon, I.-T., and M. K. Cheoun, 1999, "Axial vector current and induced pseudoscalar coupling constant on $\mu^- p \rightarrow n \nu_\mu \gamma$ reaction," e-print nucl-th/9906035.
- Cheoun, M. K., and I.-T. Cheon, 2003, "An analysis of the models for the radiative muon capture on a proton," *J. Phys. G* **29**, 293.
- Choi, S., *et al.*, 1993, "Axial and pseudoscalar nucleon form factors from low energy pion electroproduction," *Phys. Rev. Lett.* **71**, 3927.
- Christillin, P., 1981, "Radiative muon capture for $N=Z$ nuclei," *Nucl. Phys. A* **362**, 391.
- Christillin, P., and M. Gmitro, 1985, "Radiative muon capture on ^{16}O ," *Phys. Lett.* **150B**, 50.
- Christillin, P., M. Rosa-Clot, and S. Servadio, 1980, "Radiative muon capture in medium-heavy nuclei," *Nucl. Phys. A* **345**, 331.
- Christillin, P., and S. Servadio, 1977, "About low energy expansion of two current amplitudes," *Nuovo Cimento A* **42**, 165.
- Chu, W. T., I. Nadelhaft, and J. Ashkin, 1965, "Radiative μ^- capture in copper," *Phys. Rev.* **137**, B352.
- Ciechanowicz, S., 1976, "Allowed partial transitions in muon capture by ^{28}Si ," *Nucl. Phys. A* **267**, 472.
- Ciechanowicz, S., 1981, "Recoil nuclei polarization in the partial $\mu^- + ^{12}\text{C} \rightarrow \nu + ^{12}\text{B}$ transitions," *Nucl. Phys. A* **372**, 445.
- Ciechanowicz, S., F. C. Khanna, and E. Truhlik, 1998, "On the muon capture in ^{28}Si and extraction of g_p ," *Proceedings of the 7th International Conference on Mesons and Light Nuclei 98*, Pruhonice, Prague, Czech Republic, 478.
- Ciechanowicz, S., and Z. Oziewicz, 1984, "Angular correlation for nuclear muon capture," *Fortschr. Phys.* **32**, 61.
- Clay, D. R., J. W. Keuffel, R. L. Wagner, and R. M. Edelstein, 1965, "Muon capture in ^3He ," *Phys. Rev.* **140**, B586.
- Cohen, R. C., S. Devons, and A. D. Kanaris, 1963, " μ capture in oxygen," *Phys. Rev. Lett.* **11**, 134.
- Cohen, R. C., S. Devons, and A. D. Kanaris, 1964, "Muon capture in oxygen," *Nucl. Phys.* **57**, 255.
- Cohen, S., and D. Kurath, 1967, "Spectroscopic factors for the 1p shell," *Nucl. Phys. A* **101**, 1.
- Congleton, J. G., 1994, "Muon capture by ^3He : the hyperfine effect," *Nucl. Phys. A* **570**, 511.
- Congleton, J. G., and H. W. Fearing, 1993, "Determination of the nucleon pseudoscalar coupling using muon capture by ^3He ," *Nucl. Phys. A* **552**, 534.
- Congleton, J. G., and E. Truhlik, 1996, "Nuclear muon capture by ^3He : meson exchange currents for the triton channel," *Phys. Rev. C* **53**, 956.
- Conforto, G., M. Conversi, and L. di Lella, 1962, "Observation of radiative capture of negative muons in iron," *Phys. Rev. Lett.* **9**, 22.
- Conversi, M., R. Diebold, and L. di Lella, 1964, "Radiative muon capture in ^{40}Ca and the induced pseudoscalar coupling constant," *Phys. Rev.* **136**, B1077.
- Coon, Sidney A., and M. D. Scadron, 1981, "Goldberger-Treiman discrepancy and the momentum variation of the pion-nucleon form factor and pion decay constant," *Phys. Rev. C* **23**, 1150.
- Coon, Sidney A., and M. D. Scadron, 1990, " πNN couplings, the πNN form factor, and the Goldberger-Treiman discrepancy," *Phys. Rev. C* **42**, 2256.
- Culligan, G., J. F. Lathrop, V. L. Telegdi, R. Winston, and R. A. Lundy, 1961, "Experimental proof of the spin dependence of the muon capture interaction, and evidence for its (F-GT) character," *Phys. Rev. Lett.* **7**, 458.
- Cummings, W. J., *et al.*, 1992, "Energetic protons and deuterons emitted following μ^- capture by ^3He nuclei," *Phys. Rev. Lett.* **68**, 293.
- Dautry, F., M. Rho, and D. O. Riska, 1976, "Weak interactions in deuterons: Exchange currents and nucleon-nucleon interaction," *Nucl. Phys. A* **264**, 507.
- Del Guerra, A., A. Giazotto, M. A. Giorgi, A. Stefanini, D. R. Botterill, H. E. Montgomery, P. R. Norton, and G. Matone, 1976, "Threshold π^+ electroproduction at high momentum transfer: A determination of the nucleon axial vector form factor," *Nucl. Phys. B* **107**, 65.

- Delorme, J., and M. Ericson, 1994, "S-wave pion nucleus interaction and weak coupling constants," *Phys. Rev. C* **49**, 1763.
- Delorme, J., M. Ericson, A. Figureau, and C. Thevenet, 1976, "Axial polarizability and weak currents in nuclei," *Ann. Phys. (N.Y.)* **102**, 273.
- de Swart, J. J., M. C. M. Rentmeester, and R. G. E. Timmermans, 1997, "The status of the pion-nucleon coupling constant," *Proceedings of MENU97*, edited by D. Drechsel, G. Hohler, W. Kluge, H. Leutwyler, B. M. K. Nefkens, and H.-M. Staudenmaier, TRIUMF Report TRI-97-1.
- Deutsch, J., 1983, "Time dependence of neutron polarization in hydrogen muon capture: A possible experiment for LAMPF II," *Proceedings of the Third LAMPF II Workshop*, LA-9933-C, Vol II, 628.
- Deutsch, J. P., L. Grenacs, P. Igo-Kemenes, P. Lipnik, and P. C. Macq, 1968, "An experimental test of the analogy between muon and radiative pion capture," *Phys. Lett.* **26B**, 315.
- Deutsch, J. P., L. Grenacs, J. Lehmann, P. Lipnik, and P. C. Macq, 1968, "Hyperfine effect in the mu-mesonic ^{11}B atom and information on ^{11}Be from muon capture measurements," *Phys. Lett.* **28B**, 178.
- Deutsch, J. P., L. Grenacs, J. Lehmann, P. Lipnik, and P. C. Macq, 1969, "Measurement of muon partial capture rates in ^{16}O and the induced pseudoscalar coupling constant in muon capture," *Phys. Lett.* **29B**, 66.
- Devanathan, V., R. Parthasarathy, and P. R. Subramanian, 1972, "Recoil nuclear polarization in muon capture," *Ann. Phys. (N.Y.)* **73**, 291.
- di Lella, L., I. Hammerman, and L. M. Rosenstein, 1971, "Photon asymmetry for radiative μ capture in calcium," *Phys. Rev. Lett.* **27**, 830.
- Döbeli, M., M. Doser, L. van Elmbt, M. Schaad, P. Truöl, A. Bay, J.-P. Perroud, and J. Imazato, 1986, "Experimental results on radiative muon capture in complex nuclei," *Czech. J. Phys., Sect. B* **36**, 386.
- Döbeli, M., M. Doser, L. van Elmbt, M. W. Schaad, P. Truöl, A. Bay, J.-P. Perroud, J. Imazato, and T. Ishikawa, 1988, "Radiative muon capture in nuclei," *Phys. Rev. C* **37**, 1633.
- Dogotar, G. E., R. A. Eramzhyan, and E. Truhlik, 1979, "Exchange currents and extraction of a_{nn} and g_p from negative muon capture in deuterium," *Nucl. Phys. A* **326**, 225.
- Doi, M., T. Sato, H. Ohtsubo, and M. Morita, 1990, "Effect of meson exchange current on deuteron muon capture," *Nucl. Phys. A* **511**, 507.
- Doi, M., T. Sato, H. Ohtsubo, and M. Morita, 1991, "Muon capture in hyperfine states of muonic deuterium," *Prog. Theor. Phys.* **86**, 13.
- Dolinsky, E. I., and L. D. Blokhintsev, 1959, "Absorption of polarized μ^- mesons by nuclei, the neutron angular distribution," *Nucl. Phys.* **10**, 527.
- Dombey, N., and B. J. Read, 1973, "Pion electroproduction and photoproduction including PCAC," *Nucl. Phys. B* **60**, 65.
- Donnelly, T. W., and W. C. Haxton, 1979, "Multipole operators in semileptonic weak and electromagnetic interactions with nuclei: Harmonic oscillator single-particle matrix elements," *At. Data Nucl. Data Tables* **23**, 103.
- Donnelly, T. W., and W. C. Haxton, 1980, "Multipole operators in semileptonic weak and electromagnetic interactions with nuclei: General single-particle matrix elements," *At. Data Nucl. Data Tables* **25**, 1.
- Donnelly, T. W., and G. E. Walker, 1970, "Inelastic electron scattering and supermultiplets in the particle-hole model for ^{12}C , ^{16}O , ^{28}Si , ^{32}S , and ^{40}Ca ," *Ann. Phys. (N.Y.)* **60**, 209.
- Doyle, B. C., and N. C. Mukhopadhyay, 1995, "Phenomenological transition amplitudes in selected 1p-shell nuclei," *Phys. Rev. C* **52**, 1947.
- Drechsel, D., and L. Tiator, 1992, "Threshold pion photoproduction on nucleons," *J. Phys. G* **18**, 449.
- Eramzhyan, R. A., V. A. Kuz'min, and T. V. Tetereva, 1998, "Calculations of ordinary and radiative muon capture on $^{58,60,62}\text{Ni}$," *Nucl. Phys. A* **642**, 428.
- Ericson, M., 1978, "Pion field and weak interactions in nuclei," *Progress in Particle and Nuclear Physics*, edited by D. Wilkinson (Pergamon Press, New York), Vol. 1, p. 67.
- Esaulov, A. S., A. M. Pilipenko, and Yu. I. Titov, 1978, "Longitudinal and transverse contributions to the threshold cross section slope of single pion electroproduction by a proton," *Nucl. Phys. B* **136**, 511.
- Evseev, V. S., V. S. Roganov, V. A. Chernogorova, Chang Run-Hwa, and M. Szymczak, 1963, "Angular distribution of neutrons due to μ^- capture in calcium for various energy thresholds," *Phys. Lett.* **6**, 332.
- Evseev, V. S., V. S. Roganov, V. A. Chernogorova, Chang Run-Hwa, and M. Szymczak, 1967, "Angular distribution of high energy neutrons emitted in the absorption of polarized μ^- mesons in Ca," *Sov. J. Nucl. Phys.* **4**, 245.
- Faifman, M. P., 1989, "Nonresonant formation of hydrogen isotope mesic molecules," *Muon Catal. Fusion* **4**, 341.
- Faifman, M. P., and L. I. Men'shikov, 1999, "Influence of ion-molecular reactions on μ -capture in hydrogen and on fusion in $^3\text{He-d-}\mu$ muonic molecules," *Hyperfine Interact.* **118**, 187.
- Falomkin, I. V., A. L. Filippov, M. M. Kulyukin, B. Pontecorvo, Yu. A. Scherbakov, R. M. Sulyaev, V. M. Tsupko-Sitnikov, and O. A. Zamidoroga, 1963, "Measurement of the $\mu + ^3\text{He} \rightarrow ^3\text{H} + \nu$ reaction rate: final results," *Phys. Lett.* **3**, 229.
- Favart, D., F. Brouillard, L. Grenacs, P. Igo-Kemenes, P. Lipnik, and P. C. Macq, 1970, "Depolarization of negative muons in low-Z muonic atoms with nonzero nuclear spin," *Phys. Rev. Lett.* **25**, 1348.
- Fearing, H. W., 1966, "Radiative muon capture and the giant dipole resonance in ^{40}Ca ," *Phys. Rev.* **146**, 723.
- Fearing, H. W., 1975, "Theorem for the photon asymmetry in radiative muon capture," *Phys. Rev. Lett.* **35**, 79.
- Fearing, H. W., 1980, "Relativistic calculation of radiative muon capture in hydrogen and ^3He ," *Phys. Rev. C* **21**, 1951.
- Fearing, H. W., 1998a, "Comment on 'Induced pseudoscalar coupling constant' by Il-Tong Cheon and Myung Ki Cheoun (nucl-th/9811009)," e-print nucl-th/9811027 v2.
- Fearing, H. W., 1998b, "Nucleon-nucleon bremsstrahlung: An example of the impossibility of measuring off-shell amplitudes," *Phys. Rev. Lett.* **81**, 758.
- Fearing, H. W., 2000, "The off-shell nucleon-nucleon amplitude: Why it is unmeasurable in nucleon-nucleon bremsstrahlung," *Few-Body Syst., Suppl.* **12**, 263.
- Fearing, H. W., T. R. Hemmert, R. Lewis, and C. Unkmeier, 2000, "Radiative pion capture by a nucleon," *Phys. Rev. C* **62**, 054006.
- Fearing, H. W., and S. Scherer, 2000, "Field transformations and simple models illustrating the impossibility of measuring off-shell effects," *Phys. Rev. C* **62**, 034003.
- Fearing, H. W., and G. E. Walker, 1989, "Radiative muon capture in a relativistic mean field theory: Fermi gas model," *Phys. Rev. C* **39**, 2349.

- Fearing, H. W., and M. S. Welsh, 1992, "Radiative muon capture in medium heavy nuclei in a relativistic mean field theory model," *Phys. Rev. C* **46**, 2077.
- Fearing, Harold W., Randy Lewis, Nader Mobed, and Stefan Scherer, 1997, "Muon capture by a proton in heavy baryon chiral perturbation theory," *Phys. Rev. D* **56**, 1783.
- Flamand, G., and K. W. Ford, 1959, "Muon capture by ^{12}C and beta decay of ^{12}B ," *Phys. Rev.* **116**, 1591.
- Foldy, L. L., and J. D. Walecka, 1964, "Muon capture in nuclei," *Nuovo Cimento* **34**, 1026.
- Frischknecht, A., *et al.*, 1985, "Radiative muon absorption in calcium," *Phys. Rev. C* **32**, 1506.
- Frischknecht, A., *et al.*, 1988, "Radiative muon absorption in oxygen," *Phys. Rev. C* **38**, 1996.
- Froelich, P., 1992, "Muon catalyzed fusion: Chemical confinement of nuclei within the muonic molecule $\text{d}\mu$," *Adv. Phys.* **41**, 405.
- Fuchs, T., and S. Scherer, 2003, "Pion electroproduction, PCAC, chiral Ward identities, and the axial form factor revisited," e-print nucl-th/0303002.
- Fujii, A., and H. Primakoff, 1959, "Muon capture on certain light nuclei," *Nuovo Cimento* **12**, 327.
- Fukui, M., K. Koshigiri, T. Sato, H. Ohtsubo, and M. Morita, 1983a, "The average polarization of ^{12}B in the muon capture reaction," *Phys. Lett.* **132B**, 255.
- Fukui, M., K. Koshigiri, T. Sato, H. Ohtsubo, and M. Morita, 1983b, "Nuclear polarization of ^{12}B in muon capture reaction," *Prog. Theor. Phys.* **70**, 827.
- Fukui, M., K. Koshigiri, T. Sato, H. Ohtsubo, and M. Morita, 1987, "Polarizations of ^{12}B in muon capture reaction with higher order configuration mixing," *Prog. Theor. Phys.* **78**, 343.
- Galindo, A., and P. Pascual, 1968, "Asymmetry of recoil nuclei in capture of polarized muons," *Nucl. Phys. B* **4**, 295.
- Giffon, M., A. Goncalves, P. A. Guichon, J. Julien, L. Roussel, and C. Samour, 1981, " μ^- partial capture rates in ^{10}B , ^{12}C and ^{14}N ," *Phys. Rev. C* **24**, 241.
- Gmitro, M., S. S. Kamalov, T. V. Moskalenko, and R. A. Eramzhyan, 1981, "Radiative muon capture on nuclei: Microscopic calculation for ^{16}O and ^{40}Ca ," *Czech. J. Phys., Sect. B* **31**, 499.
- Gmitro, M., S. S. Kamalov, and A. A. Ovchinnikova, 1987, "Radiative capture of polarized muons on ^{16}O and ^{40}Ca ," *Nucl. Phys. A* **468**, 404.
- Gmitro, M., S. S. Kamalov, F. Šimkovic, and A. A. Ovchinnikova, 1990, "Ordinary and radiative muon capture on ^{12}C ," *Nucl. Phys. A* **507**, 707.
- Gmitro, M., and A. A. Ovchinnikova, 1981, "Current divergences, pion photoproduction and radiative muon capture," *Nucl. Phys. A* **356**, 323.
- Gmitro, M., A. A. Ovchinnikova, and T. V. Tetereva, 1986, "Continuity-equation constraint in the two-vertex nuclear processes: Radiative muon capture on ^{16}O and ^{40}Ca ," *Nucl. Phys. A* **453**, 685.
- Gmitro, M., O. Richter, H. R. Kissener, and A. A. Ovchinnikova, 1991, "Ordinary and radiative muon capture on ^{14}N ," *Phys. Rev. C* **43**, 1448.
- Gmitro, M., and P. Trüöl, 1987, "Radiative muon capture and the weak pseudoscalar coupling in nuclei," in *Advances in Nuclear Physics*, edited by J. W. Negele and E. Vogt (Plenum, New York), Vol. 18, p. 241.
- Godfrey, T. N. K., 1953, "Negative μ -meson capture in carbon," *Phys. Rev.* **92**, 512.
- Goity, Jose L., Randy Lewis, Martin Schvellinger, and Longzhe Zhang, 1999, "The Goldberger-Treiman discrepancy in $\text{SU}(3)$," *Phys. Lett. B* **454**, 115.
- Goldberger, M. L., and S. B. Treiman, 1958, "Form factors in β decay and μ capture," *Phys. Rev.* **111**, 354.
- Goldman, M. R., 1972, "Order α corrections to muon capture in hydrogen," *Nucl. Phys. B* **49**, 621.
- Gorringer, T. P., D. S. Armstrong, S. Arole, M. Boleman, E. Gete, V. Kuz'min, B. A. Moftah, R. Sedlar, T. J. Stocki, and T. Tetereva, 1999, "Measurement of partial muon capture rates in 1s-0d shell nuclei," *Phys. Rev. C* **60**, 055501.
- Gorringer, T. P., D. S. Armstrong, C. Q. Chen, E. Christy, B. C. Doyle, P. Gumplinger, H. W. Fearing, M. D. Hasinoff, M. A. Kovash, and D. H. Wright, 1998, "Isotope dependence of radiative muon capture on the $^{58,60,62}\text{Ni}$ isotopes," *Phys. Rev. C* **58**, 1767.
- Gorringer, T. P., B. L. Johnson, D. S. Armstrong, J. Bauer, M. D. Hasinoff, M. A. Kovash, D. F. Measday, B. A. Moftah, R. Porter, and D. H. Wright, 1994, "Hyperfine effect in μ^- capture on ^{23}Na and g_p/g_a ," *Phys. Rev. Lett.* **72**, 3472.
- Gorringer, T. P., B. L. Johnson, J. Bauer, M. A. Kovash, R. Porter, P. Gumplinger, M. D. Hasinoff, D. F. Measday, B. A. Moftah, D. S. Armstrong, and D. H. Wright, 1993, "Measurement of hyperfine transition rates in muonic ^{19}F , ^{23}Na , ^{31}P , and ^{nat}Cl ," *Phys. Lett. B* **309**, 241.
- Goulard, B., B. Lorazo, and H. Primakoff, 1982, "Muon capture by the deuteron with outgoing neutrinos of very small momentum," *Phys. Rev. C* **26**, 1237.
- Govaerts, Jan, and Jose-Luis Lucio-Martinez, 2000, "Nuclear muon capture on the proton and ^3He within the standard model and beyond," *Nucl. Phys. A* **678**, 110.
- Grenacs, L., 1985, "Induced weak currents in nuclei," *Annu. Rev. Nucl. Part. Sci.* **35**, 455.
- Grenacs, L., J. P. Deutsch, P. Lipnik, and P. C. Macq, 1968, "A method to measure neutrino-gamma angular correlation in muon capture," *Nucl. Instrum. Methods* **58**, 164.
- Guichon, P. A. M., 2001, "Comment about pion electroproduction and the axial form factors," *Phys. Rev. Lett.* **87**, 019101.
- Guichon, P. A. M., B. Bihoreau, M. Giffon, A. Gonçalves, J. Julien, L. Roussel, and C. Samour, 1979, " μ^- partial capture rates in ^{16}O ," *Phys. Rev. C* **19**, 987.
- Guichon, P. A. M., M. Giffon, and C. Samour, 1978, "Possible evidence for mesonic exchange correction in $^{16}\text{N}(0^-) \leftrightarrow ^{16}\text{O}(0^+) \beta$ decay and μ capture reactions," *Phys. Lett.* **74B**, 15.
- Guichon, P. A. M., and C. Samour, 1979, "Nuclear wave functions and mesonic exchange currents in the weak transition $^{16}\text{O}(0^+) \leftrightarrow ^{16}\text{N}(0^-)$," *Phys. Lett.* **82B**, 28.
- Haberzettl, H., 2000, "Pion photo- and electroproduction and the partially-conserved axial current," *Phys. Rev. Lett.* **85**, 3576.
- Haberzettl, H., 2001, "Reply to 'Comment about pion electroproduction and the axial form-factors,'" *Phys. Rev. Lett.* **87**, 019102.
- Halpern, Alvin, 1964a, "Muon capture rate in $(p\mu p)$," *Phys. Rev.* **135**, A34.
- Halpern, Alvin, 1964b, " $(p\mu p)^+$ molecule: muon capture in hydrogen," *Phys. Rev. Lett.* **13**, 660.

- Hambro, L., and N. C. Mukhopadhyay, 1975, "Effects of non-statistical hyperfine populations in muon capture by polarized nuclei," *Lett. Nuovo Cimento Soc. Ital. Fis.* **14**, 53.
- Hambro, L., and N. C. Mukhopadhyay, 1977, "Repolarization of muons in muonic atoms with polarized nuclei," *Phys. Lett.* **68B**, 143.
- Hart, R. D., C. R. Cox, G. W. Dodson, M. Eckhause, J. R. Kane, M. S. Pandey, A. M. Rushton, R. T. Siegel, and R. E. Welsh, 1977, "Radiative muon capture in calcium," *Phys. Rev. Lett.* **39**, 399.
- Hauge, P. S., and S. Maripuu, 1973, "Shell-model calculations for $A=6-14$ nuclei with a realistic interaction," *Phys. Rev. C* **8**, 1609.
- Haxton, W. C., 1978, "Threshold pion photoproduction in ^{12}C and the 15.11 MeV M1 form factor," *Phys. Lett.* **76B**, 165.
- Haxton, W. C., and C. Johnson, 1990, "Weak-interaction rates in ^{16}O ," *Phys. Rev. Lett.* **65**, 1325.
- Hayes, A. C., and I. S. Towner, 2000, "Shell-model calculations of neutrino scattering from C-12," *Phys. Rev. C* **61**, 044603.
- Hildebrand, Roger H., 1962, "Observation of μ^- capture in liquid hydrogen," *Phys. Rev. Lett.* **8**, 34.
- Hildebrand, R., and J. H. Doede, 1962, in *Proceedings of the International Conference on High Energy Physics, Geneva, 1962*, edited by J. Prentki, p. 418.
- Hirshfelder, J. O., H. Eyring, and B. Topley, 1936, "Reactions involving hydrogen molecules and atoms," *J. Chem. Phys.* **4**, 170.
- Ho, E. C. Y., H. W. Fearing, and W. Schadow, 2002, "Radiative muon capture by ^3He ," *Phys. Rev. C* **65**, 065501.
- Ho-Kim, Q., J. P. Lavine, and H. S. Picker, 1976, "Final state interactions in muon capture by deuterons," *Phys. Rev. C* **13**, 1966.
- Huang, K., C. N. Yang, and T. D. Lee, 1957, "Capture of μ^- mesons by protons," *Phys. Rev.* **108**, 1340.
- Hwang, W.-Y. P., and B.-J. Lin, 1999, "Muon capture in deuterium," *Int. J. Mod. Phys. E* **8**, 101.
- Hwang, W.-Y. P., and H. Primakoff, 1978, "Theory of radiative muon capture with applications to nuclear spin and isospin doublets," *Phys. Rev. C* **18**, 414.
- Immele, J. D., and N. C. Mukhopadhyay, 1975, "An open-shell finite Fermi systems approach to the structure of $A=12$ nuclei," *Phys. Lett.* **56B**, 13.
- Ivanov, E., and E. Truhlik, 1979a, "Hard pions and axial meson exchange currents in nuclear physics," *Nucl. Phys. A* **316**, 437.
- Ivanov, E., and E. Truhlik, 1979b, "Hard pions and axial meson exchange current effects in negative muon capture in deuterium," *Nucl. Phys. A* **316**, 451.
- Jäger, H. U., M. Kirchbach, and E. Truhlik, 1983, "Meson exchange corrections to the nuclear weak axial charge density in the hard pion model and $0^+ \leftrightarrow 0^-$ transitions in $A=16$ nuclei," *Nucl. Phys. A* **404**, 456.
- Johnson, B. L., T. P. Gorringer, D. S. Armstrong, J. Bauer, M. D. Hasinoff, M. A. Kovash, D. F. Measday, B. A. Moftah, R. Porter, and D. H. Wright, 1996, "Observables in muon capture on ^{23}Na and the effective weak couplings \tilde{g}_a and \tilde{g}_p ," *Phys. Rev. C* **54**, 2714.
- Jones, H. F., and M. D. Scadron, 1975, "Goldberger-Treiman relation and chiral-symmetry breaking," *Phys. Rev. D* **11**, 174.
- Jonkmans, G., *et al.*, 1996, "Radiative muon capture on hydrogen and the induced pseudoscalar coupling," *Phys. Rev. Lett.* **77**, 4512.
- Junker, K., V. A. Kuz'min, A. A. Ovchinnikova, and T. V. Tereva, 2000, "Sensitivity of muon capture to the ratios of nuclear matrix elements," *Phys. Rev. C* **61**, 044602.
- Kadono, R., J. Imazato, T. Ishikawa, K. Nishiyama, K. Nagamine, T. Yamazaki, A. Bosshard, M. Döbeli, L. van Elmbt, M. Schaad, P. Truöl, A. Bay, J. P. Perroud, J. Deutsch, B. Tasiaux, and E. Hagn, 1986, "Repolarization of negative muons by polarized ^{209}Bi nuclei," *Phys. Rev. Lett.* **57**, 1847.
- Kaiser, N., 2003, "Induced pseudoscalar form factor of the nucleon at two-loop order in chiral perturbation theory," *Phys. Rev. C* **67**, 027002.
- Kameyama, H., M. Kamimura, and Y. Fukushima, 1989, "Coupled-rearrangement-channel gaussian-basis variational method for trinucleon bound states," *Phys. Rev. C* **40**, 974.
- Kammel, P., 2003, "Muon capture and muon lifetime," presented at International Workshop on Exotic Atoms—Future Perspectives (EXA 2002) 2002, Vienna, Austria.
- Kammel, P., W. H. Breunlich, M. Cargnelli, H. G. Mahler, J. Zmeskal, W. H. Bertl, and C. Petitjean, 1983, "First observation of muonic hyperfine effects in pure deuterium," *Phys. Rev. A* **28**, 2611.
- Kammel, P., W. H. Breunlich, M. Cargnelli, H. G. Mahler, J. Zmeskal, W. H. Bertl, C. Petitjean, and W. J. Kossler, 1982, "First observation of hyperfine transitions in muonic deuterium atoms via resonant $d\mu d$ formation at 34K," *Phys. Lett.* **112B**, 319.
- Kammel, P., *et al.*, 2000, "Precision Measurement of μp capture in a hydrogen TPC," *Nucl. Phys. A* **663**, 911c.
- Kane, F. R., M. Eckhause, G. H. Miller, B. L. Roberts, M. E. Vislay, and R. E. Welsh, 1973, "Muon capture rates on ^{16}O leading to bound states of ^{16}N ," *Phys. Lett. B* **45**, 292.
- Kim, C. W., and H. Primakoff, 1965, "Theory of muon capture with initial and final nuclei treated as 'elementary' particles," *Phys. Rev.* **140**, B566.
- Kirchbach, M., and D. O. Riska, 1994, "The effective induced pseudoscalar coupling constant," *Nucl. Phys. A* **578**, 511.
- Klieb, L., 1982, "Impulse approximation versus elementary particle method: Radiative muon capture in ^3He and the pion- ^3He - ^3H coupling," Ph.D. dissertation, University of Groningen, the Netherlands.
- Klieb, L., 1985, "Hard meson corrections to the amplitude for radiative muon capture and the elementary particle method," *Nucl. Phys. A* **442**, 721.
- Klieb, L., and H. P. C. Rood, 1981, "Radiative muon capture in ^3He : A comparison of the impulse approximation with elementary particle calculations," *Nucl. Phys. A* **356**, 483.
- Klieb, L., and H. P. C. Rood, 1984a, "Impulse approximation versus elementary particle method: π - ^3He - ^3H coupling constant," *Phys. Rev. C* **29**, 215.
- Klieb, L., and H. P. C. Rood, 1984b, "Impulse approximation versus elementary particle method: Pion photoproduction and radiative muon capture," *Phys. Rev. C* **29**, 223.
- Kobayashi, M., N. Ohtsuka, H. Ohtsubo, and M. Morita, 1978, "Average polarization of ^{12}B in polarized muon capture," *Nucl. Phys. A* **312**, 377.
- Kolbe, E., K. Langanke, and P. Vogel, 2000, "Muon capture on nuclei with $N>Z$, random phase approximation, and in-medium value of the axial-vector coupling constant," *Phys. Rev. C* **62**, 055502.
- Kortelainen, M., M. Aunola, T. Siiskonen, and J. Suhonen, 2000, "Mean-field effects on muon-capture observables," *J. Phys. G* **26**, L33.

- Koshigiri, K., Y. Kakudo, H. Ohtsubo, and M. Morita, 1985, "Muon capture in complex nuclei of nonzero spin," *Prog. Theor. Phys.* **74**, 736.
- Koshigiri, K., R. Morita, and M. Morita, 1997, "Induced pseudoscalar weak interaction and muon capture reaction," in *Non-Nucleonic Degrees of Freedom Detected in Nucleus (NNDF'96)*, *Proc. of the Intern. Symp.*, edited by T. Minamisono, Y. Nojiri, T. Sato, and K. Matsuta (World Scientific, Singapore), p. 238.
- Koshigiri, K., H. Ohtsubo, and M. Morita, 1982, "Muon capture in hyperfine states of ^{11}B muonic atom," *Prog. Theor. Phys.* **68**, 687.
- Koshigiri, K., H. Ohtsubo, and M. Morita, 1984, "Muon capture in ^{11}B muonic atom and hyperfine spin dependence," *Prog. Theor. Phys.* **71**, 1293.
- Kozlowski, T., W. Bertl, H. P. Povel, U. Sennhauser, H. K. Walter, A. Zglinski, R. Engfer, Ch. Grab, E. A. Hermes, H. P. Isaak, A. van der Schaaf, J. van der Pluym, and W. H. A. Hesselink, 1985, "Energy spectra and asymmetries of neutrons emitted after muon capture," *Nucl. Phys. A* **436**, 717.
- Kubodera, K., J. Delorme, and M. Rho, 1978, "Axial currents in nuclei," *Phys. Rev. Lett.* **40**, 755.
- Kudoyarov, M. F., *et al.*, 1998, in *Heavy Ion Physics, Proceedings of the VI International School-Seminar, Dubna, Russia, 1997*, edited by Yu. Ts. Oganessian and R. Kalpakchieva (World Scientific, Singapore), p. 742.
- Kuhn, S. E., *et al.*, 1994, "Multinucleon effects in muon capture on ^3He at high energy transfer," *Phys. Rev. C* **50**, 1771.
- Kume, K., N. Ohtsuka, H. Ohtsubo, and M. Morita, 1975, "Asymmetry and energy spectrum of high-energy neutrons emitted in polarized muon capture by nuclei," *Nucl. Phys. A* **251**, 465.
- Kuno, Y., J. Imazato, K. Nishiyama, K. Nagamine, T. Yamazaki, and T. Minamisono, 1984, "New pulsed-beam measurement of the average polarization of $^{12}\text{B}(\text{g.s.})$ produced in the polarized-muon capture reaction $^{12}\text{C}(\mu^-, \nu_\mu)^{12}\text{B}$," *Phys. Lett.* **148B**, 270.
- Kuno, Y., J. Imazato, K. Nishiyama, K. Nagamine, T. Yamazaki, and T. Minamisono, 1986, "Measurement of the average polarization of ^{12}B in the polarized-muon capture by ^{12}C : Magnitude of the induced pseudoscalar form factor," *Z. Phys. A* **323**, 69.
- Kuno, Y., K. Nagamine, and T. Yamazaki, 1987, "Polarization transfer from polarized nuclear spin to μ^- spin in muonic atom," *Nucl. Phys. A* **475**, 615.
- Kuo, T. T. S., and G. E. Brown, 1966, "Structure of finite nuclei and the free nucleon-nucleon interaction: An application to ^{18}O and ^{18}F ," *Nucl. Phys.* **85**, 40.
- Kuz'min, V. A., A. A. Ovchinnikova, and T. V. Tetereva, 1994, "Muon capture by $^{10,11}\text{B}$ nuclei: Sensitivity to the choice of nuclear model," *Yad. Fiz.* **57**, 1954 [*Phys. At. Nucl.* **57**, 1881 (1994)].
- Kuz'min, V. A., and T. V. Tetereva, 2000, "Properties of isovector $1+$ states in $A=28$ nuclei and nuclear muon capture," *Yad. Fiz.* **63**, 1966 [*Phys. At. Nucl.* **63**, 1874 (2000)].
- Kuz'min, V. A., T. V. Tetereva, and K. Junker, 2001, "On the strength of spin-isospin transitions in $A=28$ nuclei," *Yad. Fiz.* **64**, 1246 [*Phys. At. Nucl.* **64**, 1169].
- Lee, Y. K., T. J. Hallman, L. Madansky, S. Trentalange, G. R. Mason, A. J. Caffrey, E. K. McIntyre, and T. R. King, 1987, "Energetic neutron emission from μ^- capture in deuterium," *Phys. Lett. B* **188**, 33.
- Liesenfeld, A., A. W. Richter, S. Sirca, K. I. Blomqvist, W. U. Boeglin, K. Bohinc, R. Böhm, M. Distler, D. Drechsel, R. Edelhoff, I. Ewald, J. Friedrich, J. M. Friedrich, R. Geiges, M. Kahrau, M. Korn, K. W. Krygier, V. Kunde, H. Merkel, K. Merle, U. Müller, R. Neuhausen, T. Pospischil, M. Potokar, A. Rokavec, G. Rosner, P. Sauer, S. Schardt, H. Schmieden, L. Tiator, B. Vodenik, A. Wagner, Th. Walcher, and S. Wolf, 1999, "A measurement of the axial form factor of the nucleon by the $p(e, e' \pi^+)n$ reaction at $W=1125$ MeV," *Phys. Lett. B* **468**, 20.
- Love, W. A., S. Marder, I. Nadelhaft, R. T. Siegel, and A. E. Taylor, 1959, "Helicity of negative muons from pion decay," *Phys. Rev. Lett.* **2**, 107.
- Luyten, J. R., H. P. C. Rood, and H. A. Tolhoek, 1963, "On the theory of muon capture by complex nuclei (I)," *Nucl. Phys.* **41**, 236.
- Maev, E. M., P. Ackerbauer, D. V. Balin, V. N. Baturin, G. A. Beer, W. H. Breunlich, T. Case, K. M. Crowe, H. Daniel, J. Deutsch, T. von Egidy, J. Govaerts, Yu. S. Grigoriev, F. J. Hartmann, P. Kammel, B. Lauss, J. Marton, M. Mühlbauer, C. Petitjean, T. Petitjean, G. E. Petrov, R. Prieels, W. Prymas, W. Schott, G. G. Semenchuk, Yu. V. Smirenin, A. A. Vorobyov, N. I. Voropaev, and P. Wojciechowski, 1996, "Measurement of the breakup channels in nuclear muon capture by ^3He and ^4He ," *Hyperfine Interact.* **101/102**, 423.
- Maier, E. J., R. M. Edelstein, and R. T. Siegel, 1964, "Measurement of the reaction $\mu^- + ^{12}\text{C} \rightarrow ^{12}\text{B} + \nu$," *Phys. Rev.* **133**, B663.
- Marcucci, L. E., R. Schiavilla, S. Rosati, A. Kievsky, and M. Viviani, 2002, "Theoretical study of the $^3\text{He}(\mu^-, \nu_\mu)^3\text{H}$ capture," *Phys. Rev. C* **66**, 054003.
- Martínez-Pinedo, G., and P. Vogel, 1998, "Shell model calculation of the β^- and β^+ partial half-lives of ^{54}Mn and other unique second forbidden β decays," *Phys. Rev. Lett.* **81**, 281.
- Martino, J., 1982, "Measurement of the capture ratio in liquid hydrogen by the lifetime method," Ph.D. thesis, Univ. Paris Sud (Orsay).
- Martino, J., 1984, "Muon capture in hydrogen," in *Erice 1984: Fundamental Interactions in Low-energy Systems*, edited by P. Dalpiaz, G. Fiorentini, and G. Torelli, Ettore Majorana International Science Series No. 23 (Plenum Press, New York), p. 43.
- McGrory, J. B., and B. H. Wildenthal, 1971, "A truncated shell model calculation of ^{23}Na , ^{24}Mg and ^{28}Si ," *Phys. Lett.* **34B**, 373.
- Meaday, D. F., 2001, "The nuclear physics of muon capture," *Phys. Rep.* **354**, 243.
- Meissner, T., F. Myhrer, and K. Kubodera, 1998, "Radiative muon capture by a proton in chiral perturbation theory," *Phys. Lett. B* **416**, 36.
- Mergell, P., Ulf-G. Meissner, and D. Drechsel, 1996, "Dispersion-theoretical analysis of the nucleon electromagnetic form factors," *Nucl. Phys. A* **596**, 367.
- Miller, G. H., M. Eckhause, F. R. Kane, P. Martin, and R. E. Welsh, 1972a, "Negative muon capture in carbon leading to specific final states," *Phys. Lett.* **41B**, 50.
- Miller, G. H., M. Eckhause, F. R. Kane, P. Martin, and R. E. Welsh, 1972b, "Gamma-neutrino angular correlations in muon capture," *Phys. Rev. Lett.* **29**, 1194.
- Minamisono, K., *et al.*, 2001, "New limit of the G-parity irregular weak nucleon current detected in β decays of spin aligned ^{12}B and ^{12}N ," *Phys. Rev. C* **65**, 015501.

- Mintz, S. L., 1973, "Muon capture rate in deuterium and the weak form factors in the timelike region," *Phys. Rev. D* **8**, 2946.
- Mintz, S. L., 1983, "Differential muon capture rate and the deuterium form factors in the timelike region," *Phys. Rev. C* **28**, 556.
- Moftah, B. A., E. Gete, D. F. Measday, D. S. Armstrong, J. Bauer, T. P. Gorringer, B. L. Johnson, B. Siebels, and S. Stanislaus, 1997, "Muon capture in ^{28}Si and g_p/g_a ," *Phys. Lett. B* **395**, 157.
- Morita, M., and A. Fujii, 1960, "Theory of allowed and forbidden transitions in muon capture reactions," *Phys. Rev.* **118**, 606.
- Morita, M., and R. Morita, 1992, "Muon capture in hyperfine states of muonic deuterium and induced pseudoscalar form factor," *Z. Phys. C* **56**, S156.
- Morita, M., R. Morita, M. Doi, T. Sato, H. Ohtsubo, and K. Koshigiri, 1993, "Induced pseudoscalar interaction in weak nucleon current and muon capture in hyperfine states of muonic deuterium," *Hyperfine Interact.* **78**, 85.
- Morita, M., R. Morita, and K. Koshigiri, 1994, "Induced terms of weak nucleon currents in light nuclei," *Nucl. Phys. A* **577**, 387.
- Mukhopadhyay, N. C., 1972, "On the impulse-approximation treatment of allowed muon capture in ^6Li ," *Phys. Lett.* **40B**, 157.
- Mukhopadhyay, N. C., 1977, "Nuclear muon capture," *Phys. Rep.* **30**, 1.
- Mukhopadhyay, N. C., and M. H. Macfarlane, 1971, "Transition rate for ground state to ground state in the capture of negative muons by ^{12}C ," *Phys. Rev. Lett.* **27**, 1823; **28**, 1545(E).
- Mukhopadhyay, N. C., and J. Martorell, 1978, "An improved impulse approximation treatment of the "allowed" weak and analogue electromagnetic transitions in ^{12}C ," *Nucl. Phys. A* **296**, 461.
- Mulhauser, F., *et al.*, 1996, "Measurement of muon transfer from proton to triton and $pp\mu$ molecular formation in solid hydrogen," *Phys. Rev. A* **53**, 3069.
- Myhrer, F., 1999, private communication.
- Nagele, N., W. H. Breunlich, M. Cargnelli, H. Fuhrmann, P. Kammel, J. Marton, P. Pawlek, A. Scrinzi, J. Werner, J. Zmeskal, W. Bertl, and C. Petitjean, 1989, "Experimental investigation of muon-induced fusion in liquid deuterium," *Nucl. Phys. A* **493**, 397.
- Nasrallah, N. F., 2000, "Goldberger-Treiman discrepancy," *Phys. Rev. D* **62**, 036006.
- Navarro, J., and H. Krivine, 1986, "A sum rule approach to total muon capture rates," *Nucl. Phys. A* **457**, 731.
- Newbury, N. R., A. S. Barton, P. Bogorad, G. D. Cates, M. Gatzke, B. Saam, L. Han, R. Holmes, P. A. Souder, J. Xu, and D. Benton, 1991, "Laser polarized muonic helium," *Phys. Rev. Lett.* **67**, 3219; **69**, 391(E).
- Nguyen, Nguyen Tien, 1975, "Neutrino disintegration and muon capture in the deuteron," *Nucl. Phys. A* **254**, 485.
- Nozawa, S., K. Kubodera, and H. Ohtsubo, 1986, "Exchange currents and configuration mixing effects in the $^{16}\text{O}(0^+) - ^{16}\text{N}(0^-)$ transitions," *Nucl. Phys. A* **453**, 645.
- Nyman, E. M., and M. Rho, 1977, "Probing the pion field in nuclei," *Nucl. Phys. A* **287**, 390.
- O'Connell, J. S., T. W. Donnelly, and J. D. Walecka, 1972, "Semileptonic weak interactions with ^{12}C ," *Phys. Rev. C* **6**, 719.
- Ohta, K., and M. Wakamatsu, 1974, "PCAC and renormalization of the weak axial-vector vertex in nuclei," *Phys. Lett.* **51B**, 325.
- Opat, G. I., 1964, "Radiative muon capture in hydrogen," *Phys. Rev.* **134**, B428.
- Oziewicz, Z., and N. P. Popov, 1965, " γ -neutrino correlations in first forbidden nuclear μ -meson capture," *Phys. Lett.* **15**, 273.
- Parthasarathy, R., and V. N. Sridhar, 1978, "Gamma-neutrino angular correlation in muon capture by ^{28}Si ," *Phys. Rev. C* **18**, 1796.
- Parthasarathy, R., and V. N. Sridhar, 1981, "Gamma-neutrino angular correlations in muon capture by ^{28}Si . II," *Phys. Rev. C* **23**, 861.
- Particle Data Group, 2000, "Review of particle physics," *Eur. Phys. J. C* **15**, 1.
- Pascual, P., R. Tarrach, and F. Vidal, 1972, "Muon capture in deuterium," *Nuovo Cimento A* **12**, 241.
- Peterson, E. A., 1968, "Muon capture in ^3He ," *Phys. Rev.* **167**, 971.
- Petitjean, C., *et al.*, 1990/91, "The $p\mu d$ fusion cycle," *Muon Catal. Fusion* **5/6**, 199.
- Phillips, A. C., F. Roig, and J. Ros, 1975, "Muon capture in ^3He ," *Nucl. Phys. A* **237**, 493.
- Ponomarev, L. I., 1973, "Molecular structure effects on atomic and nuclear capture of mesons," *Annu. Rev. Nucl. Sci.* **23**, 395.
- Ponomarev, L. I., and M. P. Faifman, 1976, "Calculation of the hydrogen μ -mesic molecule deexcitation rates," *Sov. Phys. JETP* **44**, 886.
- Popov, N. P., 1963, " γ -neutrino correlation in nuclear muon capture," *Zh. Eksp. Teor. Fiz.* **44**, 1679 [*Sov. Phys. JETP* **17**, 1130 (1963)].
- Possoz, A., Ph. Deschepper, L. Grenacs, P. Lebrun, J. Lehmann, L. Palffy, A. de Moura Gonclaves, C. Samour, and V. I. Telegdi, 1977, "Average polarization of ^{12}B in $^{12}\text{C}(\mu, \nu)^{12}\text{B}(\text{g.s.})$ reaction: Helicity of the π -decay muon and nature of the weak coupling," *Phys. Lett.* **70B**, 265.
- Possoz, A., D. Favart, L. Grenacs, J. Lehmann, P. Macq, D. Meda, L. Palffy, J. Julien, and C. Samour, 1974, "Measurement of the average polarization of ^{12}B produced by polarized muons in the $\mu^- + ^{12}\text{C} \rightarrow \nu_\mu + ^{12}\text{B}$ reaction," *Phys. Lett.* **50B**, 438.
- Primakoff, H., 1959, "Theory of muon capture," *Rev. Mod. Phys.* **31**, 802.
- Reifenröther, G., E. Klempt, and R. Landua, 1987, "Cascade of muonic helium atoms," *Phys. Lett. B* **191**, 15.
- Reynolds, G. T., D. B. Scarl, A. Swanson, J. R. Waters, and R. A. Zdanis, 1963, "Muon capture on carbon," *Phys. Rev.* **129**, 1790.
- Rho, Mannque, 1978, "Meson fields in nuclei," in *Progress in Particle and Nuclear Physics*, edited by D. Wilkinson (Pergamon Press, New York), Vol. 1, p. 105.
- Roesch, L. Ph., N. Schlumpf, D. Taquq, V. L. Telegdi, P. Truttmann, and A. Zehnder, 1981, "Measurement of the capture rates to the excited states in $^{12}\text{C}(\mu^-, \nu)^{12}\text{B}^*$ and a novel technique to deduce the alignment of $^{12}\text{B}^*(1^-)$," *Phys. Lett.* **107B**, 31.
- Roesch, L. Ph., V. L. Telegdi, P. Truttmann, A. Zehnder, L. Grenacs, and L. Palffy, 1981, "Measurement of the average and longitudinal recoil polarizations in the reaction $^{12}\text{C}(\mu^-, \nu)^{12}\text{B}(\text{g.s.})$: Magnitude of the induced pseudoscalar coupling," *Phys. Rev. Lett.* **46**, 1507.

- Roig, F., and J. Navarro, 1990, "Radiative muon capture and the value of g_p in nuclei," *Phys. Lett. B* **236**, 393.
- Rood, H. P. C., and H. A. Tolhoek, 1965, "The theory of muon capture by complex nuclei (III). Radiative muon capture," *Nucl. Phys.* **70**, 658.
- Rosenfelder, R., 1979, "Semileptonic weak and electromagnetic interactions in nuclei: Recoil polarization in muon capture," *Nucl. Phys. A* **322**, 471.
- Rosenstein, L. M., and I. S. Hammerman, 1973, "Photon spectrum from radiative μ capture in calcium," *Phys. Rev. C* **8**, 603.
- Rothberg, J. E., E. W. Anderson, E. J. Bleser, L. M. Lederman, S. L. Meyer, J. L. Rosen, and I-T. Wang, 1963, "Muon capture in hydrogen," *Phys. Rev.* **132**, 2664.
- Scherer, S., and H. W. Fearing, 2001, "A simple model illustrating the impossibility of measuring off-shell effects," *Nucl. Phys. A* **684**, 499.
- Scherer, S., and J. Koch, 1991, "Pion electroproduction at threshold and PCAC," *Nucl. Phys. A* **534**, 461.
- Schottmueller, J., A. Badertscher, M. Daum, P. F. A. Goudsmit, M. Janousch, P-R. Kettle, J. Koglin, V. E. Markushin, and Z. G. Zhao, 1999, "Kinetic energy of π^-p atoms in liquid and gaseous hydrogen," *Hyperfine Interact.* **119**, 95.
- Shapiro, I. S., E. I. Dolinsky, and L. D. Blokhintsev, 1957, "On the interaction between μ mesons and nucleons," *Nucl. Phys.* **4**, 273.
- Shiomi, H., 1996, "Second class current in QCD sum rules," *Nucl. Phys. A* **603**, 281.
- Siebels, B., T. P. Gorringer, W. P. Alford, J. Bauer, J. Evans, S. El-Kateb, K. P. Jackson, A. Trudel, and S. Yen, 1995, "Gamow-Teller strength in $^{23}\text{Na}(n,p)$ and a comparison to $^{23}\text{Na}(\mu^-, \nu)$," *Phys. Rev. C* **52**, 1488.
- Sigg, D., *et al.*, 1996, "The strong interaction shift and width of the ground state of pionic hydrogen," *Nucl. Phys. A* **609**, 269; **617**, 526(E).
- Siiskonen, T., J. Suhonen, and M. Hjorth-Jensen, 1999, "Towards the solution of the C_p/C_A anomaly in shell-model calculations of muon capture," *Phys. Rev. C* **59**, 1839.
- Siiskonen, T., J. Suhonen, V. A. Kuz'min, and T. V. Tetereva, 1998, "Shell-model study of partial muon-capture rates in light nuclei," *Nucl. Phys. A* **635**, 446; **651**, 437(E).
- Skibinski, R., J. Golak, H. Witala, and W. Glöckle, 1999, "Final state interaction effects in μ -capture induced two-body decay of ^3He ," *Phys. Rev. C* **59**, 2384.
- Sloboda, R. S., and H. W. Fearing, 1978, "Radiative muon capture rates and the maximum photon energy," *Phys. Rev. C* **18**, 2265.
- Sloboda, R. S., and H. W. Fearing, 1980, " $O(1/m^2)$ and nuclear effects in radiative muon capture in ^{40}Ca ," *Nucl. Phys. A* **340**, 342.
- Smekal, J., and E. Truhlik, 1998, "Comments on the last development in constructing the amplitude for the radiative muon capture," preprint nucl-th/9811080.
- Smekal, J., E. Truhlik, and F. C. Khanna, 1999, "Chiral Lagrangians and the transition amplitude for radiative muon capture," *Few-Body Syst.* **26**, 175.
- Sotona, M., and E. Truhlik, 1974, "Muon capture in deuterium with realistic potentials," *Nucl. Phys. A* **229**, 471.
- Souder, P. A., D. E. Casperson, T. W. Crane, V. W. Hughes, D. C. Lu, H. Orth, H. W. Reist, M. H. Yam, and G. zu Putnitz, 1975, "Formation of the muonic helium atom, $\alpha\mu^-e^-$ and observation of its Larmor precession," *Phys. Rev. Lett.* **34**, 1417.
- Souder, P. A., *et al.*, 1998, "Laser polarized muonic ^3He and spin dependent μ^- capture," *Nucl. Instrum. Methods Phys. Res. A* **402**, 311.
- Stoks, V., R. Timmermans, and J. J. de Swart, 1993, "Pion-nucleon coupling constant," *Phys. Rev. C* **47**, 512.
- Subramanian, P. R., and V. Devanathan, 1979, "Orientations of the recoil nucleus in muon capture," *Phys. Rev. C* **20**, 1615.
- Subramanian, P. R., R. Parthasarathy, and V. Devanathan, 1976, "Nuclear orientation following muon capture by spin zero nuclei," *Nucl. Phys. A* **262**, 433.
- Sundelin, R. M., and R. M. Edelman, 1973, "Neutron asymmetries and energy spectra from muon capture in Si, S, and Ca," *Phys. Rev. C* **7**, 1037.
- Suzuki, T., 1997, "Effects of neutron halo on μ capture by ^{11}B ," in *Non-Nucleonic Degrees of Freedom Detected in Nucleus (NNDF '96), Proc. of the Intern. Symp.*, edited by T. Minamisono, Y. Nojiri, T. Sato, and K. Matsuta (World Scientific, Singapore), p. 349.
- Suzuki, T., D. F. Measday, and J. P. Roalsvig, 1987, "Total nuclear capture rates for negative muons," *Phys. Rev. C* **35**, 2212.
- Švarc, A., and Ž. Bajzer, 1980, "The extraction of the neutron-neutron scattering length from muon capture by a deuteron," *J. Phys. G* **6**, 1397.
- Švarc, A., Ž. Bajzer, and M. Furic, 1978, "Kinematical and dynamical considerations of muon capture by deuteron," *Z. Phys. A* **285**, 133.
- Švarc, A., Ž. Bajzer, and M. Furic, 1979, "The influence of the neutron-neutron off-energy-shell interaction on the differential μ -d capture rates," *Z. Phys. A* **291**, 271.
- Tatara, Naoko, Y. Kohyama, and K. Kubodera, 1990, "Weak interaction processes on deuterium: Muon capture and neutrino reactions," *Phys. Rev. C* **42**, 1694.
- Telegdi, V. L., 1959, "Consequences of atomic conversion for the interpretation of experiments on the spin dependence of muon absorption," *Phys. Rev. Lett.* **3**, 59.
- Tkebuchava, F. G., 1978, "Determination of the induced pseudoscalar form factor of the nucleon from an analysis of the reaction $\pi^-p \rightarrow e^+e^-n$ based on current algebra," *Sov. J. Nucl. Phys.* **28**, 65.
- Towner, I. S., 1986, "Meson exchange currents in time-like axial charge transitions," *Annu. Rev. Nucl. Part. Sci.* **36**, 115.
- Towner, I. S., and F. C. Khanna, 1981, "Role of 2p-2h states in weak $0^+ \rightarrow 0^-$ transitions in $A=16$ nuclei," *Nucl. Phys. A* **372**, 331.
- Truhlik, E., 1972, "Neutron-neutron interaction and muon capture by deuteron," *Nucl. Phys. B* **45**, 303.
- Truhlik, E., 2001, "Pion electroproduction amplitude," *Phys. Rev. C* **64**, 055501.
- Truhlik, E., and F. Khanna, 2002, "On radiative muon capture in hydrogen," *Phys. Rev. C* **65**, 045504.
- Truttmann, P., H. Brändle, L. Ph. Roesch, V. L. Telegdi, A. Zehnder, and L. Grenacs, 1979, "Qualitative measurement of the longitudinal recoil polarization in the reaction $^{12}\text{C}(\mu^-, \nu)^{12}\text{B}$ (g.s.)," *Phys. Lett.* **83B**, 48.
- Vainshtein, A. I., and V. I. Zakharov, 1972, "Low energy theorems for photo- and electropion production at threshold," *Nucl. Phys. B* **36**, 589.
- Virtue, C. J., K. A. Aniol, F. E. Entezami, M. D. Hasinoff, D. Horvath, H. W. Roser, and B. C. Robertson, 1990, "Photon asymmetry in radiative muon capture on calcium," *Nucl. Phys. A* **517**, 509.
- Walecka, J. D., 1975, "Semi-leptonic weak interactions in nu-

- clei," in *Muon Physics*, edited by V. Hughes and C. S. Wu (Academic Press, New York), Vol. II, p. 114.
- Walecka, J. D., 1976, "Semileptonic weak and electromagnetic interactions with nuclei: Muon capture to discrete nuclear levels from hyperfine states," *Nucl. Phys. A* **258**, 397.
- Wang, I-T., 1965a, "Study of the "breakup" channels of muon capture by He^3 ," *Phys. Rev.* **139**, B1544.
- Wang, I-T., 1965b, "Muon capture by deuterons," *Phys. Rev.* **139**, B1539.
- Wang, I-T., E. W. Anderson, E. J. Bleser, L. M. Lederman, S. L. Meyer, J. L. Rosen, and J. E. Rothberg, 1965, "Muon capture in $(p\mu d)^+$ molecules," *Phys. Rev.* **139**, B1528.
- Warburton, E. K., 1992, "Second-forbidden unique β decays of ^{10}Be , ^{22}Na , and ^{26}Al ," *Phys. Rev. C* **45**, 463.
- Warburton, E. K., I. S. Towner, and B. A. Brown, 1994, "First-forbidden β decay: Meson-exchange enhancement of the axial charge at $A\sim 16$," *Phys. Rev. C* **49**, 824.
- Weinberg, Steven, 1960, "Muon absorption in liquid hydrogen," *Phys. Rev. Lett.* **4**, 575.
- Weinberg, Steven, 1996, *The Quantum Theory of Fields: Vol. II* (Cambridge University Press, Cambridge, England).
- Wessel, W. Roy, and Paul Phillipson, 1964, "Quantum mechanics of the $(p-\mu-p)^+$ molecular ion," *Phys. Rev. Lett.* **13**, 23.
- Wiaux, V., R. Prieels, J. Deutsch, J. Govaerts, V. Brudanin, V. Egorov, C. Petitjean, and P. Truöl, 2002, "Muon capture by ^{11}B and the hyperfine effect," *Phys. Rev. C* **65**, 025503.
- Wildenthal, B. H., 1984, "Empirical strengths of spin operators in nuclei," in *Progress in Particle and Nuclear Physics*, edited by D. H. Wilkinson (Pergamon Press, Oxford), Vol. 11, p. 5.
- Wilkinson, D. H., 2000a, "Limits to second-class nucleonic and mesonic currents," *Eur. Phys. J. A* **7**, 307.
- Wilkinson, D. H., 2000b, "Limits to second-class nucleonic currents," *Nucl. Instrum. Methods Phys. Res. A* **455**, 656.
- Winston, R., 1963, "Observable hyperfine effects in muon capture by complex nuclei," *Phys. Rev.* **129**, 2766.
- Wolfenstein, L., 1970, in *High Energy Physics and Nuclear Structure*, edited by S. Devons (Plenum, New York), p. 661.
- Wright, D. H., *et al.*, 1992, "The TRIUMF Radiative Muon Capture Facility," *Nucl. Instrum. Methods Phys. Res. A* **320**, 249.
- Wright, D. H., *et al.*, 1998, "Measurement of the induced pseudoscalar coupling using radiative muon capture on hydrogen," *Phys. Rev. C* **57**, 373.
- Wright, D. H., *et al.*, 2000, "Radiative muon capture on ^3He ," *Few-Body Syst., Suppl.* **12**, 275.
- Wullschlegel, A., and F. Scheck, 1979, "Radiative muon capture on ^{12}C and ^{16}O ," *Nucl. Phys. A* **326**, 325.
- Yovnovich, M. L., and V. S. Evseev, 1963, "On interaction constants in μ^- capture," *Phys. Lett.* **6**, 333.
- Zaimidoroga, O. A., M. M. Kulyukin, B. Pontecorvo, R. M. Sulyaev, I. V. Falomkin, A. I. Filippov, V. M. Tsupko-Sitnikov, and Yu. A. Scherbakov, 1963, "Measurement of the total muon capture rate in ^3He ," *Phys. Lett.* **6**, 100.
- Zel'dovich, Ia. B., and S. S. Gershtein, 1959, "Formation of hydrogen mesic molecules," *Zh. Eksp. Teor. Fiz.* **35**, 833 [*Sov. Phys. JETP* **8**, 451 (1959)].